Growth of abalone (*Haliotis rubra*) with implications for its productivity

by

Fay Helidoniotis, BSc (Hons)

Submitted in fulfilment of the requirements for the Degree of

Doctor of Philosophy in Quantitative Marine Science

Institute for Marine and Antarctic Studies

University of Tasmania

July 2011

Statement of Originality

This thesis contains no material which has been accepted for a degree or diploma by the University or any other institution. To the best of my knowledge and belief, this thesis contains no material published or written by another person except where due acknowledgement is made in the text of the thesis.

Fay Helidoniotis _____ Date _____

Authority of Access Statement

This thesis may be available for loan and limited copying in accordance with the *Copyright Act 1968*

Fay Helidoniotis _____ Date _____

STATEMENT OF CO-AUTHORSHIP

The following people and institutions contributed to the publication of the work undertaken as part of this thesis:

Chapter 2: Dr M. Haddon (CSIRO) supervised the research in this chapter and provided significant intellectual input and technical advice on statistical analyses and research design. Prof. C. Johnson (UTAS) provided intellectual input and discussion on the content.

Chapter 3: Dr M. Haddon suggested the approach of cross model validation in addition to co-supervising and providing intellectual input and discussion. Prof. C. Johnson provided co-supervision, intellectual input and discussion that significantly improved the Chapter. Dr G. Tuck (CSIRO) co-supervised and provided a significant contribution into the intellectual input and discussion on the interpretation of results.

Chapter 4: Dr M. Haddon provided statistical advice. Dr G. Tuck provided intellectual input and discussion of the content. Mr D. Tarbath (UTAS - Tasmanian Aquaculture and Fisheries Institute) is a collaborator and provided confirmation of the accuracy in the description of part of the methods.

Chapter 5: Prof. C. Johnson co-supervised the research and provided significant intellectual input and technical advice on statistical analyses. Dr M. Haddon provided statistical advice and suggested significant improvements on the presentation of results. Dr G. Tuck co-supervised the research and provided intellectual input and discussion. Satellite SST data was obtained from the Remote Sensing Facility at CSIRO and Mr F. Rizwi significantly contributed to the programming used to obtain the data.

Chapter 6: Dr G. Tuck conceived part of the research reported and significantly contributed to the interpretation of results. Dr M. Haddon provided the R script for the size transition matrix, as well as statistical direction and intellectual input.

We the undersigned agree with the above stated "proportion of work undertaken" for each of the above published (or submitted) peer-reviewed manuscripts contributing to this thesis:

Prof. Craig Johnson _____

Dr Geoff Tuck _____

Dr Malcolm Haddon _____

Date: _____

ABSTRACT

The use of an incorrect growth model in fisheries management may lead to inaccurate predictions about stock productivity. In Australia, three non-nested size-based growth models are generally used to describe the growth of abalone populations: the von Bertalanffy, Gompertz and inverse logistic. The models differ in their description of growth, especially in the juvenile phase. However, while data on juveniles has the greatest discriminating power between models, in reality good data on size distributions and growth of juveniles is uncommon, and this leads to ambiguity in model selection.

I use a large dataset (from the Tasmanian Aquaculture and Fisheries Institute) describing sizes and growth of juvenile and adult size classes to systematically resolve model ambiguity for blacklip abalone (*Haliotis rubra*) populations in Tasmania. Modal progression analysis of bimonthly data collected over two years from the same site identified two cohorts of juveniles between 10 – 75 mm shell lengths. The best statistical model was selected using standard statistical model selection procedures, i.e. Akaike's Information Criteria and likelihood ratio tests. Despite the large data set of 4,259 specimens, model selection remained statistically ambiguous. The Gompertz was selected as the best statistical model for one cohort and the linear model for the other. Interestingly, the biological implications of the best fitting Gompertz curve were not consistent with observations from aquaculture. The study revealed that slight differences in data quality may contribute to ambiguity in statistical model selection and that biological realism is also needed as a criterion for model selection.

The robustness of different growth models to sampling error that is inconsistent between samples was explored using Monte Carlo simulation and cross model simulation. The focus

was on simulated length increment data largely from adult size classes (55 – 170 mm shell length) as these data are more commonplace than data from juveniles. Results confirm that the two main shortcomings in length increment data contributing to model misspecification were (i) poor representation of juvenile size classes (< 80 mm) and (ii) low sample size (n<150). Results indicate that when negative growth data are included in the von Bertalanffy model, K increases and L_∞ decreases. In reality the true description of growth remains unknown. Given realistic length increment data, there is a reasonable probability that an incorrect growth model may be selected as the best statistical model. This is particularly important, because this study indicates there is a different magnitude of error associated with each growth model. The important overall finding is that while it is possible to make incorrect model selections using customary statistical fitting procedures, departures from biological reality are lower if the incorrect inverse logistic model is selected over the incorrect von Bertalanffy or Gompertz model.

The selection of the most appropriate growth model was further tested by fitting each of the three growth models to length increment data from a total 30 wild populations. The inverse logistic was the best statistically fitting model in 23 populations.

The combined results from data on the growth of juveniles, cross model simulation, and fitting to data from numerous wild populations systematically revealed that the inverse logistic model was the most robust empirical representation of blacklip abalone growth in Tasmania. With this confidence in the selected model, it was then possible to address two urgent ecological and management issues related to stock productivity; the effect of climate change on growth rates and the success of broad-scale management controls in the presence of fine-scale variability in growth rates.

The effect of ocean warming on the growth rates of blacklip abalone populations was explored from the analysis of length increment data from 30 populations across a range of water temperatures. Measurements based on the growth rates of juveniles did not reveal a clear negative relationship between temperature on growth. A decrease in growth rate was observed however it may not be directly attributable to temperature but may be forced by the onset of maturity, which does appear to be directly influenced by temperature.

Fine-scale estimates of growth rate are an implicit aspect of evaluating the success of broad-scale management control such as Legal Minimum Length (LML) for harvesting. In reality, it is not possible to obtain fine-scale growth rates given the expense of obtaining empirical length increment data at fine spatial scales. Therefore, an alternative approach was developed that exploited the correlation between the parameters of the inverse logistic model and size at maturity. The approach generated theoretical, fine scale growth parameters and population-specific LMLs for 252 populations around Tasmania. Using population specific size limits, results revealed that 46 populations were unprotected by the current Legal Minimum Length (LML) settings, potentially exposing those populations to overexploitation. The majority of unprotected populations were located in the south west, a region that is economically valuable. An important recommendation from this thesis is that the LML of the economically valuable south-west region should be increased in order to achieve the management goals of the fishery.

ACKNOWLEDGEMENTS

I am very grateful to my supervisors Craig Johnson, Malcolm Haddon and Geoff Tuck for their patience, fantastic mentoring, and for encouraging me throughout the whole process. I was fortunate to be supervised by such highly established professionals in the field. I would like to acknowledge the senior scientific officers for organizing the fieldwork that produced the dataset used in this study: Craig Mundy, Rick Officer, Warwick Nash and the technical staff of the Resource Security and Future Harvest Programme at the Tasmanian Aquaculture and Fisheries Institute, now part of the Institute for Marine and Antarctic Studies at the University of Tasmania.

A big thanks to the people at the Tasmanian Abalone Council and their partners and to the Tasmanian Department of Primary Industries, Parks, Water and Environment for sharing their extensive knowledge about the management of the abalone fishery.

I would like to thank the University of Tasmania for providing a UTAS Scholarship and the CSIRO/UTAS Quantitative Marine Science program for an incremental scholarship. The Tasmanian Aquaculture and Fisheries Institute also provided funding for this work.

A big thanks to Craig Allen, Neill Zeimer, Ginetta Basilico and Rick Porter-Smith for their valuable assistance during the progression of this thesis and for keeping me motivated.

To my family for being a source of comfort and providing me with the greatest motivating force that I could ask for. They are always in my heart and thoughts across the long distances.

Fay Helidoniotis (July 2011)

CONTENTS

LIST OF FIGURES

LIST OF TABLES

CHAPTER 1

General Introduction

1.1 Overview

The Tasmanian abalone fishery is the largest single-managed abalone fishery in the world. It supplied 30% of global wild-caught abalone production in 2008 (ABS 2009), and had a beach value of AU$93 million in 2009 (Tarbath & Gardner 2009).

The fishery relies predominantly on a single species, the blacklip abalone (*Haliotis rubra*), and consists of numerous genetically independent populations (Temby *et al.* 2007). Catches have ranged between 1,000 and 4,500 tonnes per year through the current 48 year history of the fishery (1962 – 2010), and have been relatively stable at about 2,500 tonnes per year since 1997 (Harrison 2006; Tarbath & Gardner 2009). Stable catches notwithstanding, productivity is spatially highly variable around the State and the reasons for this are not well understood.

Effective fishery management and the resolution of fisheries and related ecological questions requires that productivity is better understood (Hilborn & Mangel 1997). For example, there is a need to understand the influence of temperature on productivity in wild abalone (Tarr 1995; Rogers-Bennett 2007). This is particularly important in Tasmania, given that within the geographical range of populations around Tasmania water temperatures differ by 4 °C and maximum average temperatures typically range from 15 – 19 °C. A further reason to investigate the effect of temperature on abalone production is that climate change is expected to cause long-term warming of surface waters (Ridgway

2007a). Any potential changes in productivity along the Tasmanian east coast will require a management response.

Productivity is perceived using indirect measures such as regional catch rates (catch per unit effort) and landings (tonnes). There remains a lack of understanding about the biological and ecological causes of variation in productivity. Despite this lack in understanding, managers of the abalone fishery implement different control measures, such as regional caps on catch (tonnes) and Legal Minimum Lengths (LML) which are the minimum lengths for harvesting. These control measures vary depending on the perceived level of productivity. Improving the understanding in the variation in productivity around the State will enable fisheries managers to adopt a more proactive approach toward fisheries management. Addressing this issue will enable scientific programmes to provide more informed and sound recommendations to fisheries managers and industry.

In order to understand how and why productivity varies, it is necessary to understand the mechanisms that affect productivity. Accurate estimates of productivity depend on the quantitative analysis of three biological components; growth, recruitment, and mortality (Hilborn & Walters 1992). In this thesis I will focus on growth, in particular population mean (somatic) growth. I will investigate how best to estimate growth rates, how growth rates vary between populations and how growth varies under different temperature conditions. I will then combine this information to make scientific recommendations relating to the management of the fishery.

In Australia, the choice of growth models differs between the scientific programmes in different States (Day & Fleming 1992; Troynikov *et al.* 1998; Worthington & Andrew 1998). This was not surprising because there is inconsistency in the methods used for

selecting a growth model. Model selection appears to have been based on visual support from the particular data available (Yamaguchi 1975) rather than more robust methods based on statistical approaches.

A variety of somatic growth models have been applied to data from different abalone fisheries. However the relative utility of the different models has rarely been investigated systematically. This has compromised estimates of productivity for both ecological studies and for fisheries management.

The adoption of particular growth models continues without proper scrutiny as to their suitability for the species in question (not only in the case of abalone). The use of an incorrect growth model in fisheries management may lead to inaccurate predictions about stock productivity (Arce & León 1997). An associated problem, that remains poorly evaluated is the influence of sampling error on scientific findings. There is general agreement that data relating to population and community dynamics from harvested marine species is often incomplete or uncertain (Francis & Shotton 1997; Punt 2006). Sampling error is caused by sampling only a small proportion or subset of a population and can give rise to model uncertainty (Francis & Shotton 1997). It is therefore important that minimum data requirements are specified for the predictive methods that lead to management decisions (Francis & Shotton 1997; Punt 2006).

There are several reasons to focus this work on the Tasmanian abalone fishery. This fishery is large in terms of the harvest, the value of the fishery and the number of stakeholders involved. A suitable stock assessment model is currently being developed to predict stock productivity and a formal evaluation and appraisal of growth is therefore urgently required. The selection and implementation of a suitable growth model from an array of many will

ultimately improve the candidate stock assessment models that are being considered as part of the decision making process in the management of this fishery. The scientific programme associated with the Tasmanian fishery has accumulated growth data for a number of populations over many years. The extent and quality of this database presents an excellent opportunity for applying and comparing among different models for their suitability to describe blacklip abalone growth. Accurately characterizing growth in abalone, based on modelling length-increment data will have applications to many other fisheries that also rely on length-based models to characterise growth.

In this thesis alternative growth models will be systematically tested for their appropriateness when applied to data from blacklip abalone populations in Tasmania, Australia. I will test three different growth models using statistical approaches, based on information criteria, and evaluate their relative statistical fit to shell-length data from juvenile and adult blacklip abalone populations. The selection of a suitable growth model will be based on the following:

- The use of statistical goodness of fit tests such as likelihood ratio tests and Akaike information criterion, to identify which growth model is most relevant to the blacklip abalone over the full size spectrum from juvenile to adults.
- A quantitative assessment of the behaviour and robustness of different growth models in the presence of types of sampling error common in tag-recapture data.
- The use of biological criteria to identify which growth model is most biologically plausible to blacklip abalone.

Studies into the effect of temperature and productivity based on other abalone species have not defined a clear relationship. For example, two studies into the correlation between water temperature and growth rate in wild populations of *H. midae* abalone from South

Africa produced inconsistent results (Newman 1969a; Tarr 1995). However, many factors were not considered in those studies. For example, they did not take into account that certain temperature ranges are within the thermal tolerance for growth in abalone (Gilroy & Edwards 1998). Therefore temperature effects were not detected and thus the issue remained open to research. Furthermore, such studies used size specific growth rates, which did not take into account that the onset of maturity occurs at different shell lengths between populations and is likely to affect growth rates (Newman 1968; Lester *et al.* 2004).

The Tasmanian fishery is managed at a broad spatial scale relative to the heterogeneous nature of the populations. One important management rule is the Legal Minimum Length (LML) which is the minimum shell length at which abalone can be harvested legally. The management objective of the LML is to provide some minimum protection to the spawning stock biomass. The LML is formally calculated from estimates of growth and size at maturity. Despite their extensive use, the success of LMLs in meeting management objectives is rarely assessed (Stewart 2008). Growth needs to be modelled in order to determine the suitable LML that factors in the time taken to produce young and adequately sustain the population. Therefore population specific growth data is important in determining the size that abalone should be fished in order to manage the fishery sustainably. I will address growth related questions on productivity that require accurate estimates of growth and have implications for the ecology and management of blacklip abalone populations in Tasmania.

1.2 Thesis structure and objectives

This thesis consists of five principle chapters developed as stand-alone papers (excluding the General Introduction and the General Discussion chapters of the thesis). The five chapters form a logical sequence in examining issues of modelling growth in Tasmanian blacklip abalone populations, and in applying these models to the management of the Tasmanian fishery. The objectives addressed include:

1.2.1 Modelling growth

A. To assess the validity of three candidate growth models applied to a population of juvenile abalone (**Chapter 2**).

B. To test the relative robustness of the three candidate growth models using cross-model validation and Monte-Carlo simulation using tag-recapture data, with unbalanced sampling error (**Chapter 3**).

C. To select the growth model which best represents growth of juvenile and adult populations (**Chapter 4**).

1.2.2 Application of growth models to ecology and fishery management

D. To investigate links between temperature conditions and growth in fast and slowly growing populations (**Chapter 5**).

E. To quantify the extent of mismatch between growth rates and the Legal Minimum Length size limits and highlight the implications this has on protecting spawning stock (**Chapter 6**).

Chapters 2 through **4** systematically identify the most suitable growth model for blacklip abalone populations in Tasmania. Growth models are fitted to data and a critique of each model is provided. The three growth models are assessed biologically and statistically, for both juvenile (**Chapter 2**) and adult (**Chapters 3** and **4**) stages of the life history. The selection of the most plausible growth model is based on this assessment. **Chapter 5** applies the selected growth model to assess the potential effects of climate change on growth rates, and to assess the implications of this for stock management. **Chapter 6** addresses the implications of heterogeneous growth between different populations for fisheries management.

1.3 Chapter Summaries

1.3.1 Model selection: describing the growth of juvenile abalone (Chapter 2)

Few studies have been able to describe the growth rate of wild caught juvenile blacklip (2 – 80 mm shell length) (Prince *et al.* 1988a; Prince *et al.* 1988b). Data describing growth in the juvenile size range (i.e. the size range of the sexually immature population living in crypsis), is rare because samples are difficult to obtain (Rogers-Bennett *et al.* 2007). Fortunately a large dataset existed within the Tasmanian Aquaculture and Fisheries Institute that consisted of juvenile abalone (approx. 10 – 75 mm). This chapter compares the utility of

three different models (von Bertalanffy, Gompertz and linear) to describe growth of juvenile abalone based on empirical data.

The results in Chapter 2 confirm that a linear growth trajectory is both statistically and biologically plausible, necessitating the inclusion of a size based model with constant initial growth (e.g. the inverse logistic) as a candidate model for this species. The inverse logistic model was further examined in the following two chapters (**Chapter 3 – 4**). The major finding in **Chapter 2** is that growth in juveniles varies seasonally, regardless of model choice, with fastest growth in the warmer months (September – March). The effect of temperature on growth is investigated further in **Chapter 5**.

1.3.2 Model validation: model robustness when applied to data with unbalanced sampling error (Chapter 3)

The selection of an inappropriate growth model, i.e. model misspecification, has profound implications for stock assessment and simulation, both of which are becoming increasingly important in fisheries modelling (Schnute 1991; Polacheck *et al.* 1993; Dick 2004; Zhou 2007). Both the quality of data collected from field surveys and the sensitivity of each model to data quality and quantity can affect model outcomes (Francis & Shotton 1997)

Using Monte Carlo simulation, I examined the statistical goodness-of-fit of three growth models (the von Bertalanffy, Gompertz, and inverse logistic) for their robustness to data with unbalanced sampling error. The data examined consists of tag-recapture data (with simulated sampling error) because tag-recapture data is common in scientific programmes. The inverse logistic growth model is included because results in **Chapter 2** indicate growth

of juvenile size classes may be linear and linear growth is consistent with the inverse logistic growth model (Haddon *et al.* 2008). In Chapter 3 model misspecification is examined in the context of the robustness of each of the three models to differences in data quality and quantity (i.e. unbalanced sampling error).

Results in **Chapter 3** show that the inverse logistic model is the most statistically robust model in the presence of unbalanced sampling error. This finding is important as it establishes the inverse logistic model as a plausible candidate model for blacklip abalone offering advantages over the von Bertalanffy and Gompertz models. The von Bertalanffy and Gompertz are commonly used in stock assessments and the inverse logistic model would be a novel addition to stock assessment modelling.

1.3.3 Model selection: selecting a growth model to describe the full growth trajectory of blacklip abalone (Chapter 4)

In Australia techniques used in model selection often vary between scientific programmes and are sometimes inconsistent with most widely accepted methods that rely on information criteria (Burnham & Anderson 2002). In **Chapter 4,** I further tested the suitability of the three candidate growth models to determine whether one was statistically and biologically optimal for describing the growth of blacklip abalone. The three candidate growth models were fitted to tag recapture data from 30 samples of wild blacklip abalone populations around Tasmania. The best statistical model was identified using the relative statistical fit, likelihood ratio tests, Akaike's Information Criterion and Akaike weights as diagnostics.

The results indicate that the inverse logistic model is statistically and biologically the most suitable model for the majority of blacklip abalone populations for size classes ranging from 50 – 182 mm.

The combined results of the first three data chapters established that the inverse logistic model is the most suitable for blacklip abalone populations. This growth model can therefore be confidently applied in the final two chapters (**Chapters 5 and 6**) to address growth related questions on productivity.

1.3.4 Ecological implications: climate change (Chapter 5)

Climate change is expected to lead to warming of surface waters in south-east Australia at 3.8 times the global average (Ridgway 2007a). Productivity of abalone populations in Tasmania tends to be relatively lower in warmer waters. In Chapter 5, I examine variability in growth rates and size at maturity among blacklip abalone populations under a temperature gradient and relate this to productivity. The quantification of the effect of temperature on growth potentially allows the effects of climate change to be incorporated into fisheries stock assessment models.

Results based on the correlation between water temperature and size at maturity show that as water temperature increases, the size at maturity decreases. Although a slight correlation between water temperature and growth residuals was apparent, the correlation between water temperature and size at maturity was stronger and consistent around the coast of Tasmania. Given that the onset of sexual maturity may have a strong bearing on decreasing growth rates (Lester *et al.* 2004) a synthesis of all the three factors in this chapter (i.e.

temperature, growth and maturity) indicates warmer temperatures may lead to a decrease in the size at maturity which in turn leads to a decrease in growth rates.

1.3.5 Management implications: protecting spawning biomass (Chapter 6)

Legal Minimum Lengths (LML) are the oldest management tool used to minimise the risk of overfishing (Martin & Maceina 2004). In Tasmania the calculation of the LML requires estimates of growth and size at maturity. The findings in **Chapter 5** show that growth and size at maturity may vary at fine spatial scales, finer than the scale at which the fishery is managed, making it more difficult to manage appropriately as a sustainably fished resource. This mismatch in spatial scales was the motivation for the final chapter of the thesis. Ideally, in order to be truly successful at achieving its management goal, the LML should vary at a spatial scale that is consistent with the variability in growth rate and size at maturity. However, in reality, the extent of the mismatch in spatial scale between the broad-scale LML and the biology is not known i.e. the number of populations and their location. The mismatch potentially compromises optimum yields and/or sustainability. Furthermore LMLs are estimated in the absence of information on growth due to the paucity of growth data and are often adjusted after considering historical catch data which are irrelevant within the formal method of calculating the LML (i.e. which use growth and maturity estimates). In this chapter I developed an approach for estimating fine scale, population-specific growth parameters in the absence of growth data. I also address the question of how well the current LML settings account for the variability in growth rates

and if they are successful in achieving the intended management goal of protecting the spawning stock.

Although the current LML settings applied by management reflect some of the variability in growth rate and size at maturity, the results in this chapter show that the variability in growth rate is at such a fine spatial scale that the broad-scale LML settings fail to achieve their management goal particularly in the south west of Tasmania. This south-west region is economically valuable to the Tasmanian abalone fishery and populations there are at risk of being overfished. This is partly because those populations have the highest combined initial growth rates and size at maturity of any populations within the geographical range of the Tasmanian abalone fishery. This leads to generally large abalone, and the current management controls do not take this into consideration.

To summarise, an accurate description of growth has profound implications for the management of abalone fisheries. Furthermore, the methods applied within this thesis are also relevant to other fisheries that rely on length based descriptions of growth.

CHAPTER 2

Fitting growth models to length frequency distributions of a population of juvenile blacklip abalone (*Haliotis rubra*) from southern Tasmania: statistical fit versus biological plausibility

2.1 Abstract

I consider the problem of selecting the most appropriate growth model to describe the growth trajectory of a population of juvenile (10 – 75 mm) blacklip abalone (*H rubra*) from a site in south-east Tasmania. Using modal progression analysis, I identified two cohorts of juvenile blacklip abalone. Non-seasonal and seasonal versions of three growth models (the von Bertalanffy and Gompertz models, and a linear model) were fitted to the data and examined for statistical fit using likelihood ratio tests and Akaike's Information criteria. Selection of the statistically optimal model for juvenile growth remained ambiguous. The seasonal-Gompertz model was the best fitting for one cohort whereas the seasonal-linear model was best for the other. However in the first cohort the best fitting seasonal-Gompertz predicted a growth rate of 24μm/d which is not consistent with published findings of growth in juveniles (>2mm shell length). In contrast, the statistically suboptimal models for that cohort predicted growth rates of 67μm/d for the seasonal-von Bertalanffy and 60 μm/d for the seasonal-linear which were consistent with published findings. In the second cohort, the best fitting seasonal-linear model predicted a growth rate of 60 $\mu m.d^{-1}$, consistent with published findings. The seasonal-Gompertz model varied in the growth rate predictions between the two cohorts, which were from the same geographical stock, whereas the von Bertalanffy and linear models were more consistent in their growth rate predictions between cohorts. The seasonal von Bertalanffy and Gompertz models

approximated seasonal, linear-like growth over a size range of 10 – 75 mm shell length. After considering both statistical and biological criteria it is concluded that the most appropriate growth model for blacklip abalone between 10 – 75 mm shell length is a linear model with an underlying seasonal trend. Juvenile abalone at Hope Island grew faster during the warmer months of September – March where mean monthly temperatures ranged between 11- 16 °C.

2.2 Introduction

2.2.1 The importance of information on juveniles in modelling growth

Quantifying mean population growth is one of the three main components required for predicting stock productivity (Hilborn & Walters 1992). Mean somatic growth is quantified using various growth models that are selected *a priori*. The most widely used growth models are the von Bertalanffy and Gompertz models (Ricker 1975; Katsanevakis & Maravelias 2008), However, the appropriateness of these models (von Bertalanffy or Gompertz) to juvenile size classes is questionable because constant growth rates have been reported for juveniles and these models do not incorporate constant growth rates in that size region (Haaker *et al.* 1998). The appropriateness of these growth models to size classes of juvenile animals has not been systematically evaluated. Consideration of the growth of juveniles is important because it is in this size range that discriminating power between growth models is greatest. Furthermore, it is important to resolve the growth trajectory through the juvenile phase because this is where growth occurs most rapidly (Morgan & Colbourne 1999). It follows that selection of a growth model without data on juveniles may lead to low confidence in model selection. However, despite recognition of the issue, juveniles remain poorly represented in fisheries data because samples of juveniles are difficult to obtain for many marine species. Fortunately, data on the

growth in juvenile blacklip abalone (*H. rubra*) was available from the Tasmanian Aquaculture and Fisheries Institute. This enabled a systematic evaluation of both the statistical fit of a set of candidate models, and the biological validity of their predictions are used to select the most appropriate growth model for juvenile blacklip abalone populations in Tasmania

2.2.2 Measuring growth in blacklip abalone

The Tasmanian blacklip abalone (*H rubra*) fishery is the largest single managed abalone fishery in the world (ABARE 2007), and a clear understanding of growth and productivity is necessary to underpin robust management. However achieving such an understanding is complicated because the somatic growth rate of abalone stocks is known to be spatially variable (Worthington *et al.* 1998). Moreover, data on growth of populations of juvenile blacklip abalone in the wild is rarely available due to the cryptic nature of juveniles. Abalone are classified as juveniles when the first respiratory pore appears, at approximately 2 mm in length two to three months into the post larval stage (Cropp 1989). Maturity into the adult stage often coincides with emergence from crypsis (Peck *et al.* 1987; Prince *et al.* 1988b; Nash *et al.* 1994) although a proportion of mature abalone can remain cryptic (Prince *et al.* 1988b; Catchpole *et al.* 2001). In south-east Tasmania, the onset of maturity and the size at emergence is known to be variable but tends to be greater than 100 mm. Therefore the size range of juvenile blacklip abalone in south-east Tasmania is generally regarded to be between 2 – 100 mm shell length. Because of their cryptic habit on the underside of boulders, juvenile abalone are difficult to sample by SCUBA divers. Hence, most growth studies on blacklip abalone are based primarily on data from emergent, and therefore adult, individuals that are relatively easy to sample by SCUBA divers, and data on juveniles is usually under represented. The large dataset available for this study, made availale from the

Tasmanian Aquaculture and Fisheries Institute, consisted of shell measurements of juveniles within the 10-75 mm size range.

2.2.3 Techniques and models used to estimate growth

There are three main techniques for measuring growth in blacklip abalone and each have their disadvantages. These include mark–recapture, growth ring analysis, and modal progression analysis (Proudfoot *et al.* 2008). The main disadvantage of mark–recapture studies is that the stress of tagging on juveniles may affect growth (Prince 1991). For this reason, modelling the growth of juvenile abalone based on mark-recapture data is ill advised. The main disadvantage with analysis of growth rings is that growth rings in blacklip abalone cannot be assumed to be annual (McShane & Smith 1992). In contrast to these techniques, reliable growth estimates for juvenile size classes are possible using modal progression analysis (Proudfoot *et al.* 2008). Unlike the other two techniques, which measure the growth increment of individuals, modal progression analysis measures the mean population growth. Regardless of the technique used, sampling abalone is prone to a bias known as Rosa Lee's phenomenon that can affect growth measurements (Ricker 1975). Rosa Lee's phenomenon is the selective removal of fast or slow growing individuals as a result of natural predation. This bias applies equally to all three sampling techniques used for measuring growth (Ricker 1975). Modal progression analysis is therefore arguably the most robust option for estimating growth of juvenile blacklip abalone since it has fewer disadvantages than mark–recapture or growth ring analysis. Although modal progression analysis has been successful in describing the mean population growth for many marine species, it remains untested for juvenile blacklip abalone.

To measure growth using modal progression analysis, length frequency distributions need to be obtained at regular time intervals and decomposed into modal groups (Rogers-Bennett *et al.* 2007). Modal groups usually increase in length through time and the progression of the modal groups through time is assumed to represent the mean population growth of a cohort (Britton & Harper 2008). Growth models are fitted to the progression of the modal groups within each cohort (Basson *et al.* 1988; Gulland & Rosenberg 1992; Chatzinikolaou & Richardson 2008).

2.2.4 Statistical fit of growth models

Studies into the somatic growth of blacklip abalone over the last 30 years have predominantly used two mathematical models (Day & Fleming 1992): the von Bertalanffy (von Bertalanffy 1938) and Gompertz (Gompertz 1825; Winsor 1932). Both models are assumed to describe the entire growth pattern from juvenile to adults (Harrison & Grant 1971; Shepherd & Hearn 1983; McShane *et al.* 1988; Nash 1992; Worthington *et al.* 1995; Troynikov *et al.* 1998), however the appropriateness of the growth trajectory over the juvenile size classes is questionable. The majority of studies that used the von Bertalanffy in Day and Fleming's (1992) review were based on tagging analysis, and included mainly adult abalone while juveniles were poorly represented. Of the two studies cited in Day and Fleming's (1992) review that used the Gompertz model one was based on growth ring analyses later shown to be invalid, and the other was based on data from tagging studies consisting mainly of adult size classes. Prince's study (1988a; 1988b) was the only study thus far to explicitly measure growth in juvenile blacklip abalone (shell length <80 mm) and in that study the linear model was more appropriate for juvenile size abalone.

The work presented in this chapter explicitly considers the growth of juvenile blacklip abalone and examines which model best describes the growth trajectory of juveniles within a particular

population. The usefulness of modal progression analysis in discriminating between the three growth models is also reviewed. The availability of a 2.5 year dataset of shell length measurements, collected once every two months from a single population in southern Tasmania, made it possible to characterise the growth of a population of juvenile abalone (< 100 mm shell length) before they emerge from crypsis. The overall null hypothesis tested is that there is no significant difference in statistical fit to these data between three growth models following modal progression analysis of juvenile abalone between 10-75 mm at Hope Island, Tasmania. There were four objectives in the study. First, to compare the statistical fit of three different growth models to the progression of modal groups that appear in 16 length-frequency samples collected over a 2.5 year period. Second, to compare the growth rate derived from modal progression analysis to published studies that report on the mean growth rate in a wild population and the growth rates of individual juvenile abalone under controlled conditions. The third objective was to determine whether the three growth models predict different growth rates for different cohorts from the same geographic stock. The final objective was to determine the most appropriate growth model by evaluating statistical and biological criteria, identifying their advantages and shortcomings.

2.3 Methods

2.3.1 The data

A population of cryptic abalone was sampled on 16 occasions between November 1992 and May 1995, from the shallow sub-tidal area around the leeward side of Hope Island in Dover Bay, Tasmania (Figure 2.1). Individual specimens were measured only once (i.e. sampled destructively through removal and not replaced). Each sample of the population was collected at

approximately two monthly intervals from a fixed location. In total, 5,238 individuals were collected with shell lengths ranging from 7 - 109 mm (Table 2.1).

Each sub-tidal collection involved carefully turning small boulders for 1.0 hour by two divers within the same location. The sizes of boulders turned ranged from 100 cm^2 up to 4500 cm^2. Depth of collections ranged between 1 - 10 m. During the first 11 sampling occasions, the collections were limited to shell lengths less than 80 mm. Generally, abalone larger than 80 mm were not collected because earlier work by Prince *et al.* (1988a) indicated that specimens greater than 80 mm could not be separated into cohorts and the software was unable to converge on a solution. This length restriction had the advantage of ensuring that the lower size modal groups were represented adequately within the total sample size, which was restricted to approximately 300 individuals.

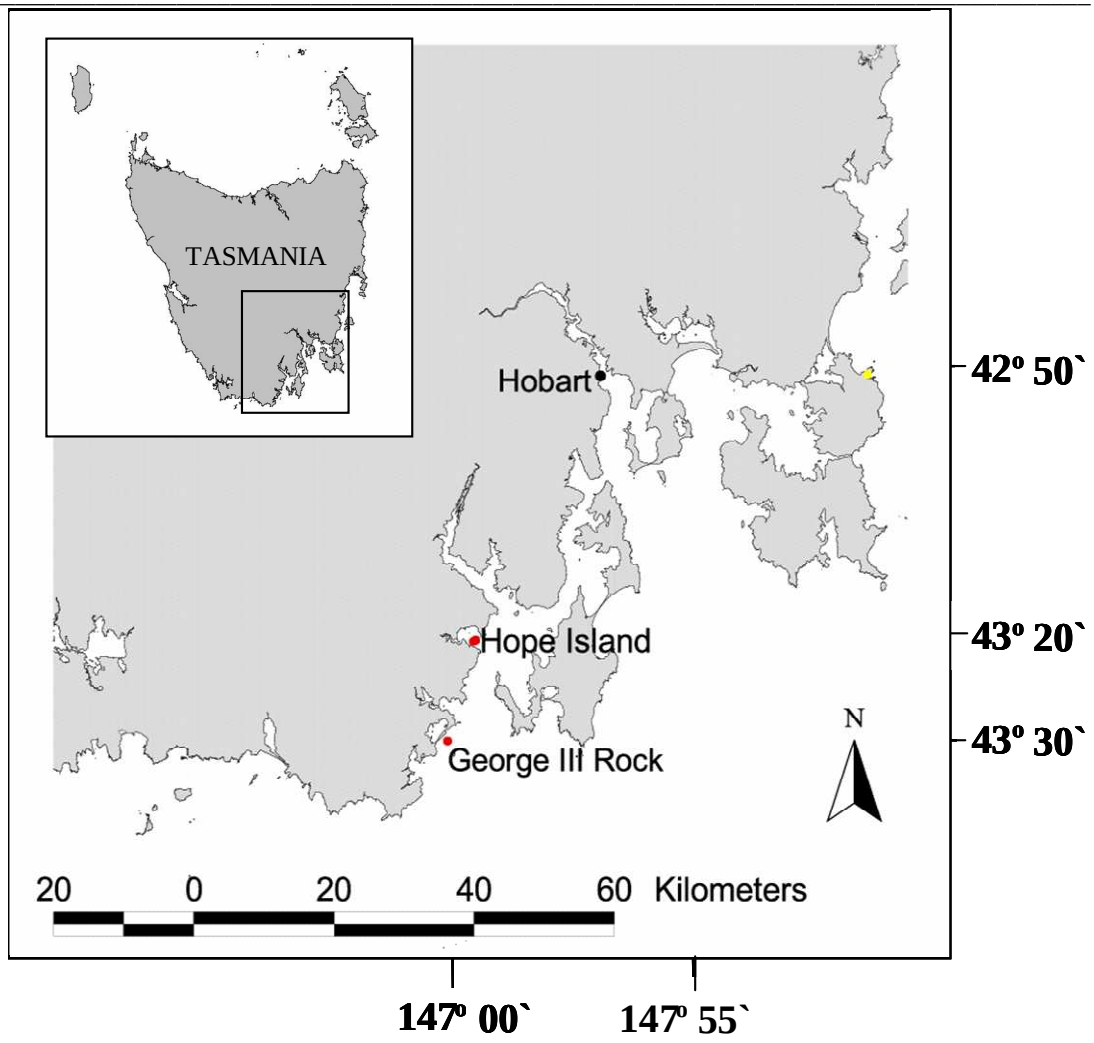

Figure 2.1: Hope Island, 43.20ºS, 147.05ºE, is a smal l island located in a sheltered bay within the D'Entrecasteaux Channel, approximately 50 kms south of Hobart. Samples of blacklip abalone (*Haliotis rubra*) were collected from a small stretch of coast in an area accessible by boat.

Table 2.1. Modal characteristics of each sample for each cohort, showing results of the predicted and observed shell lengths (mm), s.e. indicates standard error of the mean while std. dev. is the standard deviation. VB is von Bertalanffy model and Gz is Gompertz model

cohort	sample date		predicted mean (seasonal)			observed mean		std dev	proportion (no. of specimens)
			linear	VB	Gz	estimate	s.e	estimate	estimate
C	1992	Nov	15.4	15.3	17.1	16	0.27	3.1	141
	1993	Jan	21.7	21.8	21.9	23	0.27	4.3	256
		Mar	26.4	26.5	26.3	26	0.25	3.6	208
		May	28.6	28.6	28.8	29	0.31	5.5	309
		Jul	29.2	29.1	29.3	29	0.39	5.6	208
		Sep	30.9	30.8	30.6	31	0.44	7.0	260
		Nov	36.2	36.2	35.4	36	0.38	6.3	276
	1994	Jan	43.0	43.0	42.2	43	0.41	7.4	322
		Mar	47.8	47.8	47.3	47	0.6	8.5	186
		May	50.0	50.0	49.6	49	0.61	8.8	208
		Jul	50.6	50.6	50.3	50	0.92	9.9	113
		Sep	52.4	52.3	52.3	54	0.84	12.4	226
		Nov	56.9	56.8	57.3	56	0.93	12.0	163
	1995	Jan	64.4	64.4	65.3	65	0.81	10.6	173
		Mar	68.8	68.8	69.5	71	1.02	9.9	95
		May	71.5	71.4	71.8	71	0.7	9.6	184
B	1994	Mar	11.6	11.7	11.7	12	0.3	2.8	92
		May	15.1	15.1	15.0	15	0.33	3.5	109
		Jul	17.5	17.5	17.5	17	0.36	3.8	117
		Sep	19.7	19.7	19.7	20	0.35	4.1	130
		Nov	23.4	23.4	23.4	24	0.36	4.4	150
	1995	Jan	29.8	29.8	29.8	29	0.45	5.8	154
		Mar	34.3	34.3	34.3	36	0.66	4.8	53
		May	38.4	38.4	38.4	38	0.5	5.6	126
A	1995	Mar	-	-	-	9	0.64	1.3	4
		May	-	-	-	15	0.57	2.5	20

A major assumption of this work is that modal groups (cohorts) identified in the bi-monthly samples are representative of the entire population of juvenile abalone. However, given that the size of boulders that can be successfully overturned is a subset of all boulders at the site, if a relationship exists between boulder size and the size of cryptic abalone attached to them, then there is potential for any modes of larger-sized abalone to be biased low ('boulder bias'). On the

other hand, the smallest modal groups are made up of animals < 10 mm shell length and the very smallest are more difficult to see or detect underwater ('visibility bias'). This could bias the modes of the smallest-sized abalone high. In these data 'visibility bias', and 'boulder bias' are assumed to be small, and subsequent modal progressions analysis assumes that the mean length of the identified modes propagated through time represents the mean growth of the surviving population. It is noted that these biases would apply equally to the other measurement techniques that might have been used, i.e. tagging and growth ring analysis. This bias, if present, is a consequence of the sampling and is not specific to modal progression analysis. The most common size classes in the samples were between 10–75 mm and there are no obvious processes that might bias these modal groups either high or low.

2.3.2 Modal progression analyses

The shell lengths of all juvenile abalone taken on the 16 sampling occasions were measured to the nearest millimetre using vernier callipers. These data were aggregated into 2 mm size classes, which provided a useful compromise between detail and noise given the available sample sizes. This also permitted a comparison with an earlier length frequency study that also used 2 mm size classes (Prince *et al.* 1988a). In all calculations the size classes are represented by their mid-points (e.g. size class 11 mm includes animals ≥10 mm and <12 mm).

To select a probability density function to describe the various modal groups, a preliminary analysis was conducted on a selection of modal groups that were clearly separated from other modes (Figure 2.2, Table 2.1). A comparison was made of the relative quality of fit provided by normal, log-normal, and gamma distributions (not shown). The frequency distribution of each modal group was well described using the normal probability density function, which was used in

all subsequent analyses. Each mode was described using a separate normal distribution, the parameters of which consisted of the mean size, the variance, and the proportion of the overall sample contained in each mode.

$$(\hat{f}_j \mid \mu_m, \sigma_m, p_m) = \sum_{m=1}^{m\max} \sum_{j=1}^{j\max} \left\{ \left(\int_{l=L_j}^{U_j} \frac{1}{\sigma_m \sqrt{2\pi}} e^{\left[\frac{-(l-\mu_m)^2}{2\sigma_m^2} \right]} \right) \times p_m \right\} \quad (2.1)$$

$(\hat{f}_j \mid \mu_m, \sigma_m, p_m)$ is the expected frequency of length class *j* given the parameters of the *m* normal probability density functions; μ_m is the estimated mean length for the modal group *m*; σ_m is the estimated standard deviation for the modal group *m*; p_m is the estimated number of observations in each modal group *m*; *j*max is the number of 2 mm length classes while *j* identifies each length class (1 to *j*max); *m* identifies the modal group and *m*max is the maximum number of modal groups, ; U_j is the upper bound of each particular 2 mm length class *j*; L_j is the lower bound of each particular length class *j*; and *l* is length as used in the integration (ranging from L_j to U_j for each length class).

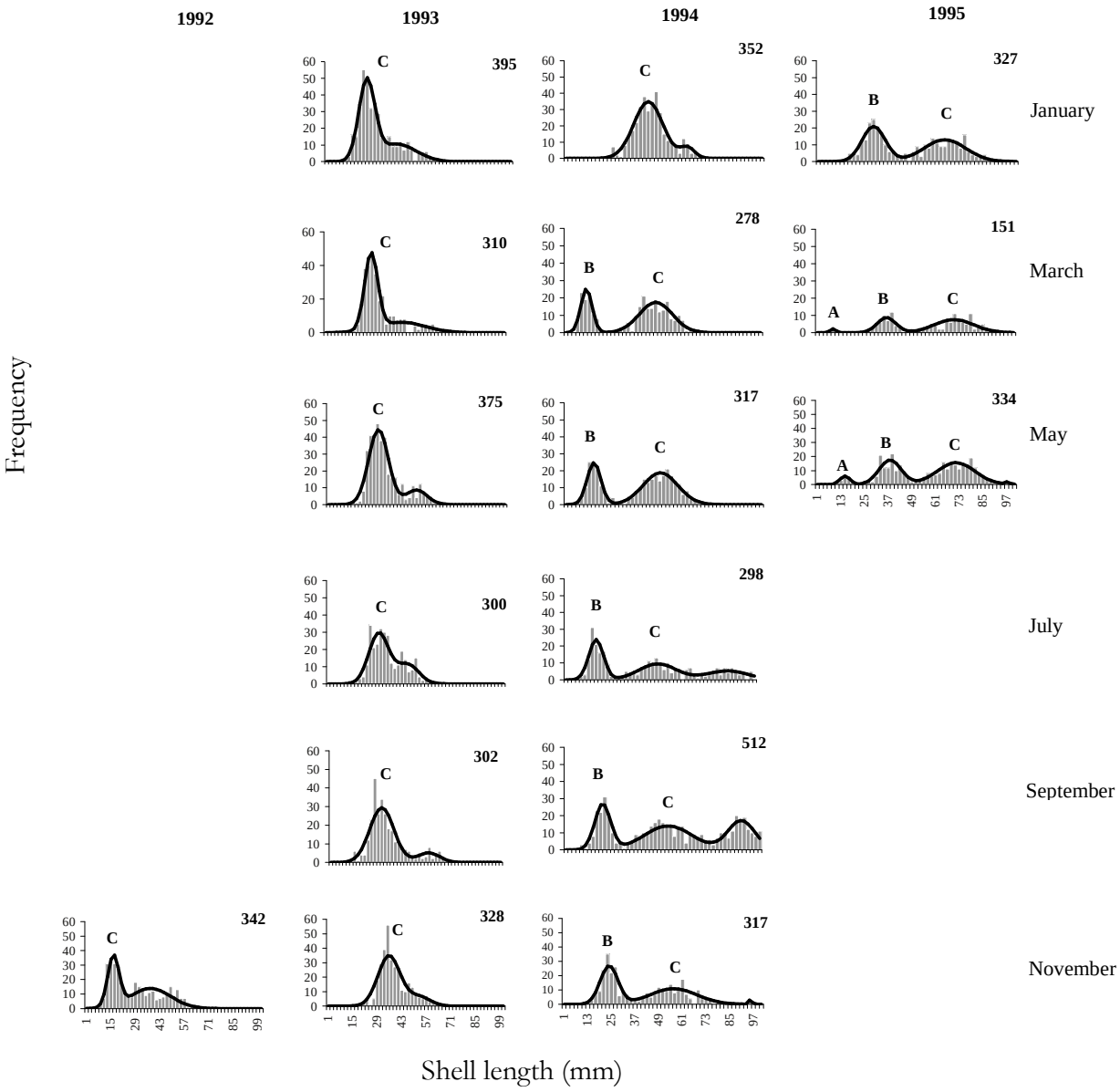

Figure 2.2. Size frequency of juvenile blacklip abalone (*Haliotis rubra*) from Hope Island, Tasmania. Bi-monthly size frequency distributions are separated into normally distributed modal groups. Inferred sequences of modal growth are represented by the capital letters A to C at 2 monthly intervals from Nov 1992 – May 1995. Measurements are aggregated into 2 mm size increments. The sample size (number of abalone collected) is given in the top right hand corner of each graph (total n = 5,238). Samples were taken from depths ranging between 1-10 m. All surveys aimed to collect at least 300 small abalone (< 80 mm shell length).

Modes were identified using two criteria. The first criterion was whether modal progressions could be visually identified, which implied that a mode should exist given the existence of a related mode in a previous or following sample. The second criterion was the expectation that both the mean size and variance of each modal group would either stay stable or increase through time. These two criteria maintained continuity of modal groups through time and avoided over-fitting. The statistical fit between the observed and expected frequencies was optimized by maximizing the logarithm of the multinomial likelihood using the Solver™ add-in in Excel™ (Microsoft Office 2003)

$$LL(f \mid \mu_m, \sigma_m, p_m) = \sum_{j=1}^{j\max} f_j Ln\left(\frac{\hat{f}_j}{\sum \hat{f}_j}\right) \qquad (2.2)$$

where *LL* is the log-likelihood of the *f*'s (that is the observed frequencies of length classes 1 to *j*max given μ_m, σ_m, and p_m, which are the means, standard deviations, and the predicted number of observations in modal group *m*), and $\hat{f}_j$ is the expected frequency of length class *j*. A penalty function $\left(N - \hat{N}\right)^2$ was subtracted from the log-likelihood to force the sum of the predicted number of observations ($\hat{N} = \sum p_m$) to equal *N*, the observed number of observations (Haddon 2001). The value of the penalty function always became trivial during the fitting process. The predicted frequencies for each length class were summed to give the total predicted frequencies across all length classes. The objective function (i.e. *LL*- penalty) was maximised by adjusting the parameter values (mean, variance, proportion) for each hypothesized mode.

2.3.3 Growth models

Juvenile growth was characterized by identifying cohorts from the progression of modal groups over the 16 sampling events. Three candidate growth models: the von Bertalanffy, Gompertz and linear, were fitted to the data from the separate cohorts. Having between five and six samples a year provided sufficient samples to enable seasonal versions of the growth curves to be fitted (Pitcher & MacDonald 1973). The models used were all age-based models. By assuming that the age of the 10mm size class is 6 months it is possible to treat size based modal progression data as age based data. The following age based models were then fitted to the modal progression data:

Von Bertalanffy (VB) $$L_t = L_\infty \left(1-\exp^{-\left(A\sin\left(\frac{2\pi(t-p)}{C}\right)+K\right)(t-t_0)}\right)+\varepsilon \quad (2.3)$$

Gompertz (Gz) $$L_t = L_0 \exp\left[G\left(1-\exp^{-\left(A\sin\left(\frac{2\pi(t-p)}{C}\right)+g\right)(t-t_0)}\right)\right]+\varepsilon \quad (2.4)$$

Linear $$L_t = (\mathrm{b}\times t)+\mathrm{a}+A\sin\left(\frac{2\pi(t-p)}{\mathrm{C}}\right)+\varepsilon \quad (2.5)$$

Seasonality term $$\left(A\sin\left(\frac{2\pi(t-p)}{C}\right)\right) \quad (2.6)$$

For the von Bertalanffy curve, L_t is the length at age or date t, L_∞ is the asymptotic average maximum size (mm), K is the growth constant, and t_0 is the hypothetical age or date of zero length (days). For the Gompertz curve, L_0 is the length at $t = 0$ and ($L_0 \exp G$) is the asymptotic length L_∞ (as $t \rightarrow \infty$), and g is the growth constant. For the linear model, b is the growth rate and a is the mean initial length of each modal group from the first sample

in which it appears. Within each seasonal term, A is the amplitude of the sine wave representing the seasonal variation in growth rate, t is the age or date, p is the time offset from the start of the cycle (this relates to the phase of the sine wave), and C is the period of the sine wave in units of days. The ε's are the independent additive normal random error terms. In each case, the seasonal curves can represent non-seasonal growth through setting the A parameter to zero.

The modal analysis was used to identify and sub-divide the 2 mm size class length frequency counts into separate cohorts through time. The 2 mm size class data for each cohort was subsequently used in the growth model fitting rather than just using the mean estimates of the modal groups (see Figure 2.3). Non-seasonal versions of the linear, von Bertalanffy and Gompertz models (equations (2.3) –(2.5), but removing the seasonality term) were fitted to the two most clearly defined cohorts (in this case cohorts B and C, see Figure 2.2). In each case the models were fitted by minimizing the negative log-likelihood using normal random residual errors. The distribution of the residuals in each case was examined for any obvious trends.

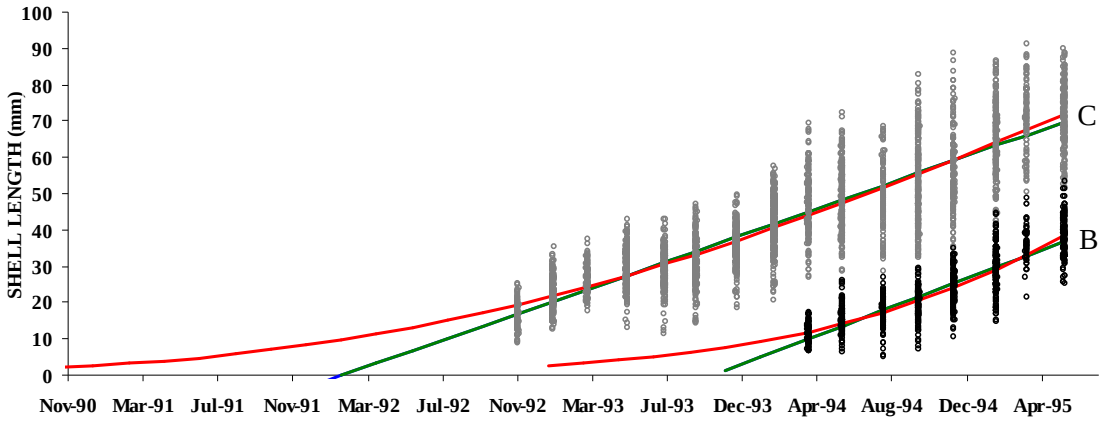

Figure 2.3. Comparison of non-seasonal growth of shell-length in a population of immature blacklip abalone (*Haliotis rubra*) at Hope Island, Tasmania. Linear (green line), von Bertalanffy (blue line, hidden under the green line) and Gompertz models (red) were fitted using maximum likelihood.

Growth trajectories indicate that the linear and von Bertalanffy models are not visually discernible while the Gompertz exhibits its sigmoidal nature and tails away.

The selection of both the optimum non-seasonal and seasonal models was based on four statistical and two biological criteria. The first statistical criterion related to the quality of model fit. This involved identifying the model with the minimum negative log-likelihood estimate (the best fitting model). The second criterion was to compare the models using a log-likelihood ratio test (Haddon 2001) to determine whether the model fits were significantly different. The third criterion was to rank the models according to the smallest Akaike Information Criteria (*AIC*). The *AIC* balances the trade-off between the quality of fit and the number of parameters used (Burnham & Anderson 2002) and is defined as $AIC = -\Sigma LL + 2K$, where K is the total number of parameters (including σ^2) and $-\Sigma LL$ is the negative log-likelihood given by

$$-\Sigma LL = -\sum_{m=1}^{m\max}\sum_{i=1}^{n_m} Ln\left(\frac{1}{\sigma_m\sqrt{2\pi}}e^{-\left[\frac{(x_i-\mu_m)^2}{2\sigma_m^2}\right]}\right) \quad (2.7)$$

where x_i relates to each of the $i = 1$ to n_m observations of length in modal group m, and -ΣLL is minimised using the Solver™ add-in in Excel™. The fourth criterion was to determine the probability of the relative weight of evidence when comparing pairs of models, sub-optimum (AIC_k) to optimum $(AIC_{\min})$, using Akaike weights (w_k) (Buckland et al., 1997). These are defined by first comparing the relative AIC values $\Delta_k = AIC_k - AIC_{\min}$, where k indexes the three growth models, and substituting these into $w_k = \exp(-0.5\Delta_k)/\sum_{k=1}^{3}\exp(-0.5\Delta_k)$. The first biological criterion was an assessment of the realism of those parameters that have specific biological interpretations. Some parameter estimates relate to conditions extrapolated well beyond the available data and are likely to be unrealistic artifacts (Francis 1988a, 1988b; Lester *et al.* 2004). Nevertheless, their values indicate how the curve is responding to the available data, biases notwithstanding. In this study the parameter values with potentially real biological interpretations related only to the von Bertalanffy and Gompertz and included the implied asymptotic maximum size for both the von Bertalanffy (L_∞) and Gompertz ($L_0\exp[G]$). Finally, the second biological criterion was to estimate growth rates ($\mu m.d^{-1}$) for juvenile abalone surviving into the first year of post settlement growth. This was compared with published growth rates from studies of early growth under controlled conditions and from one study under wild conditions.

2.3.4 Residual deviance using bootstrapping

Cohorts B and C both had sufficient data (numbers of observations and separate modal groups) to permit the construction of confidence bounds around the best fit of each of the growth models. The percentile 95% confidence limits around the optimal trajectories were estimated using a structured non-parametric bootstrap (Efron & Tibshirani 1993). Each cohort consisted of a size progression of modal groups and the variance of those groups increased with the mean size. A structured bootstrap was therefore required to avoid mixing different variances among modal groups within each cohort. Residuals were resampled from within each modal group and then added to the optimum predicted values for each growth model. This assumes that the residuals are independent and identically distributed within each modal group. The growth curves were then refitted to the bootstrap samples. A total of 500 bootstraps were used in the analysis. The upper and lower 95% confidence interval boundaries for all three growth models were compared graphically to determine the extent of overlap between the three models. The mean of the 500 bootstraps were calculated for all three growth models. The residual deviance for each modal group was determined to quantify the difference between the mean lengths predicted by each growth model, according to the equation

$$\text{residual deviance} = \left| \left(100 \times \left(\hat{\mathrm{L}}_i - \hat{\mathrm{L}}_j \right) \div \hat{\mathrm{L}}_i \right) \right| \qquad (2.8)$$

The residual deviance is the pair-wise difference in mean predicted length (from 500 bootstraps) for each modal group between model *i* and model *j* expressed as a percentage of mean modal length from model *i*. The total residual deviance between pair-wise model

comparisons was estimated by taking the sum of the residual deviance for each modal group, as follows

$$\text{residual deviance} = \sum_{m=1}^{m\max} \left| \left(100 \times \left(L_{mi} - L_{mj}\right) \div L_{mi}\right) \right| \quad (2.9)$$

where *m* identifies the modal group.

2.4 Results

2.4.1 Modal progression analysis

In total, three cohorts were detected in the modal progression analysis from the single site (16 sampling occasions; 5,238 measurements) (Table 2.1, Figure 2.2). Due to modal selection criteria only two of these cohorts, B and C (4,259 measurements), were used to examine the relative fit of the three candidate growth models. These cohorts satisfied the criteria for modal selection, namely an increase in variance as modal lengths increased, and modal lengths increased or remained stable through time. Cohort B consisted of eight modal groups spanning over 15 months and cohort C consisted of 16 modal groups spanning over 31 months. The combined shell length measurements from cohorts B and C ranged between 7- 89 mm (Table 2.1).

The limited data from cohort A exhibited growth that was not inconsistent with that exhibited by cohorts B and C, but as there were only 24 observations across two sampling periods it was not considered further (Figure 2.2).

2.4.2 Non-seasonal growth curves

Overall, the resulting mean growth models were all similar within the size range limits of the data (Figure 2.3). The von Bertalanffy and linear models were visually indistinguishable, implying that the von Bertalanffy approximates a straight line over the 10-75 mm mean size range (Figure 2.3). The Gompertz exhibited a slight curve but was similar to the von Bertalanffy and linear model over the range of the data (Figure 2.3). The biological plausibility of the growth models and the validity of the model parameters were assessed by comparing their predicted estimates of growth rate ($\mu m.d^{-1}$), with published findings. Growth rates were calculated from model parameters. In the von Bertalanffy curve, K and L_∞ parameter values were used for determining growth rates. In the Gompertz model the growth rate was estimated using the L_0, G and g parameters. In the linear model growth rate was estimated by parameter b in equation (2.5) (for all parameter values see Table 2.2). Growth rates estimated from the non-seasonal linear model within the first year of the juvenile phase (from 2 mm onwards) were 60.8 and 56.9 μm/d for cohorts B and C respectively (coefficient of variation between the cohorts, c.v. = 2.9%). Growth rates from the non-seasonal von Bertalanffy curve were similar to that of the linear model, estimated at 60.7 and 58.3μm/d for cohorts B and C respectively (c.v. = 2.8%). Growth rates within the first year for the non-seasonal Gompertz were slightly more variable at 20.3μm/d and 17.2 μm/d for cohorts B and C respectively (c.v. = 11.6%), and were notably much lower than estimates from either the linear or von Bertalanffy. The L_∞ from the von Bertalanffy model varied between cohorts B and C (5526 mm and 6374 mm respectively, c.v. = 9.7%), and were biologically implausible. Estimates of L_∞ this large for both cohorts implies that the von Bertalanffy is adopting a linear-like trajectory to fit the observed data. For the Gompertz model L_∞ (L_0*exp$G$) varied substantially between the two cohorts (CV = 133%),

being too high for cohort B (5,139mm) and substantially lower for cohort C (146mm). When the non-seasonal growth curves were fitted, the Gompertz growth model provided the best statistical fit out of the three candidate models (Table 2.3). The seasonality of growth apparent in the modal analysis showed that the smallest modes had a slightly flatter start to growth. When seasonal effects on growth were ignored in fitting models, this underlying seasonality imparted an advantage to the non-seasonal Gompertz curve, which follows such a trend naturally in the smaller modes (Figure 2.3).

Table 2.2. Parameter estimates of juvenile blacklip abalone (*Haliotis rubra*) cumulative somatic growth according to three growth models, viz. linear, von Bertalanffy (VB) and Gompertz (Gz). Parameter values are shown for models excluding and including seasonality in growth. All individuals sampled were between 7 - 109 mm shell length, and taken from cryptic habitat at Hope Island between November 1992 – May 1995. *A* is the amplitude of the sine wave representing the seasonal variation in growth rate, *p* is the time offset from the start of the cycle (relates to the phase of the sine wave), and *C* is the period of the sine wave in units of days. The ε's are the independent additive normal random error terms.

parameters		cohort B		cohort C	
		non-seasonal	seasonal	non-seasonal	seasonal
linear	a	10	10	17	17
	b	0.061	0.057	0.060	0.060
	A	-	1.9	-	3.08
	p	-	-69	-	25
	C (d)	-	375	-	371
	ε	4.8	4.6	7.9	7.6
VB	L∞	5526	2265	6345	2567
	K	1.1E-05	2.8E-05	9.2E-06	2.3E-05
	t_0 (d)	-160	-156	-290	-282
	A	-	8.7E-04	-	1.2E-03
	P	-	-70	-	23
	C (d)	-	376	-	373
	ε	4.9	4.6	7.9	7.6
Gz	Lo	21	34	19.74	22.5
	G	5.5	0.2	2.0	1.9
	g	5.0E-04	2.1E-02	8.5E-04	1.1E-03
	t_0	196	190	10	88
	A	-	-3.8	-	-0.06
	P	-	116	-	221
	C	-	1253	-	360
	ε	4.7	4.6	7.8	7.6
	L∞	5139	40	220	153

2.4.3 Seasonal growth curves

Although all three non-seasonal growth curves generated acceptable fits to the observed data (Table 2.3), analysis of residuals for both cohorts B and C clearly demonstrated an oscillation above and below the approximate linear fits indicating a seasonal trend. This seasonality trend persisted throughout the time interval sampled (Figure 2.4). Adding seasonality improved the statistical fit between the predicted curves and the observations as demonstrated by the improvement in the negative log-likelihood (Table 2.3). In cohort B, the *AIC* indicated that the seasonal-linear model provided the best fit for the least number of parameters however there was no significant difference between the different model fits for cohort B. Nevertheless, Akaike weights (w_i), for cohort B, indicate that the seasonal-linear model had a greater probability of being the best model relative to the seasonal-von Bertalanffy and the seasonal-Gompertz (Table 2.3). For cohort C, the *AIC* indicated that the seasonal-Gompertz model was clearly optimal ($w_i = 1.00$) with the seasonal-linear and seasonal-von Bertalanffy models being statistically very unlikely ($\Delta AIC > 10$; Table 2.3).

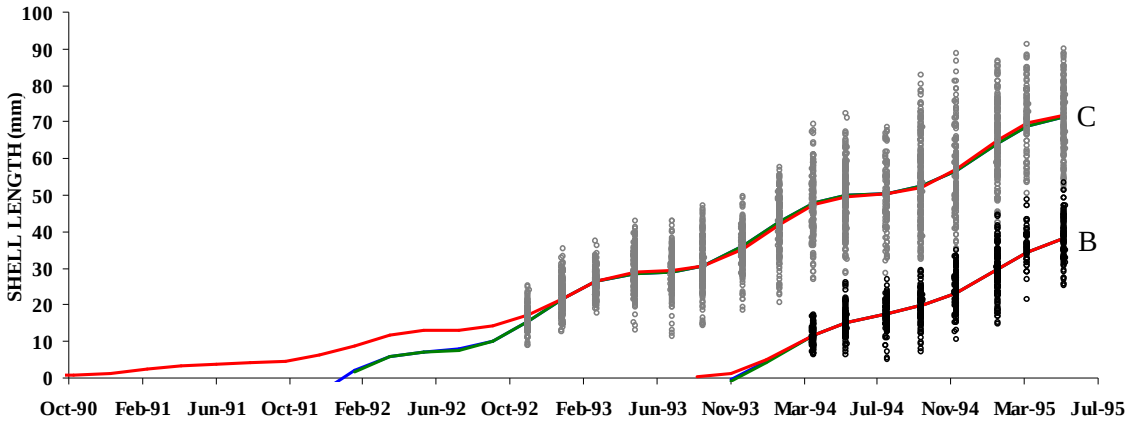

Figure 2.4. Comparison of growth of shell-length in a population of immature blacklip abalone (*Haliotis rubra*) at Hope Island and predicted growth trajectories between Nov 1992 – May 1995 based on modal analyses and including effects of seasonality on growth. Linear, von Bertalanffy and Gompertz models were fitted using maximum likelihood. Growth trajectories indicate that the linear, von Bertalanffy and Gompertz models are not visually discernible in cohort B while the Gompertz (red line) exhibits its sigmoidal nature and tails away in cohort C.

Table 2.3. Comparing the fits of three growth models (non-seasonal and seasonal) to growth in juvenile blacklip abalone (*Haliotis rubra*) from Hope Island. Quality of fit was assessed using log-likelihood values, likelihood ratio tests, AIC values and Akaike weights (w_i). In cohort B the linear von Bertalanffy and Gompertz models are equally supported by the data. The number of parameters for each model is shown in parentheses and includes the error term ε. The addition of more parameters (von Bertalanffy or Gompertz) does not significantly improve the fit upon the simpler linear model. For cohort C the Gompertz model was a significant improvement upon the linear and von Bertalanffy models. The addition of a term for seasonality significantly improved the fit. No constraints were placed on any parameters. The likelihood ratio test determines whether a fit is statistically different to the best (lowest AIC) model (p=0.05). -veLL is the negative log-likelihood, AIC is the Akaike Information Criterion, -veLL diff is the difference in negative log-likelihood between each model and the best model, Δ AIC is the change or difference in AIC, and w_i is the relative Akaike weights.

		non-seasonal			seasonal		
		linear	VB	Gz	linear	VB	Gz
		(3)	(4)	(5)	(6)	(7)	(8)
cohort B	-veLL	2798	2798	2765	2754	2754	2754
	AIC	5602	5604	5540	5520	5522	5524
	-veLL diff	33	33			0	0
	ratio test	Signif	Signif	best	best	Not Signif	Not Signif
	Δ AIC	62	64	0	0	2	4
	wi	0.00	0.00	1	0.67	0.24	0.09
cohort C	-veLL	11197	11200	11176	11075	11075	11066
	AIC	22400	22408	22362	22162	22164	22148
	-veLL diff	21	24		9	9	
	ratio test	Signif	Signif	best	Signif	Signif	best
	Δ AIC	38	46	0	14	16	0
	wi	0.00	0.00	1	0.00	0.00	1

As outlined in the Methods (section 2.3.3), the selection of the seasonal growth models was also subject to biological criteria. Within the first year of the juvenile phase, estimates of growth rate of the two cohorts varied between growth models. For the seasonal-linear model both cohorts B and C grew at an average of 60 μm/d. Growth in the first year of

the juvenile phase for the seasonal-von Bertalanffy differed slightly, being 58 and 67 μm/d for cohorts B and C respectively (CV = 9.2%). For the seasonal-Gompertz model, growth rates in the first year were notably more variable (CV = 88%) between cohorts, at 107 μm/d and 24 μm/d for cohort B and C respectively. The L_∞ parameter estimates were not always biologically plausible, being too large for the seasonal-von Bertalanffy (cohort B = 2265mm, cohort C = 2567mm) and too small for the seasonal-Gompertz (cohort B = 40mm, cohort C = 153 mm) (Table 2.2).

The selection of the statistically optimum growth model may have been partly affected by inconsistencies in the data given that the two cohorts from the same population were not equally represented in the data. In cohort C, the sample size was 3328 and the size range was 16 - 71 mm and the seasonal-Gompertz was selected as the best statistical model. In cohort B the sample size and size range was lower (n = 921 and 12 - 38 mm, respectively) and the seasonal-linear was best. The ambiguity in model selection and the corresponding variability in parameter estimates may have been influenced by spurious fits to sampling error in the data which may subsequently skew inferences about variability in growth. Sampling error could have influenced which model performed best statistically. When seasonality was included, the Gompertz model was more sensitive to sampling error in the data, because parameter estimates varied between two cohorts, compared with the linear and von Bertalanffy model. The greater consistency in growth rates between cohorts for the seasonal-linear and seasonal-von Bertalanffy models suggest that these models are less affected by inconsistencies in data than the seasonal-Gompertz model. Nevertheless all seasonal models demonstrate that growth is fastest (3.75 mm month-1) during the warmer months of September - March; and slowest (0.3 mm month-1) during the colder months of March – August.

2.4.4 Residual deviance

A post hoc analysis using non-parametric bootstrapping identified those modal groups that contributed to differences in statistical fit between the three seasonal growth models (Table 2.4). For cohort B, which extended over 15 months, the residual deviance within modal groups did not exceed 0.4%. The highest total residual deviance between any two models occurred between the linear and the Gompertz with a total residual deviance of 1.2% (Table 2.4). For cohort C, which extended over 31 months, the residual deviance within modal groups was as high as 11.7%. The greatest difference occurred between the Gompertz and the von Bertalanffy, although the residual deviance between the Gompertz and linear models was similarly high (11.4%). This high residual deviance was specific to the first modal group (sample of November 1992) which contributed 45% of the total residual deviance for the full time series (Table 2.4). For the remaining modal groups, i.e. the last 15 of the 16 modal groups, the linear and von Bertalanffy models were similar to the Gompertz model having a maximum residual deviance in any single modal group of only 2.3%. The results of 500 bootstrapped confidence intervals indicate that modal groups with relatively high deviance are a possible source of idiosyncrasies in the data and may contribute to differences in statistical fit between the three growth models when seasonality is included.

Table 2.4. Percentage residual deviance for each pair-wise comparison of three seasonal growth models for cohorts B and C. VB = von Bertalanffy; Gz = Gompertz.

modal	cohort B			cohort C		
group	linear vs VB	linear vs Gz	VB vs Gz	linear vs VB	linear vs Gz	VB vs Gz
Nov-92				0.27	11.40	11.70
Jan-93				0.16	0.87	0.71
Mar-93				0.16	0.41	0.57
May-93				0.03	0.64	0.68
Jul-93				0.19	0.50	0.70
Sep-93				0.18	0.88	0.70
Nov-93				0.01	2.27	2.25
Jan-94				0.11	1.84	1.95
Mar-94	0.30	0.40	0.11	0.13	1.02	1.14
May-94	0.04	0.24	0.20	0.08	0.67	0.75
Jul-94	0.15	0.14	0.29	0.03	0.63	0.60
Sep-94	0.02	0.23	0.25	0.10	0.19	0.09
Nov-94	0.08	0.03	0.05	0.11	0.72	0.83
Jan-95	0.04	0.01	0.03	0.06	1.36	1.42
Mar-95	0.01	0.06	0.04	0.04	1.09	1.13
May-95	0.02	0.08	0.06	0.04	0.44	0.48
TOTAL	0.66	1.20	1.03	1.69	24.9	25.7

2.5 Discussion

2.5.1 Modal progression analysis

Given distinct modal groups and year round sampling, it was straightforward to follow the progression of modal groups within a cohort. As blacklip abalone grew larger, the variance increased and the modal definition decreased. This was expected, as it is indicative of natural variability in growth. As the variance in growth increased with size of individuals, a larger sample size was required to clearly define each mode. The poor definition in some larger modal groups may partly be an artifact of inadequate sampling of the larger animals since collections were generally limited to 80mm and ~300 individuals. The larger and broader modal groups may be made up of both fast and slowly growing individuals, possibly as a result of density-dependent effects (Huchette *et al.* 2003) and leading to the presence of multiple minor modes. Larval settlement studies at George III Rock (19 km south of Hope Island (Figure 2.1), demonstrate that very high densities (1,916 m^{-2} in August-November 1991) of settled post larvae can occur (Nash *et al.* 1995), so density-dependent effects might be expected.

2.5.2 Statistical fit of the growth models

According to the *AIC* values the Gompertz model was the best fitting non-seasonal growth model for both cohorts B and C (Table 2.3), however seasonality improved the fit of all models and consequently the seasonal-Gompertz was the best fitting model only for cohort C. The seasonal-linear model best described cohort B, but was not significantly different from the statistical fit of the other models (Table 2.3). For cohort C the source of

the deviance between models was mainly attributable to the November 1992 modal group, which was not fitted as well by the seasonal-von Bertalanffy or linear models and as a result the seasonal-Gompertz model provided the best fit. The statistically optimum seasonal model differed between the two cohorts and overall model selection remains somewhat ambiguous (Table 2.5), despite the availability of a comprehensive dataset on juvenile size classes.

The von Bertalanffy and Gompertz curves were only able to fit the data with parameter estimates that, when extrapolated, were implausible for blacklip abalone populations. The implausibly high L_∞ values for the von Bertalanffy and the implausibly low L_∞ values for the Gompertz models were obtained because they needed to approximate linearity in order to fit the data. Therefore given the approximate linear-like growth indicated by both the von Bertalanffy and Gompertz models, the season-linear model is selected as the optimal growth model describing growth of the population of juvenile blacklip abalone at Hope Island.

Table 2.5. Summary table assessing the performance of three growth models [von Bertalanffy (VB), Gompertz (Gz) and linear] against four statistical selection criteria and one biological criterion Results are for both the non-seasonal and seasonal growth models. n.a. = not applicable. Ticks (√) indicate best fitting model. Crosses (×) indicate parameter values with poor biological meaning.

		non-seasonal			seasonal		
cohort	criteria	linear	VB	Gz	linear	VB	Gz
B	1. best fit (LL)			√	√	√	√
	2. differs from best model	signif	signif	best	not signif	not signif	not signif
	3. lowest AIC			√	√		
	4. Akaike weights (w_i)	very unlikely	very unlikely	best	best	less support	very unlikely
	5. biologically plausible	√	√	×	√	√	×
C	1. best fit (LL)			√			√
	2. differs from best model	signif	signif	best	signif	signif	best
	3. lowest AIC			√			√
	4. Akaike weights (w_i)	very unlikely	very unlikely	best	very unlikely	very unlikely	best
	5. biologically plausible	√	√	×	√	√	×

2.5.3 Biological plausibility of growth models

The mixed and therefore ambivalent results of the statistical selection of the most appropriate growth model across the two cohorts made it difficult to confidently select any one of the three models (Table 2.5). When no single model is preferred across all cohorts on statistical grounds, a biological assessment of each model improved confidence in

model selection. A useful biological evaluation in this case was to compare growth rates estimates predicted by each growth model with published growth rate estimates reported from empirical observation in controlled and wild conditions. In Australia the growth rate of juvenile blacklip abalone under controlled conditions have been estimated in a number of studies. Tasmanian trials report that "growth was consistently about 60 micron per day for the first 500 days" (Cropp 1989, p. 12) in juveniles. In a separate study, large post larvae abalone at 2 mm shell length (i.e. at the commencement of the juvenile phase), had growth rates between 40.3 and 60.32μm/d (Daume 2003 p51, Table 15). The consistency in growth rates of 2 mm abalone reported in these separate studies is noteworthy. Overall, the growth rates estimated in the current study using both the non-seasonal and seasonal linear and von Bertalanffy models in the first year of juvenile growth ranged between 56.9 - 67 $\mu m.d^{-1}$, and these values were clearly consistent with growth rates measured in controlled laboratory studies by Cropp (1989) and Daume (2003).

In contrast, the Gompertz model yielded growth rate estimates of 17, 20, 24, and 107 $\mu m.d^{-1}$, across both cohorts and with and without the seasonality term. None of the predicted estimates of the Gompertz are consistent with the published observations of growth in controlled environment for 2 mm abalone. Therefore, the seasonal-Gompertz model, while it gave the best fit at least for one cohort, is not considered in this instance to correctly describe the biological growth rate of juvenile blacklip abalone. The seasonal-von Bertalanffy and seasonal-linear models were more biologically plausible in their estimates of growth rate for abalone of ~2 mm shell length. Of the two, the linear model was also the more optimal than the seasonal-von Bertalanffy in terms of statistical fit. The linear model that includes seasonality is therefore considered the most biologically plausible model of growth in juvenile blacklip abalone at Hope Island, Tasmania. Using the seasonal-linear

model, annual growth increments ranged between 20.8 and 21.9 mm/y for the population of juveniles (10 – 75 mm) at Hope Island. This result is also consistent with published results from a study on a wild population of juvenile blacklip abalone only 1 km from Hope Island where growth rates of juveniles were 19.1 mm/y (Prince *et al.* 1988a).

There is confusion over the plausibility of the lag phase in growth as depicted by a sigmoidal growth model such as the Gompertz. Studies under controlled conditions indicate a lag phase in growth in the post larval phase <2 mm. However, this does not concern the present study since the post larval phase precedes the juvenile phase and there is no evidence that the lag phase continues into the size range of juveniles examined here (10 - 75mm). Therefore, the distinction between the post larval phase and beginning of the juvenile phase (which commences at ~ 2 mm shell length; Cropp 1989) is important. Results from controlled experiments indicate that a sigmoidal pattern of growth may be associated only with the post-larval size range between 0-2 mm (Daume 2003). The growth rate (18 $\mu m.d^{-1}$) of small (shell length < 540 μm) post larval abalone (Nash *et al.* 1995), is clearly not comparable with that of juveniles >2 mm shell length.

2.5.4 Differences between cohorts

The expectation was that the three growth curves should not differ appreciably in their estimates of growth rates between the two cohorts because the two cohorts were from the same geographic stock and only two years apart. However the Gompertz model resulted in large differences in growth rate estimates between cohorts B and C whereas the linear and von Bertalanffy resulted in consistent growth rates, as expected, for both non-seasonal and

seasonal versions. Variability in parameter estimates between non-seasonal and seasonal models was also greater in the Gompertz than in the linear and von Bertalanffy.

It might be argued that the Gompertz is sensitive to real, but subtle, differences in the growth of the two cohorts which may confer an advantage for detecting growth related differences between samples. However it is important to also consider if these differences are real or artificial and associated with inconsistencies in sampling (i.e. sampling error) (Francis & Shotton 1997). The data between the two cohorts differed in various aspects including the length of time series, sample size and the size classes represented. In one cohort of juvenile abalone, the sample size was 3328 and the size range was 16 - 71 mm and the seasonal-Gompertz was selected as the best statistical model. In the other cohort the sample size and size range was lower (n=921 and 12- 38 mm, respectively) and the seasonal-linear was best. The unexpected differences in growth rate between cohorts B and C predicted by the Gompertz model may probably reflect the influence of the extra parameter of the Gompertz model, relative to the von Bertalanffy, which confers more flexibility to the Gompertz and greater sensitivity to small differences in data quantity and quality.

The ambiguity in model selection and the corresponding variability in parameter estimates may have been influenced by spurious fits to sampling error which may subsequently skew inferences about variability in growth. Further work is therefore required to explore the influence of sampling error on the outcomes of model selection based on statistical model fitting procedures. This is particularly important given that growth studies rely upon parameter values to characterize differences between populations across geographic scales (Worthington *et al.* 1995). Unless the differences between growth rates are real, variability in parameter values and hence differences between populations that are due to sampling

error are not helpful in quantifying differences in growth characteristics between populations. The seasonal-von Bertalanffy and seasonal-linear models were more consistent in their estimation of growth rate between cohorts than the Gompertz and therefore these models are considered to be more reliable.

2.6 Conclusion

The major finding was that growth is seasonal in juvenile abalone at Hope Island. Juvenile abalone grew faster during the warmer months of November – March where mean monthly temperatures ranged between 11- 16 °C. This is the first study to demonstrate the effect of temperature on wild populations of juveniles for any abalone species.

A comparison of growth rates estimated from modal progression in a wild population and from controlled experiments clearly demonstrated that growth rates can be derived via the analysis of modes progressing over time. The growth rates obtained from the best fitting Gompertz model consistently differed to the growth rates obtained from the von Bertalanffy and linear model. However, results obtained from the Gompertz model could not be validated with any published literature whereas results obtained from the von Bertalanffy and the linear models were more readily validated. It is clear from this result that the best statistical model may not always be biologically plausible.

In this study the growth of juvenile blacklip abalone (10 – 75 mm) is best described by a linear model. The annual growth increment of cohort B was approximately 21.9 mm in shell length (60.8 $\mu m.d^{-1}$) while for cohort C it was 20.8 mm in shell length (56.9 $\mu m.d^{-1}$).

CHAPTER 3

Growth models for fisheries: the effect of unbalanced sampling error on model selection, parameter estimation and biological predictions

3.1 Abstract

Field studies on population mean somatic growth usually yield unbalanced data consisting of various forms of sampling error. These data are then analysed using growth models that are selected based on their statistical fit to the data. However the selection of the best statistical model may be a result of fits to data that are unrepresentative of the population, due to sampling error, and this may mislead biological predictions. In this context there has been little evaluation of the robustness of growth models to sampling error. A Monte Carlo simulation study was performed to test the robustness of four growth models *viz.* the von Bertalanffy, Gompertz, inverse logistic and Schnute models, using tag-recapture data of abalone populations as a case study. Cross model validation was performed on simulated unbalanced data which consisted of eight typical scenarios of sampling error in tag-recapture data. The robustness of each growth model was evaluated according to a three stage approach: (1) model fitting criteria, (2) biological validity and (3) the risk of making false biological predictions. Results from statistical criteria indicate that an inadequate size range in the data was the most likely form of sampling error that led to an incorrect model being selected as the 'best' statistical model. Results from biological criteria indicate that the incorrect von Bertalanffy and Gompertz models were more biologically inaccurate,

compared with the incorrect inverse logistic model. The inverse logistic model produced absurd parameter estimates, but generated more accurate biological predictions. Results from the risk assessment indicate that unknowingly selecting an incorrect growth model can potentially have far more serious implications to fishery stock assessments than is currently appreciated. However, the risk of making false biological implications are minimised if the 'incorrect' inverse logistic growth model is unknowingly selected over the 'incorrect' von Bertalanffy or Gompertz models. Given widespread use of the von Bertalanffy and Gompertz models, selected solely on the basis of goodness of fit tests, it is clear that greater care and scrutiny is warranted in the selection of growth models in the presence of sampling error.

3.2 Introduction

Mean population somatic growth is one of three population parameters, along with recruitment and mortality, used in the assessment and consequent management of fish stocks (Hilborn & Walters 1992). For example, growth models, combined with mortality and recruitment, are used for modelling stock dynamics and predicting sustainable harvests (Walters & Martell 2004; Rogers-Bennett *et al.* 2007). It follows that the selection of an appropriate growth model is fundamental to robust fisheries management. In Tasmania, where the blacklip abalone fishery (*H. rubra*) accounts for ~30% of the global abalone wild catch (FAO 2006), precise and unbiased descriptions of growth are critical to effective management (Haddon *et al.* 2008).

The Tasmanian abalone fishery consists of hundreds of spatially explicit stocks which are ecologically dissimilar at fine spatial scales (tens or hundreds of metres) (Prince *et al.* 1987; Nash 1992). Ideally, populations would be sampled consistently but rarely is this possible when there are numerous populations to sample. In the case of tag-recapture data, there is usually an inconsistent number of observations per size class between samples and this gives rise to unbalanced sampling error in the data. This presents a particular problem where inter-population comparisons are important to the scientific understanding and management of the Tasmanian abalone fishery. Lapses in sampling consistency may obscure biological findings and thwart comparisons between populations. It is therefore important to consider the effect of unbalanced sampling error data (including measurement error) on model uncertainty (Francis & Shotton 1997).

Uncertainty in growth model selection is caused, at least in part, from lack of data on growth of juveniles, which is the size range with the greatest discriminating power between candidate models (Urban 2002; Rogers-Bennett *et al.* 2007). Unfortunately, for many species, including abalone, tagging smaller juveniles (< 50 mm in the case of *H. rubra*) is not a viable option because the process of tagging may itself affect the growth of juveniles (Day & Fleming 1992; Wang 1998). It is clearly important to specify minimum data requirements that lead to management decisions (Francis & Shotton 1997; Punt 2006), and therefore it is important to determine whether a paucity of data on juvenile size classes affects the robustness of predictive methods.

Another problem of model uncertainty arises partly from a thin choice in candidate models (Katsanevakis & Maravelias 2008). This may lead to "retrospective regret" in the selected model because a larger range of plausible models was not considered (Hamilton *et al.* 2007; Katsanevakis & Maravelias 2008). With the exception of one study (Rogers-Bennett *et al.*

2007), the selection of growth models for abalone has generally been limited to two models, namely the von Bertalanffy and the Gompertz models (Day & Fleming 1992). Historically, there has been strong reliance on the von Bertalanffy model and if the von Bertalanffy was not the best fitting model, then the Gompertz was selected, effectively by default. However other alternative models are available. The inverse logistic model was recently developed to describe the growth of blacklip abalone populations in Tasmania (Haddon *et al.* 2008). The Schnute model (Schnute 1981; Francis 1995) is another alternative that has been used for its flexibility and offers the prospect of accurately describing different growth trajectories (Worthington *et al.* 1995), however it still assumes a growth trajectory similar to either the von Bertalanffy or Gompertz models.

Aspects of sampling error that can affect model reliability include sample size, the size range of observations (Rogers-Bennett *et al.* 2007), and the relative density of samples within a size range (Wang 1998). Typical tag-recapture data consists of relatively fewer small and large specimens and more specimens in the mid-size range (Wang *et al.* 1995). In addition, observations of apparent negative growth increments are common in tagging studies despite being biologically absurd. It is unknown whether growth models are robust to these kinds of data characteristics, and so the possibility and consequences of selecting an incorrect model must be considered.

Selecting an incorrect model can lead to misleading outcomes and invalid conclusions (Cox 2002). In practice, the true growth trajectory is usually not known. Nonetheless, key decisions in fisheries management must be made, usually on an annual basis, and rely on information from models. One approach towards evaluating the robustness of growth models to unbalanced sampling error is to use simulation testing based on Monte Carlo techniques. In the present work, the simulation framework consists of an operating model

which represents biological reality, and which is used to generate simulated data consisting of typical characteristics of sampling error. These simulated data are used to evaluate the robustness of the growth models to unbalanced sampling error. Growth model robustness is evaluated according to three criteria: (1) statistical criteria, (2) biological criteria and (3) the risk of making false biological predictions. Blacklip abalone is used as a case study, and the robustness of four growth models are tested against eight realistic scenarios of sampling error. The eight scenarios combined address the unbalance in the data. The null hypothesis tested is that there is no difference between the mathematical form of the operating model and the best fitting assessment model for any given scenario of sampling error. Accompanying this is an identification of the relative contributions that different forms of sampling error have on the selection of the growth models considered.

3.3 Methods

3.3.1 Growth models

Assessments were made of four deterministic candidate growth models used to describe growth in abalone, *viz.* the Von Bertalanffy, Gompertz, inverse logistic and Schnute models. The candidate growth models include a reparameterised analogue of the von Bertalanffy model for tag-recapture data used for estimating expected length increments following specific time increments (Fabens 1965; Haddon 2001).

The standard VB model is given as

$$\Delta\hat{L} = \left(L_\infty - L_i\right)\left(1 - e^{-K\Delta t}\right) + \varepsilon \tag{3.1}$$

The reparameterised Gompertz (Troynikov *et al.* 1998) for estimating length increments following time increments is

$$\Delta\hat{L} = L_\infty \left(\frac{L_i}{L_\infty}\right)^{\exp(-g\Delta t)} - L_i + \varepsilon \tag{3.2}$$

The inverse logistic model (Haddon *et al.* 2008) is

$$\Delta\hat{L} = \frac{Max\Delta L}{1 + e^{Ln(19)\frac{\left(L_i - L_{50}^m\right)}{\left(L_{95}^m - L_{50}^m\right)}}} + \varepsilon \tag{3.3}$$

A length-based analogue of the Schnute model (Francis 1995) suitable to use with length increment data (Worthington *et al.* 1995) is given following (and for simplicity this will be referred to as the Schnute model):

$$\Delta\hat{L} = \left[L_i^b e^{-a\Delta t} + c\left(1 - e^{-a\Delta t}\right)\right]^{1/b} - L_i + \varepsilon \quad \text{if } a \neq 0,\ b \neq 0 \tag{3.4}$$

where $\Delta\hat{L}$ is the expected length increment, L_∞ is the shell size where the mean length increment is zero (VB and Gz), L_i is the initial length when first tagged and released, K is the rate of change in length increment with increasing shell size, g is the exponential decrease and is > 0, Δt is the time at liberty (as a fraction of a year), $Max\Delta L$ is the maximum growth increment, L_{50}^m = initial length that produces a growth increment of $0.5Max\Delta L$, L_{95}^m is the initial length that produces a growth increment of $0.05Max\Delta L$, b describes curvature in the Schnute Model, a "has no simple biological meaning" (Francis

1995) but scales the rate at which the curve approaches an asymptote, if there is one, C is the growth curve shape parameter and ε is the independent, additive, normal random residual

3.3.2 The simulation testing framework

The simulation testing framework consisted of a training dataset, testing datasets (simulated), operating models, and assessment models (Butterworth *et al.* 1997; Smith *et al.* 1999; Sainsbury *et al.* 2000). The parameters for the operating models were derived by fitting the models to a training dataset. Simulation testing involved systematically selecting a particular growth model as the operating model and then generating simulated testing datasets using Monte Carlo methods. The four assessment growth models were fitted, in turn, to the simulated testing datasets. The operating models represented the underlying biological reality, which defined the correct model, and the simulated testing datasets, generated from the operating models, represented a population with known growth parameters. It was assumed that the simulated growth data incorporated both stochastic process and observation uncertainty.

3.3.3 Training dataset

To select realistic parameters for each operating model, a training dataset of tag-recapture data were selected from a field survey at Black Island, Tasmania, Australia (42.86°S, 148.00°E; Figure 3.1). The selection of the training dataset was independent of the growth models and was representative of growth increments for blacklip abalone in some populations of Tasmania's blacklip abalone fishery. This dataset was made up of yearly length increments from juvenile and mature abalone whose size at tagging ranged between 57-171 mm. Growth increments that were more negative than -3 mm were removed (Figure 3.1). Note that -3 mm was selected because it was assumed to allow for measurement error applicable to all size classes that is not necessarily related to shell chipping; this is common practice in treating growth increment data in abalone (see Naylor *et al.* 2003). The final sample consisted of 116 observations, which is a typical sample size of tag-recapture data for populations around Tasmania. Moreover, these data were sufficient to produce reliable growth model parameters.

3.3.4 Operating model and starting parameters

Operating model parameters were obtained by fitting three of the growth models (von Bertalanffy, Gompertz, inverse logistic) to the training data. Despite its flexible nature, the Schnute encompassed the Von Bertalanffy and Gompertz growth forms, and others, as special cases. The Schnute model was not suitable as an operating model because it does not have a unique form. Only the von Bertalanffy, Gompertz, and inverse logistic were

used as operating models, but all four, including the Schnute, were used as assessment models.

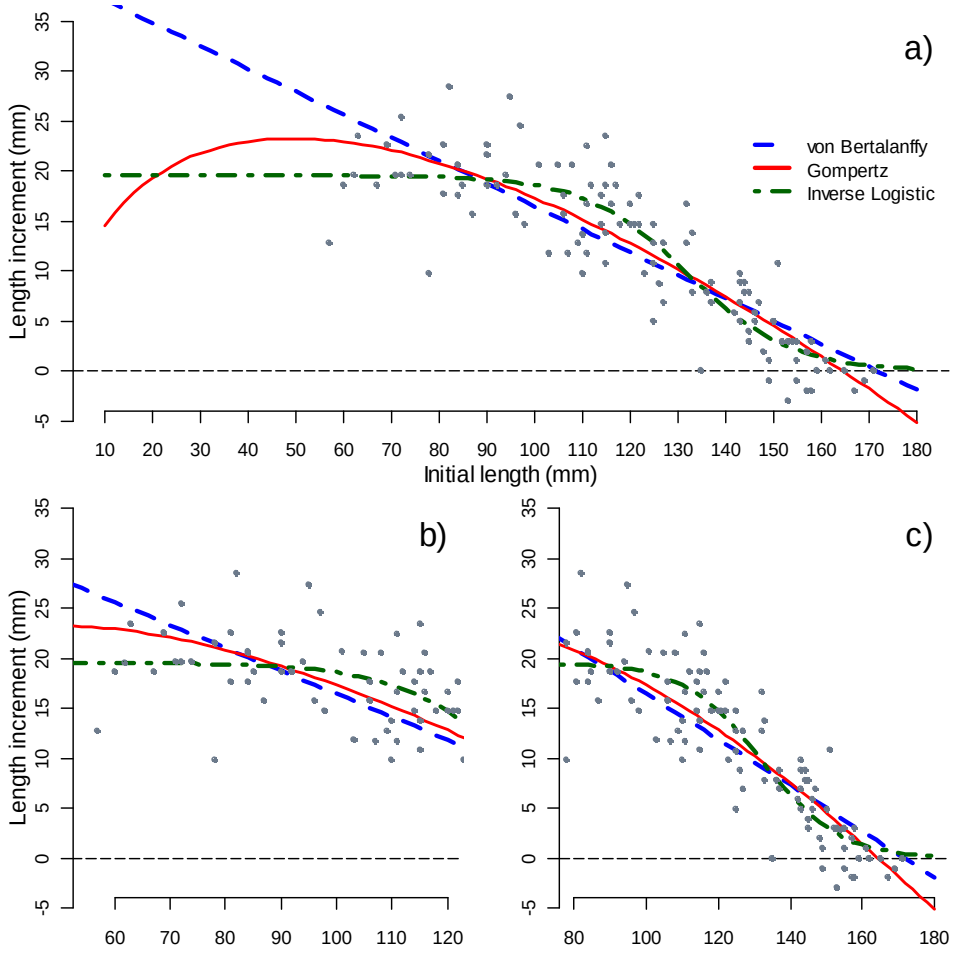

Figure 3.1: Shown are the von Bertalanffy, Gompertz, and inverse logistic growth models fitted to tag-recapture data that was used as the training dataset. The data is from Black Island (42.9687°S, 145.4924°E) and was the best example of tag recaptur e data in terms of sample size and initial size range (Fig. a). In this data set the size region mostly underrepresented is in the juvenile size range i.e. where initial length (L_t) is <60mm. The lower panels (Fig. b and c) illustrate the relationship of the models relative to two different size ranges. Fig b) indicates the relationship of the model with respect to smaller abalone (L_t 55 – 120 mm) where most of the discriminating power takes place, (although the high degree of scatter in this region may reduce the discriminating power between models). Fig. c) illustrates the relationship of the models with respect to larger abalone (L_t 80 – 170 mm) which is adequately represented in typical tag-recapture data. The Schnute model is not represented here since it assumes either a Gompertz or von Bertalanffy growth trajectory.

3.3.5 Simulating testing datasets

The Monte Carlo involved simulating testing datasets from each operating model. Normal random residuals were added to the predicted length increments produced by each operating model using a sample of abalone of initial lengths selected randomly from the chosen size range. For each data scenario, 500 testing datasets were generated by each of the three operating models. A normal distribution with a constant variance was used as the source of residuals added to each simulated dataset, with the same variance used for each operating model. This gave all three operating models equal process and observation errors (Zhou 2007). The alternative of using a non-constant variance was avoided because that would have led to the four growth model forms receiving unequal treatment with respect to residuals. Examination of growth data from nine sites collected around Tasmania (unpublished data) revealed a range in standard deviations of 3.45 – 6.02. A standard deviation of 3.69 was selected for all operating models in the simulations because this was the mean standard deviation of the all three models when fitted to the training dataset when obtaining starting parameters.

3.3.6 Scenarios of unbalanced sampling error

Two categories of test datasets were considered, namely ideal datasets and non-ideal datasets which consisted of eight scenarios of sampling error. The properties of the ideal datasets were determined from virtual ideal properties of optimal field data (Table 3.1). These included a large sample size (N=540) and an initial size range that extended over both the juvenile and adult size ranges (50-180 mm).

Table 3.1: Eight scenarios (A-H) of censorship in the data that reflect characteristics of sampling error typical of abalone tag recapture surveys in Tasmania. The data were censored according to three aspects that are typically encountered during abalone tag-recapture surveys in Tasmania; sampling size, sampling density and the initial length sizes tagged. For sampling density, 'low' correspond to the size range that is in the lower 25% of the initial length range, 'mid' = 25-75% of initial length range, and large = >75% initial length range

	scenario	sample size (N)	sampling density (P) low-mid-large	length range (mm) (R)	increments
ideal data		540	0.33-0.33-0.33	50-180	all negative increments
		540	0.33-0.33-0.34	50-181	beyond -3mm
		540	0.33-0.33-0.35	50-182	positive increments only
sampling scenarios	A	100	0.1-0.3-0.6	55-120	beyond -3mm
	B	100	0.1-0.3-0.6	80-170	beyond -3mm
	C	100	0.1-0.7-0.2	55-120	beyond -3mm
	D	100	0.1-0.7-0.2	80-170	beyond -3mm
	E	500	0.1-0.3-0.6	55-120	beyond -3mm
	F	500	0.1-0.3-0.6	80-170	beyond -3mm
	G	500	0.1-0.7-0.2	55-120	beyond -3mm
	H	500	0.1-0.7-0.2	80-170	beyond -3mm

The ideal dataset was used in two ways: firstly, to act as a control to test the capacity of the assessment models to recover the correct underlying growth model when available data are

ideal, and secondly, to examine the effect of negative growth increments on parameter estimation. Negative increments are commonplace in tag-recapture data (Quinn II & Deriso 1999) and reflect measurement error or, in the case of abalone, occasional shell damage (Francis & Shotton 1997). Adding normal random deviates to simulated growth increment data can also result in negative increments, especially for the larger initial lengths. Using the ideal dataset, the effect on parameter estimation of measurement errors arising from negative increments was examined in three ways, 1) by removing all negative increments, 2) by removing data with increments that are more negative than -3 mm, and 3) no removal.

The characteristics of the sampling error were determined by considering typical scenarios of sampling error exhibited in 20 populations around Tasmania. Characteristics of sampling error consisted of three main categories, *viz.* 1) inadequate sample size, 2) small size range consisting of small or large size individuals, and/or 3) relative density of observations taken within size classes. There were two levels within each of these three categories, which were considered in factorial combination to yield the eight realistic scenarios of sampling error. For sample size the two levels were N=100 and 500, encompassing the lower and upper limits of the 20 available empirical datasets (where N=100 - 250 is typical). For size range, observed size ranges indicate that the minimum initial lengths at release from 20 populations ranged from 47 – 82 mm (unpublished data). Thus, two different initial size ranges at tagging were used (55 – 120 mm, and 80 – 170 mm) to reflect a lack of large animals and small animals respectively. The 55 – 120 mm size range represents predominantly juvenile animals that are still growing (minimum change in length increment, ΔL, >10 mm) while the size range 80 – 170 mm includes both growing animals and animals with negligible growth (minimum $\Delta L=0$) which is more typical of real tag-

recapture data. For the relative density of observations, two different density ratios for mid- and large-sized animals (0.3 and 0.6; 0.7 and 0.2) were used, while there was a constant density of 0.1 for the smaller sized animals. Relative density is associated with the relative probability of recovering abalone of different size classes (Wang 1999). Growth increments more negative than -3 mm were omitted from all simulated datasets to reflect typical practice involving tag-recapture data (Haddon et al. 2008).

3.3.7 Fitting assessment models to data

With the exception of the ideal test datasets, all four candidate growth models were fitted to each of the 500 testing datasets simulated by the three operating models. The Schnute model was not fitted to the ideal testing dataset because it was not used as an operating model and therefore it had no utility as a possible control or in tests for effects of negative increments. To improve the efficiency of the fitting process, the parameters generated for the operating models (and the Schnute model) from the training data were used as the starting parameters when fitting to simulated testing data (Table 3.2). Each assessment model was fitted to each of the testing datasets using maximum likelihood methods. The model fitting criterion used was Akaike's Information Criteria (AIC), which is defined as $AIC = -\Sigma LL_m + 2K_m$, where K_m is the total number of parameters for model m (including σ_m^2, the standard deviation for model m), and $-\Sigma LL_m$ is given by

$$-\Sigma LL_m = -\sum_{Lt=1}^{n} Ln\left(\frac{1}{\sigma_m\sqrt{2\pi}}e^{-\left[\frac{\left(\Delta L_{Lt}-\Delta\hat{L}_{Lt}\right)^2}{2\sigma_m^2}\right]}\right) \tag{3.5}$$

ΔL_{Lt} is the observed length increment for each of the n initial lengths at tagging, Lt; and $\Delta\hat{L}_{Lt}$ is the expected length increment for initial length Lt. The negative log-likelihood for model m, $-\Sigma LL_m$, was minimised using the 'optim' function in R (R Development Core Team 2008). The standard deviation of the residuals was estimated and stored along with model parameter values and related model fits at each run. In each case, the assessment model that was mathematically related to the operating model was termed the 'correct' model while models that were unrelated to the operating model were termed the 'incorrect' models (Zhou 2007).

Table 3.2: Starting parameter values for the operating and assessment models used in tagging simulations. Starting parameters were obtained from a realistic data set of tag recapture data from a population of blacklip abalone in Tasmania. Three operating models were used; the von Bertalanffy, Gompertz, and inverse logistic. The values of the assessment model were the same as the starting values of the operating model. The Schnute model was used only as a assessment model to all three operating models. Two combinations of starting parameters were necessary for the Schnute assessment model: Gz-Schnute simulates a Gompertz model, while VB-Schnute simulates a von Bertalanffy model.

	parameters	starting values	
von Bertalanffy	L_{∞}	172	
	K	0.261	
	s	3.69	
Gompertz	L_{∞}	165	
	g	0.387	
	std. dev.	3.69	
inverse logistic	MaxΔL	20	
	L_{50}	132	
	L_{95}	166	
	std. dev.	3.69	
Schnute		Gz-Schnute	vB-Schnute
	b	0.002	0.854
	a	0.387	0.278
	c	1.012	80.7
	std. dev.	3.69	3.69

The assessment model with the smallest AIC was selected as the 'best', or statistically optimum model, regardless of whether it was a 'correct' or 'incorrect' model. The probability of selecting the best model was the proportion of the 500 simulations, for each of the eight scenarios of data quality, for which the correct model had a lower AIC than other assessment models (Table 3.3). If the three main assessment models, ignoring the Schnute, were to perform equally well under the eight data scenarios (Table 3.1) the expectation would be that the probability of the correct assessment model being selected as the statistically best model should be P=0.33. The Schnute model was omitted because it was found invariably to mimic either a von Bertalanffy or the Gompertz model. A

probability gradient between P=0.33 - 1.0 was used to evaluate the best assessment model where P<0.33 indicates ambiguity and $P \geq 0.95$ indicates unambiguous results.

Table 3.3. A summary of the probabilities of the assessment model being selected as the best statistical model, as determined by the AIC, when fitted to simulated data from the four operating models. All four assessment models were fitted to each operating model for both ideal and the eight data scenarios (A-H). The ideal data is included as a positive control for the simulation against which the eight data scenarios are compared. A probability of 0.33 meant that the correct assessment model had an equal chance of being selected as do the other two assessment models (Schnute excluded). A probability greater than 0.95 meant that the correct assessment model was unambiguously the best statistical model. For each operating model the 'correct' assessment models is identified in bold. The probability of type I error is shown for each scenario under each operating model. For a description of scenarios A-H refer to Table 3.1.

		operating model	von Bertalanffy				Type I	Gompertz				Type I	Inverse Logistic				Type I
		assessment model	***VB***	*Gz*	*IL*	*Sch*	error	*VB*	***Gz***	*IL*	*Sch*	error	*VB*	*Gz*	***IL***	*Sch*	error
ideal data		all negative increments	**1**	0	0	0	0.00	0	**1**	0	0	0.00	0	0	**1**	0	0.00
	N=540	beyond -3mm	**0.9**	0	0	0	0.14	0	**1**	0	0	0.00	0	0	**1**	0	0.00
		positive increments (>0mm)	**0.1**	0.0	0.9	0	0.89	0	**1**	0	0	0.00	0	0	**1**	0	0.00
Censored data		A	**0.65**	0.28	0.07	0	0.35	0.25	**0.69**	0.06	0	0.31	0.07	0.56	**0.37**	0	0.63
	N=100	B	**0.59**	0.09	0.32	0	0.41	0.41	**0.35**	0.24	0	0.65	0.02	0.01	**0.97**	0	0.03
		C	**0.69**	0.26	0.05	0	0.31	0.28	**0.69**	0.03	0	0.31	0.15	0.68	**0.17**	0	0.83
		D	**0.62**	0.17	0.21	0	0.38	0.35	**0.47**	0.18	0	0.53	0.01	0.03	**0.96**	0	0.04
		E	**0.80**	0.07	0.13	0	0.20	0.11	**0.82**	0.07	0	0.18	0.00	0.13	**0.87**	0	0.13
	N=500	F	**0.67**	0.01	0.31	0	0.33	0.55	**0.25**	0.20	0	0.75	0.00	0.00	**1.00**	0	0.00
		G	**0.82**	0.06	0.12	0	0.18	0.08	**0.85**	0.07	0	0.15	0.01	0.22	**0.77**	0	0.23
		H	**0.72**	0.00	0.28	0	0.28	0.40	**0.43**	0.17	0	0.57	0.00	0.00	**1.00**	0	0.00

The effect of negative increments on the consistency of parameter estimates across each of the 500 simulated datasets was examined by plotting pairs of parameters from the sets generated by each assessment model. If the available data adequately represents the growth trajectory for a given assessment model then the expectation is that estimated parameters values of the assessment model are distributed approximately normally about the true value (the known parameter values from the operating model) and will be centered around this parameter value (Hilborn & Mangel 1997). If the available data are not adequate for a given assessment model then the expectation is that the scatter of the assessment model parameter estimates around the known 'true' parameters, from the operating model, would be skewed or otherwise distorted. A robust model is considered to be the assessment model with the narrowest coefficient of variation (CV) for its parameter estimates, and more accurately recovers the parameters of the related operating model.

3.3.8 Assessing robustness using biological criteria

The robustness of the growth models were also assessed using biological criteria. A biological criterion used in other studies of abalone growth is the time taken for abalone to recruit to the fishery (Rogers-Bennett *et al.* 2007). In Tasmania, abalone recruit to the fishery once they reach a Legal Minimum shell Length (LML). The LML differs across regions around Tasmania and the appropriate LML at Black Island (the site of the training dataset) is 140 mm. Since the juvenile stage for abalone is considered to commence at the formation of the first respiratory pore at about 2 mm shell length (Cropp, 1989), the time-to-fishery is determined by the number of years taken for an abalone to grow from 2 - 140

mm. Given that time-to-fishery is a useful biological criterion for model selection, time-to-fishery estimates for the assessment models were compared to the equivalent estimates from the operating model (which represents the true time-to-fishery estimate).

The Von Bertalanffy and Gompertz models can be rearranged with respect to Δt to estimate the time taken (in years) for abalone to recruit to the fishery:

Time-to-fishery for Von Bertalanffy:

$$\Delta t = \frac{-\ln\left(1-\left(\Delta L/\left(L_\infty - L_t\right)\right)\right)}{k} \tag{3.6}$$

Time-to-fishery for Gompertz:

$$\Delta t = \ln\left(\ln\frac{\Delta L + L_t}{L_\infty} \times \left(\ln\frac{L_t}{L_\infty}\right)^{-1}\right) \times g^{-1} \tag{3.7}$$

Time-to-fishery for inverse logistic:

For the inverse logistic, estimating time-to-fishery is more involved. Growth has to be simulated iteratively to generate length-at-age in estimating the time taken to reach the LML (i.e. to enter the fishery). To estimate the time taken to reach the LML, the process starts with L_t = 2.0 and iterated with time steps of one week until $L_{t+1} \geq 140$ mm using:

$$L_{t+1} = Lt + \frac{Max\Delta L\left(\Delta t + C\sin\left(2\pi\left(t_R - p\right)\right) - C\sin\left(2\pi\left(t_T - p\right)\right)\right)}{1 + e^{Ln(19)\left(\frac{L_t - L_{50}}{L_{95} - L_{50}}\right)}} \tag{3.8}$$

where C = amplitude of the seasonality effect for ΔL; t_R and t_T = dates of recapture and tagging respectively (as fractions of a year, e.g. June 30th = 0.5; $t_R = t_T + \Delta t$), and p = the date of maximum growth rate (as a fraction of a year).

Time-to-fishery for Schnute:

$$\Delta t = -\ln \frac{\left(\Delta L + L_t\right)^{b} - c}{L_t^{\,b} - c} \times a^{-1} \tag{3.9}$$

The growth model equations were re-arranged according to equations (3.6) to (3.8) to obtain time-to-fishery estimates (Δt) for each of the 500 simulations under eight data scenarios. The parameters returned by the 500 simulations were substituted into these equations to obtain time-to-fishery estimates for each of the 500 simulations of the eight data scenarios. Fixed estimates of L_t and ΔL were used with L_t = 2 mm, and ΔL 138 mm (i.e. 140-2 mm, being the length increment between the commencement of the juvenile phase and the size when individuals enter the fishery). A robust assessment model is considered to be one where the biological estimates (e.g. time-to-fishery estimates) of the assessment model closely resemble the estimates of the related operating model across all scenarios of sampling error.

3.3.9 Risk assessment

To quantify the possible consequence of unknowingly selecting the incorrect model a simple risk assessment was conducted. This involved two components: 1) the biological accuracy (i.e. the residuals in time-to-fishery estimates determined as the difference

between the 'incorrect' assessment models and the unrelated operating model (Figure 3.2) and 2) the standard error of these residuals for each incorrect assessment model across all combined data scenarios under each incorrect operating model (Table 3.4).

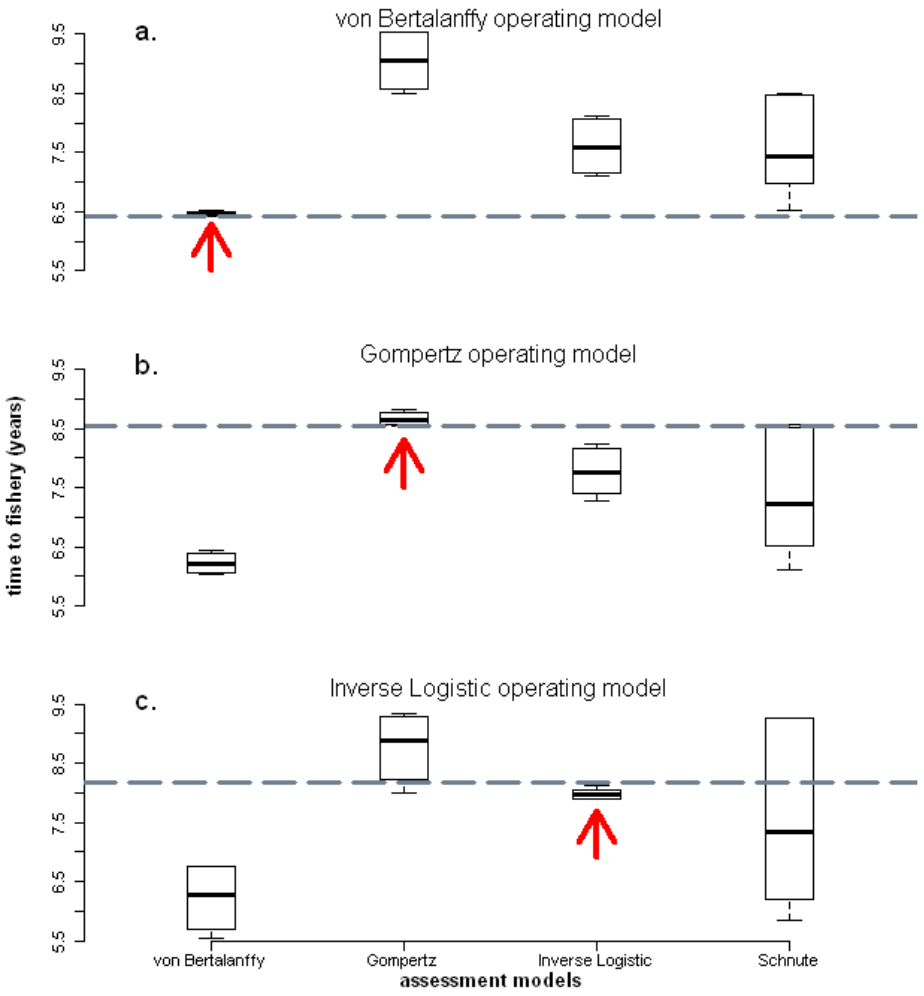

Figure 3.2: Mean values for time-to-fishery estimates are presented from 500 simulations generated from three operating models a) von Bertalanffy, b) Gompertz and c) inverse logistic. The horizontal dashed line represents the expected true time-to-fishery estimate as determined by the operating model in each case. Time-to-fishery estimates for four assessment models (von Bertalanffy, Gompertz, inverse logistic, and Schnute) are shown for all eight data quality scenarios combined. The arrows indicate the correct assessment model within each plot.

Relatively high residuals are an indication of a high risk level and are assigned a high risk index.

$$\text{Mean Risk Index} = \left(\sum_{o=1}^{o_i} \left(\sum_{d=1}^{8} r_{\text{mod}}^2 \times se_{mo} \right) \right) / o_i \qquad (3.10)$$

where r is the mean residual (i.e. difference in time-to-fishery estimates between the 'incorrect' assessment model m and unrelated operating model o for each data scenario d), s.e. is the total standard error of the mean residuals (for the 'incorrect' assessment model m under unrelated operating model o for all data scenarios combined), o is the unrelated operating model (von Bertalanffy, Gompertz or inverse logistic), o_i is the number of unrelated operating models (i.e. o_i =2 for the 'incorrect' von Bertalanffy, Gompertz and inverse logistic assessment models), o_i =3 for the 'incorrect' Schnute assessment model and d is the data quality scenario (Table 3.1).

The higher the Mean Risk Index for a given assessment model, the higher the potential risk in using that growth model for fishery management. A weighting was applied by squaring the residual to help differentiate between a high-residual/low-standard error score and a low-residual /high-standard error score. This weighting reflects that a high-residual/low-standard error score was more risky than a low-residual /high-standard error score.

Table 3.4: A biological risk assessment (Mean Risk Index, equation (3.10)) of the implications of selecting the incorrect assessment model. Mean residuals in time-to-fishery estimates between the assessment model and operating models from 500 simulations generated from three operating models a) von Bertalanffy, b) Gompertz and c) inverse logistic are tabulated. The residuals for each assessment model (von Bertalanffy, Gompertz, inverse logistic, and Schnute) are shown for eight data quality scenarios (A-H; refer to Table 1 for description of scenarios).

assessment model	von Bertalanffy		Gompertz		inverse logistic		Schnute		
operating model	Gz	IL	VB	IL	VB	Gz	VB	Gz	IL
A	-2.12	-1.42	2.08	1.10	0.72	-1.18	2.07	0.01	1.10
B	-2.45	-2.33	3.11	0.30	1.60	-0.38	0.10	-2.44	-2.33
C	-2.17	-1.41	2.29	1.16	0.68	-1.27	0.68	-1.27	-0.13
D	-2.49	-2.59	2.98	-0.18	1.53	-0.51	1.32	-1.36	-1.55
E	-2.13	-1.40	2.06	1.10	0.78	-1.10	2.04	-0.02	1.08
F	-2.46	-2.38	3.11	0.24	1.70	-0.31	0.56	-2.03	-1.97
G	-2.20	-1.45	2.21	1.13	0.74	-1.08	2.25	0.04	1.18
H	-2.52	-2.62	3.11	-0.11	1.67	-0.37	0.33	-2.29	-2.41
$\Sigma(\text{residual}^2)$	75.85		61.82		18.74		56.16		
total std.error	0.16		0.41		0.39		0.55		
Mean Risk Index	6.07		12.80		3.64		10.25		

3.3.10 Assessing model robustness

The robustness of the assessment models was evaluated according to three criteria: 1) statistical criteria assessing the statistical fit of the model to the data (i.e. the probability of selecting the correct model and the distribution of parameter estimates relative to true values), 2) biological criteria, such as time taken to reach the Legal Minimum Length and enter the fishery (Rogers-Bennett *et al.* 2007), and 3) the risk of making false biological predictions (e.g. differences in time-to-fishery estimates between the operating model and the assessment models) as a result of unknowingly selecting the incorrect model.

3.4 Results

The von Bertalanffy, Gompertz, and inverse logistic growth models differ in their description of growth characteristics of juvenile abalone (Figure 3.1), indicating that juvenile size classes are necessary for minimising model uncertainty. Typical tag-recapture data do not adequately represent the full size range of juveniles, and where there is a (characteristic) lack of data on juveniles, it is expected that the ability to discriminate between growth models would be weak (Figure 3.1). These expectations were systematically examined using a three stage approach for evaluating model robustness and the findings are presented in the following sections.

3.4.1 Stage 1a, statistical criteria: effect of negative increment on model robustness

In ideal data where sample size is large (N=540) and growth increments more negative than -3 mm are removed, the probability of obtaining the correct von Bertalanffy, Gompertz and inverse logistic models were all high (P>0.9). Results indicate that when negative growth data are included in the von Bertalanffy model, the K increases in the L_∞ decreases (Figure 3.3). Given a similar sample size (N=500) but in the presence of sampling error (scenarios E-H) the probability of the von Bertalanffy and Gompertz models being correct decreased substantially relative to the ideal data, with *P* ranging from 0.59-0.82 for the von Bertalanffy and from 0.25-0.85 for the Gompertz model. Removing all negative increments reduced the probability of the von Bertalanffy model being selected as the best statistical model using likelihood ratio tests (P=0.1, Table 3.3), while the inverse logistic model had a high probability (P=0.9, Table 3.3) of being selected under a von Bertalanffy operating model. The other assessment models (i.e. the Gompertz and inverse logistic) were selected in all instances under their corresponding operating model and were therefore unaffected by removing negative increments (Table 3.3; Figure 3.3). Removing all negative increments had a marked affect on the outcome of fitting the von Bertalanffy curve, in which the greatest bias occurred with the L_∞ and K parameters (Figure 3.3). In contrast, parameters of the Gompertz and inverse logistic assessment models were not biased by the removal of negative increments (Figure 3.3).

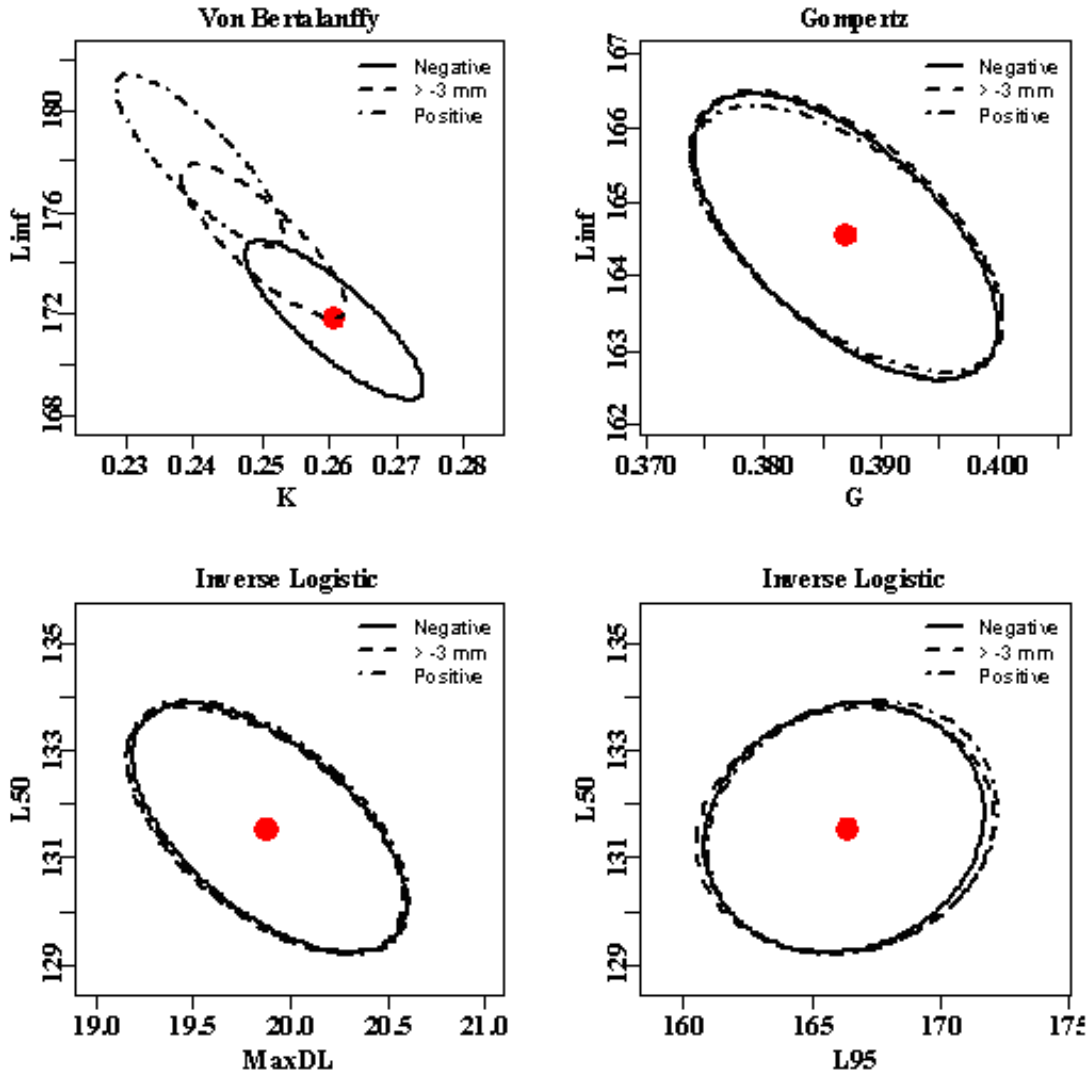

Figure 3.3: The effect of removing negative growth increments on the distribution of parameter estimates for three assessment models; von Bertalanffy, Gompertz, inverse logistic. The distribution of parameter estimates are shown for 500 simulations of ideal data adjusted by the incremental removal of negative increments; negative (no removal of negative increments), -3mm (removal of increments more negative than -3mm) and positive (all negative increments removed). The ellipses represent 95% confidence limits around the distribution of assessment model parameters estimates. The stronger the parameter correlation the more oval the 95% confidence limits. In each plot, the red point represents the parameter values used in the operating model. The greater the overlap between ellipses, the lesser the effect of removing negative increments on the distribution of parameters.

3.4.2 Stage 1b, statistical criteria: effect of unbalance sampling error on model robustness

Von Bertalanffy

In non-ideal data the probability of the correct von Bertalanffy model being statistically selected was relatively low (P= 0.59 and 0.82 across all scenarios), indicating that the von Bertalanffy is not robust to all scenarios of data quality (Table 3.3). The two data scenarios which were best for the von Bertalanffy were E and G (*P*= 0.80 – 0.82), where sample size was high (N=500) but with initial size range consisting of smaller animals (50 – 120 mm). Nevertheless these probabilities were still below the (arbitrary) unambiguous probability of P ≥ 0.95. There were five scenarios which recovered the correct model less than 70% of the time. Scenarios B and D resulted in the lowest probability of the correct von Bertalanffy being selected as the best statistical model. This suggests that a low sample size combined with a lack of smaller animals is the weakest scenario for a von Bertalanffy model.

Gompertz

The probability of the correct Gompertz model being selected for any scenario ranged between 0.25-0.85 (Table 3.3). The assessment Gompertz model was not robust to all scenarios of sampling error, especially when data covered the range of larger sizes of juveniles (80 – 170 mm). The Gompertz assessment model best recovered the correct model (probability of 0.82 and 0.85; scenarios, E and G) when sample size was high (N=500) and initial sizes were low (50 – 120 mm) (Table 3.3). Nevertheless, these

probabilities remain below the unambiguous probability of P ≥ 0.95. For the Gompertz operating model the greatest disadvantage was when data were only available for larger juveniles (80 – 170 mm; scenarios B, D, F, H) where there was ambiguity in the selection of the best model (P = 0.25-0.47) (Table 3.3). The level of ambiguity was such that for scenarios A, C, B, and F, the von Bertalanffy model showed a greater likelihood than the Gompertz of fitting data generated by the Gompertz operating model. In scenarios B, D, F and H, the incorrect assessment models (i.e. von Bertalanffy or inverse logistic) had a similar probability of being statistically the 'best' model under the Gompertz operating model (Table 3.3). Similar to the Von Bertalanffy model, a lack of smaller animals from the juvenile stages is the weakest scenario for fitting a Gompertz curve.

Inverse logistic

Out of all three assessment models tested only the inverse logistic was able to recover the simulations with a probability > 0.95 (scenarios B, D, F, and H) under its related operating model (Table 3.3). The inverse logistic model resulted in the widest range of probabilities of being correctly selected, ranging from 0.17-1.00 under its operating model. In contrast to the von Bertalanffy and Gompertz models, the data quality criterion that had the biggest disadvantage on robustness was when the length of initial sizes was restricted to 55-120 mm (particularly for scenarios A and C), under which circumstances the Gompertz had the highest probability of being selected as the best statistical model under the inverse logistic operating model.

A large sample size N=500 enables the inverse logistic to become more robust to a lack of data on smaller size classes (55 – 120 mm). Surprisingly, a size range encompassing smaller

animals is a disadvantage to the robustness of inverse logistic, because the available size range of the data was not able to define the L_{50} and L_{95} parameters of the inverse logistic. For example, the L_{50} parameter estimate (132 mm) was greater than the maximum initial shell length of 120 mm. For scenarios that included the range of larger sizes (i.e. 80 – 170 mm; B, D, F, H) the probability of correctly selecting the inverse logistic was unambiguous (P = 0.96 – 1.0, Table 3.3). Unlike the von Bertalanffy and Gompertz models, a lack of animals from the smaller portion of the size range of juveniles (< 80 mm) was not a disadvantage when fitting an inverse logistic curve. Where the initial size range was restricted to 55 – 120 mm, particularly for scenarios A and C, some estimates of parameter values of the inverse logistic were highly skewed (Figure 3.4). Increasing the sample size to N=500 (scenarios E and G) greatly reduced the skew in parameter estimates and improved the performance of the inverse logistic model (Figure 3.4).

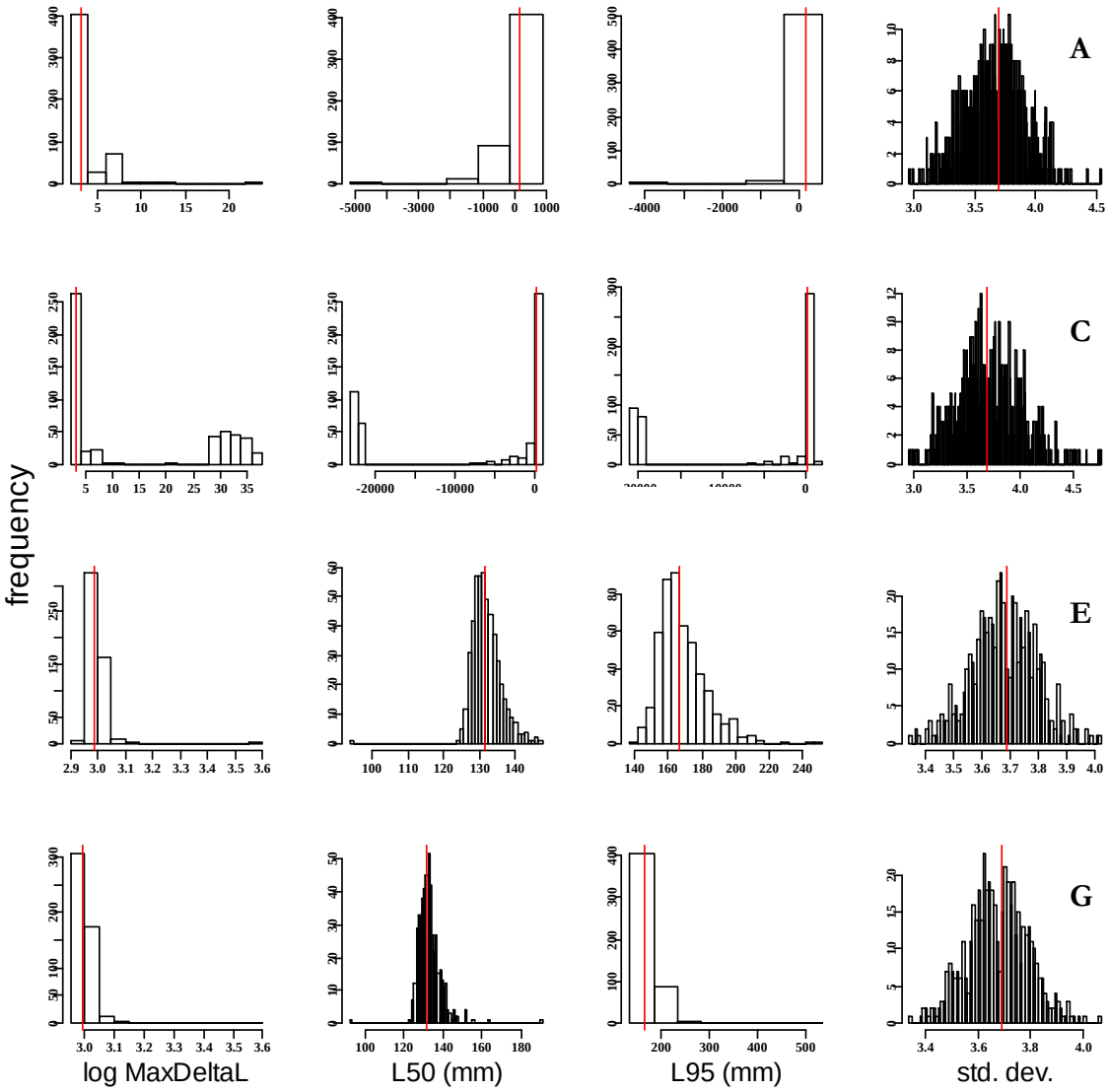

Figure 3.4: Parameter estimates for the inverse logistic model for data scenarios A, C, E and G where the initial size range of 55 – 120 mm was common to all scenarios (refer to Table 3.1 for description of scenarios). Row 1 is scenario A, row 2 is scenario C, row 3 is scenario E, row 4 is scenario G. Scenarios A and C illustrate the skewed distribution of parameter estimates of the assessment model fits. The estimates for MaxΔL (log MaxDeltaL) were often so highly skewed that a natural log transformation was required. The red line represents the estimate of the operating model parameter.

Schnute

Interestingly, but not unexpectedly, the Schnute model was never selected as the best model (Table 3.3), except under scenario F with the von Bertalanffy operating model, but even then P = 0.01. The flexibility conferred by the many submodel forms of the Schnute model, through the *a* and *b* parameters, enables it to assume either the Gompertz or the von Bertalanffy form, depending on the underlying data (Table 3.2), however, it cannot characterize constant growth of juveniles. Out of the eight alternative shapes that the Schnute model can adopt (Francis 1995), none are similar to an inverse logistic model. In addition, fitting the Schnute model to real data can be difficult because the shape of the predicted growth trajectory is very sensitive to the selection of starting parameters. For blacklip abalone, the starting parameters selected for the Schnute model greatly influenced whether it assumed a von Bertalanffy or Gompertz like growth pattern. When the starting parameters of the Schnute simulated a Gompertz-like model (Table 3.2), the Schnute converged on a false minimum and always simulated a Gompertz model regardless of the operating model (the Gompertz model in such cases would exhibit the same maximum likelihood value as that for the Schnute model). When the starting parameters of the Schnute resembled a von Bertalanffy-like growth trajectory (Table 3.2), the Schnute became flexible enough to simulate either a von Bertalanffy or Gompertz like growth trajectory, depending on the operating model. When fitted to data from the inverse logistic model the Schnute could not assume an inverse logistic like growth trajectory and would reproduce either von Bertalanffy or Gompertz like growth.

Having more parameters than either a von Bertalanffy or Gompertz, the Schnute model always had a larger AIC and would need to fit the growth data rather more closely than either of the other assessment models to be selected as the best model according to AIC. It

is therefore unlikely to be selected as the best model by likelihood ratio test. As the model fits were always very similar in quality, the difference in fit (likelihood estimates) between the Schnute, Gompertz and von Bertalanffy models was negligible for all scenarios regardless of operating model. Therefore the simplest models with fewest parameters tended to be selected on the basis of minimum AIC.

Summary

The initial size classes that produced the best performance in the von Bertalanffy and Gompertz models were the lower size classes of 55-120 mm shell length, where the minimum length increment was >10 mm. However, this form of data is atypical of what is usually encountered in typical tagging surveys. Conversely, the inverse logistic model performed best under an initial size range consisting of larger animals (80-170 mm) in which the minimum shell length increment was 0 mm, which is the kind of data more typical of that obtained from tag-recapture surveys. Therefore, the inverse logistic model had a high probability of recovering the correct or true underlying growth based on data with typical characteristics of sampling error.

3.4.3 Stage 2, biological criteria: time-to-fishery estimates

The 'correct' von Bertalanffy assessment model produced accurate and precise time-to-fishery estimates under its own operating model (range of time-to-fishery estimate 6.4-6.5 y). Accuracy in time-to-fishery estimates were determined by taking the difference between

the 'correct' assessment model and the operating model (Figure 3.2). The von Bertalanffy generated the most precise time-to-fishery estimates (CV = 0.01-0.05; Table 3.5).

The 'correct' Gompertz assessment model expressed accurate time-to-fishery estimates under its own operating model (range of time-to-fishery estimate 8.5-8.8 y). Time-to-fishery estimates were also reasonably precise for the Gompertz under its own operating model (CV = 0.01-0.05; Table 3.5).

The 'correct' inverse logistic function expressed accurate time-to-fishery estimates under its own operating model (range of time-to-fishery estimate 7.8-8.1y). The range in time-to-fishery estimates for the inverse logistic under its own operating model was 0.23 y, which is comparable with both the von Bertalanffy (0.1 y) and Gompertz (0.3 y) models under their related operating models.

Table 3.5: Range of CV estimates from all data quality scenarios combined. Estimates are presented for biological (time-to-fishery) and statistical criteria (parameter values).

	time-to-fishery (CV)	model parameter (CV)		
		L_∞	K	
von Bertalanffy	0.01-0.05	0.7-5.1	3.4-11.9	
		L_∞	g	
Gompertz	0.01-0.05	0.4-3.7	2.8-7.5	
		$Max\,\Delta L$	L_{50}	L_{95}
inverse logistic	0.03-0.08	3.4-1019	1.0-600	1.0-821

3.4.4 Comparing statistical and biological criteria

Absurd parameter estimates do not necessarily lead to absurd biological estimates. The results of the time-to-fishery estimates for the inverse logistic were more accurate than expected given the highly skewed and excessively wide distribution of parameter estimates (Figure 3.4). The range of the CV for parameter estimates was greater than the range of CV for the biological estimates (i.e. time-to-fishery estimates), particularly for the inverse logistic (Table 3.5). For example the range of the CV for the von Bertalanffy (CV = 0.7 - 5.1 and 3.4 - 11.9 for L_∞ and K respectively) was more than ten times the range of CV for time-to-fishery estimates (CV = 0.01- 0.05). The range of the CV for the inverse logistic (CV = 3.4-1019 and 1.00-821 for MaxΔL and L95 respectively) was at least 100 – 10 000 times the range of CV for time-to-fishery estimates (CV = 0.03 - 0.08).

3.4.5 Stage 3, risk assessment: biological implication of selecting the incorrect model

In reality the true growth trajectory of abalone populations may be obscured by sampling error. It is common practice among research programs to indiscriminately select a growth model, which may be unknowingly incorrect, and fit it to data which has an unknown degree of sampling error. It is therefore important to assess the biological risk of unknowingly using the incorrect growth model. Time-to-fishery estimates were used as the basis to assess the implications of selecting an incorrect model, and estimates were compared between the four assessment models (Figure 3.2). The difference in time-to-fishery estimates was calculated between each correct assessment model and the unrelated

operating model. Relatively large differences indicated a high risk associated with that assessment model. Of all four assessment models, the 'incorrect' Gompertz model was the most inaccurate in terms of departures from true time-to-fishery estimates, deviating a maximum of 3.1 years under the von Bertalanffy operating model. The 'incorrect' von Bertalanffy model was the second most inaccurate model, with the second highest departures from true time-to-fishery estimates, yielding an absolute maximum of 2.7 years under the inverse logistic operating model. The 'incorrect' Schnute model was the third most inaccurate, with an absolute maximum deviation of 2.4 years under the inverse logistic operating model. The 'incorrect' inverse logistic model was the most accurate of all the models in estimating time-to-fishery (maximum deviation = 1.69 years). The risk assessment produced a Mean Risk Index across the three operating models and eight data scenarios. This indicated that the Gompertz model implied the greatest risk (Mean Risk Index = 12.8) (Table 3.4), followed by the Schnute (10.25) then the von Bertalanffy (6.07), and the least risky option was the inverse logistic model (3.64).

3.5 Discussion

3.5.1 The effect of sampling error on model selection

There are differing views as to which model most appropriately describes abalone growth (Day & Fleming 1992), and this is not surprising. Results in this Chapter indicate that eight different data simulations of the same population resulted in ambiguous outcomes as to which growth model is statistically the best for that population. Statistical results show the inverse logistic assessment model had a higher probability of recovering its own operating

model than the von Bertalanffy or Gompertz had of recovering their relative operating models (Table 3.3). Therefore under the most typical scenarios of sampling error the inverse logistic model is the more robust model to tag-recapture data of blacklip abalone in Tasmania.

The statistical selection of the best fitting model can also be influenced by measurement error such as negative increments (Francis 1988b). With ideal data, where growth increments are available for both juveniles and adults, the removal of negative increments had no effect on the selection of the correct assessment model for the Gompertz and inverse logistic, and only affected the robustness of the von Bertalanffy model. The occurrence of increments more negative than– 3 mm might favour the selection of von Bertalanffy, or even the Gompertz model, over the selection of the inverse logistic model, because both of those models have better fits to that portion of the data. The von Bertalanffy may therefore have been selected as the best fitting model for the wrong reason, i.e. because it fits relatively well to negative increments.

To avoid fitting to negative increments, the L_∞ parameter of the von Bertalanffy and Gompertz have been reinterpreted using stochastic modelling by truncating the distribution of the L_∞ parameter (Sainsbury 1980; Troynikov *et al.* 1998). Once measurement error is properly removed from the data it is possible that the robustness of the stochastic von Bertalanffy model may be improved. Although negative increments are conspicuous in the larger size classes, they imply that uncertainties in shell length could occur across the entire initial size range and this need to be investigated further.

3.5.2 The effect of sampling error on variability in parameter estimates

Growth parameters are often used to discriminate between fast and slow growing populations and for determining the spatial scale of stocks (Worthington *et al.* 1995). However, claims of fine spatial scale heterogeneity in growth would be questionable if variability in growth parameters was due to artifacts of sampling error in the data.

Parameters of the von Bertalanffy are routinely used to compare between populations. For example in a study of three blacklip populations from South Australia, K ranged between 0.32 – 0.41 /yr and L_∞ ranged between 139 – 144 mm (Shepherd & Hearn 1983). Similarly in a study of three populations from Victoria, K ranged between 0.15 – 0.37 /yr (0.22 difference) and L_∞ ranged between 117 – 152 mm (35 mm difference). It is reasonable to assume that these populations are biologically different. The geographic extent between the SA and Victorian populations are approximately 700 km (McShane *et al.* 1988; McShane & Smith 1992). However the differences in the range of parameter estimates with this magnitude of geographic separation are approximately within the difference in range observed in this Chapter for a single population in Tasmania affected by typical scenarios of sampling error. The parameter estimates for the von Bertalanffy ranged between 0.19 – 0.34 /yr for K (0.15 difference) and 150 – 194 mm for the L_∞ (44 mm difference) due to sampling error. It is important to consider these ranges when making inter-population comparisons and raises the question whether the biological differences reported among wild populations are an artifact of sampling error in the data.

3.5.3 The effect of sampling error on biological predictions

In most cases, model selection stops at statistical goodness-of-fit tests such as AIC and likelihood ratio tests. However, biological criteria should be considered as important as statistical criteria in assessing how well models perform in recovering the underlying true growth characteristics (Rogers-Bennett *et al.* 2007). Ultimately this is important for the safe exploitation of stocks.

All assessment models performed well under their related operating model forms, accurately recovering the true time-to-fishery estimates regardless of the data scenario (Figure 3.2). The various scenarios of sampling error had a lesser effect on biological criteria (variations in time-to-fishery-estimates) than on the statistical criteria and their parameter estimates. Although all models indicated clear discrepancies between the correct assessment and operating model for statistical and parameter properties, such seemingly large discrepancies were not apparent in biological time-to-fishery estimates (Table 3.5).

Interestingly, and potentially more importantly, although some parameter estimates were absurd for the inverse logistic, accurate time-to-fishery estimates were achieved under the unrelated von Bertalanffy and Gompertz operating model (Table 3.6). The strengths of the inverse logistic model lie in its ability to capture the biological growth dynamics regardless of data quality.

Table 3.6. A summary of the robustness of four growth models according to a three criteria: 1) statistical criteria and the distribution of assessment model parameters around the operating model parameters 'good' indicates a relatively small distribution and 'poor' a relatively wide distribution, 2) biological criteria i.e. the accuracy in time-to-fishery estimates between the incorrect assessment model and operating models, 'poor' indicates relatively large inaccuracy and 'good' relatively low inaccuracy and 3) the biological risk of selecting an incorrect model as determined by the Mean Risk Index, see equation. (3.10).

	Criteria	von Bertalanffy	Gompertz	inverse logistic	Schnute
1)	parameter estimates	good √	good √	bad	n.a
2)	biological estimates	poor	poor	good √	poor
3)	risk	more risky	more risky	less risky √	more risky

3.5.4 Minimal data requirements

For parameter estimates to be reliable, data need to be sufficient to define the parameters of interest (Haddon 2001), and for that to occur, field surveys need to be model driven (Scandol 2004). A large range of initial size classes is more important for model robustness than large sample size alone. Typical datasets however consist mostly of large sized animals and, fortunately, the inverse logistic model is robust to this type of data scenario. Statistically, the inverse logistic has a requirement for data to be available across the size ranges that are extensive enough to allow the estimation of at least two parameter values, i.e. a combination of either MaxΔL and L_{50}, or MaxΔL and L_{50} or L_{50} and L_{95}. The data typical of tag-recapture studies tends to encompass the size ranges predicted by the latter two parameters (i.e. L_{50} and L_{95}) consisting of medium to large abalone. Fortunately there is clear evidence in this study that the inverse logistic model is robust to data consisting of medium to large abalone.

3.5.5 Implications of unknowingly selecting the incorrect model

In practice the true form of growth in the populations is likely to be unknown and it is valuable to assess the risk of making inaccurate biological predictions as a result of unknowingly using the 'incorrect' model. Of the four assessment models considered, the incorrect inverse logistic model provided the most accurate time-to-fishery estimates relative to the incorrect von Bertalanffy, Gompertz or Schnute models (Figure 3.2). In practice, the inverse logistic model may have been rejected early at the model fitting stage, owing to the generation of absurd parameter estimates if there is sampling error (Figure 3.4, Table 3.5), thereby limiting the selection to just two growth models. This restriction means that sampling error can lead back to the original problem, which is having a limited choice in model selection.

3.5.6 Implications of different models to fisheries management

The choice of growth model can have significant implications for fisheries management. For example, growth models are used in setting the Legal Minimum Length (LML) for harvesting and protecting spawning stock. The Gompertz model implies slower initial growth, which may imply low productivity and may lead to more conservative fishing policies (Rogers-Bennett *et al.* 2007), but may result in larger lost opportunity costs to the fishery. However, if the Gompertz model was incorrectly used to generate the LML, it would under estimate LML for an intended level of protection, thereby under-protecting the spawning stock and increasing the risk of recruitment overfishing. The use of the von

Bertalanffy curve would indicate more rapid initial growth than actually occurs, suggesting that the stock is more productive than in reality, and so this model could not be considered as being risk averse in fisheries policy decisions (Rogers-Bennett *et al.* 2007). If the von Bertalanffy is used in stock assessments, surplus stock production may be overestimated leading to risky harvest strategies. On the other hand if the von Bertalanffy model was incorrectly used to generate the size related LML, it would estimate an LML larger than necessary to provide a given level of protection, therefore overprotecting spawning stock resulting in lost opportunity costs to the fishery, which is risky to the economy but conservative to stock protection. Improving the techniques that inform the management of the blacklip abalone fishery in Tasmania is important because this is the largest managed wild abalone fishery in the world and makes a major contribution to the local economy (~AUD$100M pa before processing). The von Bertalanffy and Gompertz model are commonly used in Australia to describe the growth of abalone based on tag-recapture data. Their widespread use could potentially have serious implications in biasing fishery stock assessments.

CHAPTER 4

The suitability of the von Bertalanffy, Gompertz and inverse logistic models for describing growth in blacklip abalone populations (*Haliotis rubra*) in Tasmania, Australia

4.1 Abstract

A variety of methods are used for selecting the most appropriate growth model from a set of candidate models, and the model selected may vary depending on the method used. A length-based growth model is selected using a method that adheres to a widely accepted general method for model selection. Thirty wild populations of blacklip abalone (*H. rubra*) around the coast in Tasmania, Australia were each sampled for growth using tag-recapture methods. Three candidate, non-nested, growth models, (von Bertalanffy, Gompertz and inverse logistic) were fitted to each sample of tag-recapture data. The best statistical model was identified in each sample using criteria based on measuring relative statistical fit, including likelihood ratio tests, Akaike's Information Criteria, and Akaike weights. According to these criteria, the best fitting statistical model of the three models considered was the inverse logistic in 23 of the 30 samples. The von Bertalanffy model was the best fitting model in four samples and the Gompertz was the best in three samples. The inverse logistic was unambiguously the best fitting model, as indicated by the high Akaike weight values ($w_i > 0.8$). In contrast, the highest possible Akaike weights between the von Bertalanffy or Gompertz growth models ranged between 0.37-0.52. Results conclude that the use of either the von Bertalanffy or Gompertz growth models in the assessment of

Tasmanian blacklip abalone would be statistically sub-optimal and may mislead assessments of Tasmanian abalone stocks.

4.2 Introduction

Growth models are a key component of stock assessments used in the management of commercially important invertebrate marine species. However, the methods used to select a growth model for abalone populations vary between studies and this has resulted in different growth models being used in the biological assessment for a given species (e.g. (Worthington *et al.* 1995; Troynikov *et al.* 1998) . The model selection methods adopted among studies are not always clear despite the availability of systematic techniques for making such choices (Burnham & Anderson 2002). In Australia, and elsewhere there has generally been little explicit consideration given to the selection of a length-based growth model to fit tagging data from blacklip abalone (*H. rubra*) populations. For example, where the von Bertalanffy model was rejected the Gompertz model was selected as the most appropriate growth model because it was considered to provide a 'better fit' than the von Bertalanffy (Troynikov *et al.* 1998). However, there was no clear and widely acceptable definition as to what constituted a 'better fit'. In a more recent study of *Haliotis rufescens* in northern California, the selection of a growth model was based on information criteria (Burnham & Anderson 2002) and provided a more systematic method (Rogers-Bennett *et al.* 2007). However, the best fitting model was eventually rejected on biological grounds. In this case, biological validity effectively overrides the principle of data based model selection (Burnham & Anderson 2002).

In a review of Australian abalone growth studies by Day and Fleming (1992), model selection was usually limited to two models: the von Bertalanffy and the Gompertz growth model. The von Bertalanffy growth model tends to be the default model both currently and historically (Jákupsstovu & Haug 1988; Katsanevakis & Maravelias 2008). Despite its widespread use, the systematic selection of a growth model, such as the von Bertalanffy, from a range of competing models does not appear to be common. The plausibility of the von Bertalanffy growth model has been questioned for blacklip abalone and other fish species (Day & Taylor 1997; Katsanevakis & Maravelias 2008). Even so, owing to its extensive use the von Bertalanffy model may be helpful for making consistent comparisons between studies. Day and Fleming (1992) also report constant growth rates for juvenile abalone, and, at that time, there was no associated length increment growth model available that incorporated constant growth. Recently, the inverse logistic model was developed as a growth model for blacklip abalone populations in Tasmania (Haddon *et al.* 2008). The development of the inverse logistic model was based on earlier observations made on age-at-length measurements and modal analysis of length frequencies that suggested a linear growth trajectory on juvenile size classes which implies constant growth rate in juvenile size classess (10-70 mm) (Prince *et al.* 1988a). The size-based von Bertalanffy and Gompertz models do not predict constant growth increments in the juvenile phase. The inclusion of the inverse logistic model therefore offers greater choice for model selection.

In considering which models to include as a set of candidate growth models, it is important to assess the biological plausibility of the growth trajectories in addition to statistical methods of model selection (Burnham & Anderson 2002). A set of biologically plausible candidate models is firstly established. The best model is then selected according to statistical fitting criteria which measure the relative support for a model given the data

(Sorensen & Gianola 2002). With the exception of one study (Rogers-Bennett *et al.* 2007), multiple candidate growth models (i.e. greater than two models) have not been explicitly tested on abalone using formal model selection methods. Where model selection is explicit, the minimum AIC is customarily used to identify the optimal model (Shono 2000). Usually, the statistically best fitting candidate model is considered to be the optimal model. However biological factors also contribute. For example, a candidate model with a growth trajectory similar to that of the inverse logistic, was the best fitting model to Californian data (Rogers-Bennett *et al.* 2007) but was rejected because a section of the predicted growth trajectory could not be interpreted as being biologically valid (Rogers-Bennett *et al.* 2007). Under such circumstances the best fitting candidate growth model may be rejected following post-hoc assessment of its biological validity. For the present study, model selection is therefore based on a combination of biological and statistical criteria.

Three non-nested candidate growth models were fitted to tag-recapture data from 30 populations from around Tasmania, Australia, to identify the optimal model in terms of statistical fit and parsimony guided by systematic model selection techniques. Each growth model was fitted to multiple populations of tag-recapture data from predominantly adult-sized animals (80 - 210 mm shell length). The aims of this study were twofold; firstly to identify the best fitting growth model using goodness-of-fit tests and model selection techniques and secondly to examine the biological relevance of the predicted growth trajectory and parameters of three growth models to blacklip abalone populations in Tasmania.

4.3 Methods

4.3.1 Site selection

The 30 sites sampled represent a range of currently fished abalone reefs in the Tasmanian fishery (Figure 4.1). The sites selected were generally chosen on the advice of commercial divers who were actively fishing and familiar with the region (Tarbath, Haddon *et al.* 2001).

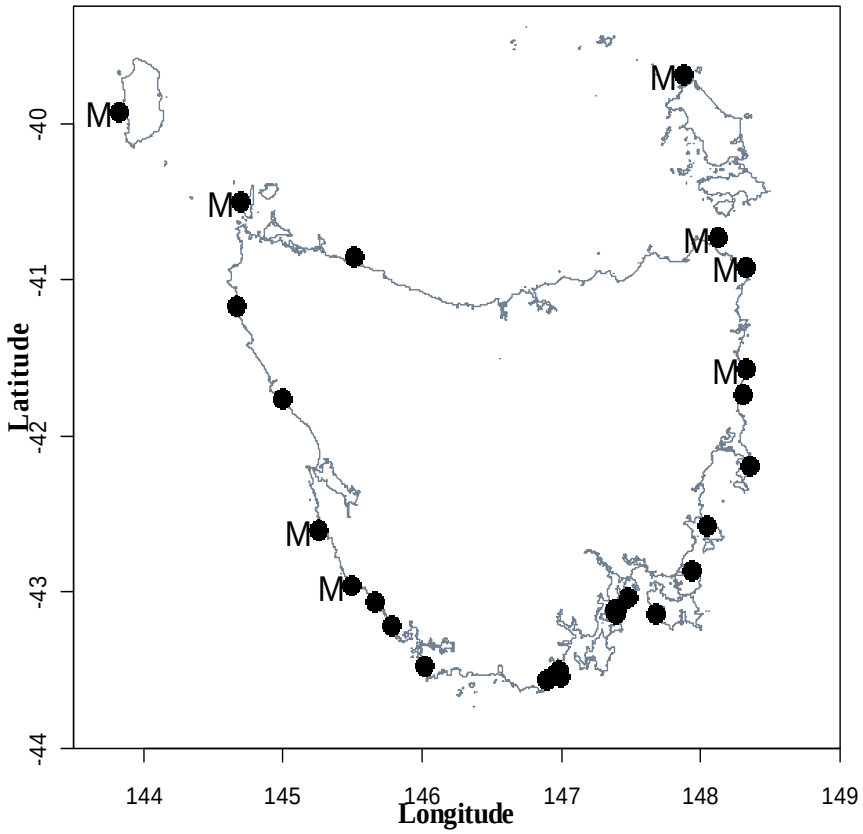

Figure 4.1. Map of the distribution of the 30 sampling sites of tag-recapture data from wild populations of blacklip abalone around Tasmania. The eight sites which had both growth and maturity data from the same site and year are indicated with an M.

4.3.2 Growth data

Tag-recapture data for blacklip abalone from 30 sites used in the analyses were collected during fishery independent surveys conducted by research divers over a total period of 15 years (from 1994-2008). Data collected during surveys that differed in both time and/or spatial location were treated as separate samples.

Five quality criteria were applied to the data within each sample:

1) negative growth increments less than -3mm were excluded (these are attributable to measurement or recording errors),

2) the sample must include juveniles to define the full growth curve i.e. < 100 mm shell length,

3) large abalone with negligible or zero growth increments had to be included in the sample so that the full range of growth was included,

4) the time increment between mark and recapture was approximately one year (between 0.9 and 1.2 years),

5) sample size was greater than 90 recaptures.

Negative increments were found to affect the parameters of the von Bertalanffy growth model (Sainsbury 1980; Chapter 3). To minimize this effect, data with length increment < -3mm were removed (-3mm was selected to allow for some sampling error). Negative increments had negligible affects on model parameters fitted to the Gompertz and inverse logistic models (Chapter 3). Length increments were corrected for the time-at-liberty by

dividing the observed length increment by the observed time-at-liberty (i.e. between 0.9 and 1.2 years) to normalize the length increments to one year exactly.

4.3.3 Growth models

The deterministic forms of the three candidate growth models include a re-parameterized size-based analogue of the von Bertalanffy model for tag-recapture data used for estimating length increments from time increments (Fabens 1965) (Figure 4.2):

$$\Delta L = \left(L_\infty - L_i\right)\left(1 - e^{-K\Delta t}\right) + \varepsilon \tag{4.1}$$

The re-parameterised Gompertz (Troynikov *et al.* 1998) for estimating length increments from time increments (Figure 4.2):

$$\Delta L = L_\infty \left(\frac{L_i}{L_\infty}\right)^{\exp(-g\Delta t)} - L_i + \varepsilon \tag{4.2}$$

The inverse logistic model (Haddon *et al.* 2008) (Figure 4.2):

$$\Delta L = \frac{Max\Delta L}{1 + e^{Ln(19)\frac{\left(L_i - L_{50}\right)}{\left(L_{95} - L_{50}\right)}}} + \varepsilon \tag{4.3}$$

where ΔL is the expected length increment, $L\infty$ is the shell size where the mean length increment is zero (VB & Gz), L_i is the initial length when first tagged and released, K is the rate of change in length increment with increasing shell size (VB), g is the rate of change in length increment with increasing shell size (Gz), Δt is the time at liberty (as a fraction of a

year), $MaxΔL$ is the maximum length increment, L_{50} is the initial length at 0.5 times the difference between $MaxΔL$ and lowest length increment and L_{95} is the initial length at 0.95 times the difference between $MaxΔL$ and lowest length increment. The constant ε s are independent additive normal random error terms. Using an identical error structure simplified the statistical comparison of these three models.

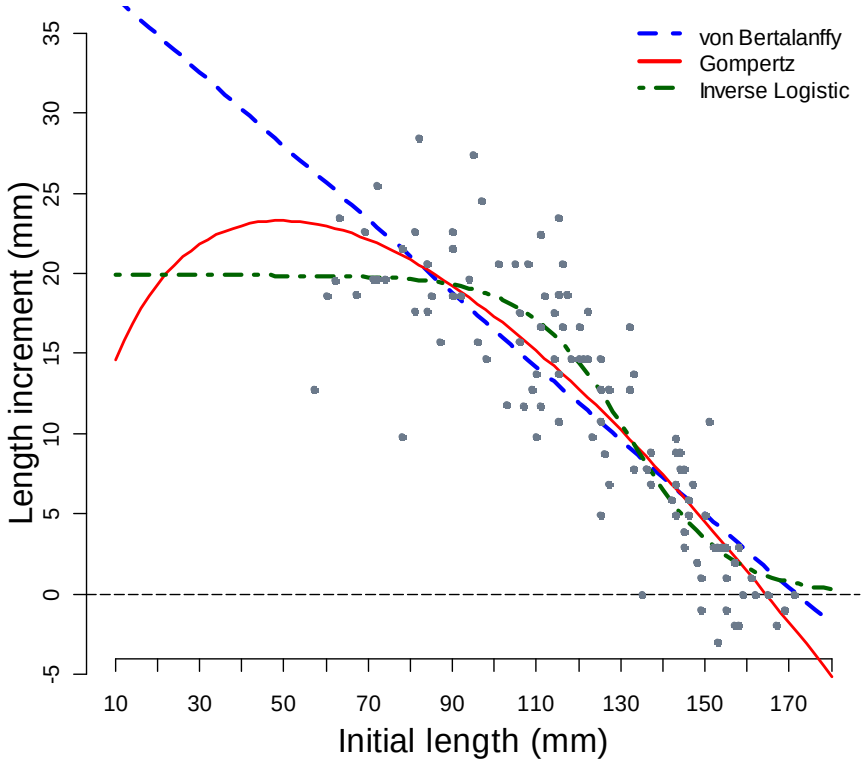

Figure 4.2. The von Bertalanffy, Gompertz, and inverse logistic growth models fitted to a dataset that was the best example of tag-recapture data in terms of sample size and initial size range. Presented are tag-recapture data from Black Island 42.9687°S, 145.4924° E.

4.3.4 Model selection using statistical criteria

The optimal growth model was identified using four statistical criteria. The first criterion involved identifying the model with the minimum negative log-likelihood estimate (the best fitting model). In each case the likelihood function based on length increments to be minimized was,

$$-LL = -\sum_{i=1}^{n} Ln\left(\frac{1}{\sigma\sqrt{2\pi}}\exp\left(-\left[\frac{\left(\Delta L_i - \Delta\hat{L}_i\right)^2}{2\sigma^2}\right]\right)\right) \tag{4.4}$$

where ΔL_i is the observed growth increment for each of the $i = 1$ to n observations at each site, $\Delta\hat{L}_i$ is the predicted growth increment for observation i from one of the three candidate growth models, equations (4.1) to (4.3), and σ is the standard deviation of the normal random errors. Rogers-Bennett et al (2007) used least squared residuals when comparing six candidate models. In an equivalent manner normal random residuals errors were used. However, the use here of a maximum likelihood framework simplified the use of model selection methods and permitted the use of likelihood ratio tests and Akaike weights. The negative log-likelihood (-*LL*) was minimized in each case using the 'optim' function in R (R Development Core Team 2008).

The second criterion was to compare the models using a likelihood-ratio test to determine whether the optimum model was significantly different to the sub-optimum models (Burnham & Anderson 2002). The likelihood-ratio test formally compares the fit of the optimal model fit to the suboptimal model fits using the χ^2 distribution which indicates if differences are statistically significant (Haddon *et al.* 2008).

$$\chi^2 = 2(LL_{IL} - LL_{Gz/vB}) \quad (4.5)$$

where χ^2 is the estimate chi-squared value, LL_{IL} is the log-likelihood of the fit to the inverse logistic (note not the negative log-likelihood), and $LL_{Gz/VB}$ is the log-likelihood of either the fit to the von Bertalanffy or the Gompertz models. If the estimated χ^2 value is greater than the χ^2 distribution with one degree of freedom (being the difference in the number of parameters between the inverse logistic and the von Bertalanffy or the Gompertz models, $\chi^2 > 3.84$) then a significant difference is indicated. The performance of the inverse logistic was the focus of the current study: therefore the likelihood ratio test was restricted to examining the fit of the inverse logistic model to the alternative two parameter model (von Bertalanffy or Gompertz) with the lowest maximum likelihood.

The third criterion was to identify the model with the smallest Akaike Information Criteria (AIC_{min}). This identifies the model that more closely represents the biological reality expressed in the data (Burnham & Anderson 2002). The AIC balances the trade-off between the quality of fit and the number of parameters used (Burnham and Anderson, 2002) and is defined as AIC = -2*LL + 2K, where K is the total number of parameters (including σ^2) and -2*LL is two times the negative log-likelihood at its optimum.

The fourth criterion was to determine the relative weight of evidence of each model (AIC_i, including the sub-optimum and optimum models) relative to the optimum model (AIC_{min}), using Akaike weights (w_i) (Buckland et al., 1997). These are defined by first comparing the relative AIC values $\Delta_i = AIC_i - AIC_{min}$, where *r* indexes the three growth models, and substituting these into the expression.

$$w_i = \exp(-0.5\Delta_i) / \sum_{r=1}^{3} \exp(-0.5\Delta_r) \quad (4.6)$$

4.3.5 Biological plausibility of growth model parameters

When analyzing the link between growth parameters and biology, two biological characteristics were used: median shell length of adults and size at maturity. The L_∞ of the von Bertalanffy and Gompertz represents the initial shell length where the predicted mean increment is zero. The L_{95} of the inverse logistic is consistently close to the shell lengths where growth increments become small. The L_∞ of the von Bertalanffy and Gompertz models does not represent the asymptotic maximum shell length of the abalone population (Ratkowsky 1986). Instead it represents the mean of the distribution of maximum lengths for the population as a whole (Sainsbury 1980). Therefore, assuming a normal distribution for the L_∞ and L_{95}, the most relevant biological estimate that could be compared to these parameters is the median length of catches. These are obtained annually from fishery-dependant commercial surveys and represent the median length of fished adult abalone from year to year. A range of median length estimates are accumulated over the years. In some years size selective fishing occurs where divers exclude very large abalone. This will affect year to year estimates of median length of catches causing a downward bias. To overcome this downward shift, only the maximum value within the year to year range of median estimates is selected for comparison with the L_∞ and L_{95} parameters. The fishing locations with median shell-length data were matched as closely as possible to the locations of the tagging survey sites. Parameter estimates of L_∞ (from the von Bertalanffy and

Gompertz) and L_{95} (from the inverse logistic model) were compared with median shell length data using ANOVA.

The L_{50} parameter of the inverse logistic model in equation (4.3) is the initial shell-length at which the decline in growth rate is most rapid (Haddon *et al.* 2008). Declines in growth rate are commensurate with the onset of maturity as energy is transferred from somatic growth to reproductive growth and a reduction in shell growth rate is expected (Lester *et al.* 2004). This decline in growth rate was claimed to be biologically implausible in red abalone (*H rufescens*) in northern California, as the decline in growth rate was considered to be too rapid (Rogers-Bennett *et al.* 2007). To explore if this rapid decline in growth rate is biologically valid in blacklip abalone, population estimates of size at maturity (SM_{50}) were compared with population estimates of the L_{50} parameter from the inverse logistic model. In total, eight sites (each representing a different population) were extracted from the database where each site had data for both growth and maturity taken at the same time (Figure 4.1). L_{50} parameter estimates (variable 1) were calculated for each site as well as the corresponding size at maturity data (SM_{50}, variable 2) and potential differences between these two variables were examined using ANOVA.

4.4 Results

4.4.1 Statistical fit

The best fitted parameters of all three models exhibited wide variation around Tasmania (Table 4.1). The relative quality of fit of the three candidate growth models was gauged

against multiple sites to determine which model was best able to describe growth in the majority of locations. The AIC values (Table 4.2) indicate that the inverse logistic model was statistically optimal in 23 samples out of the 30 samples of length-increment data considered. The von Bertalanffy model was the best fitting model for only four samples and the Gompertz was the best for three samples. In all cases the ordering of the Akaike weights matched the minimum AIC, however, there were large differences in Akaike weights between the best inverse logistic model and best von Bertalanffy or Gompertz model (Table 4.2). The high Akaike weight values ($w_i > 0.8$) for the best inverse logistic models (n = 20 sites, Table 4.2) indicate that the best fitting inverse logistic model is more certain than the best fitting von Bertalanffy or Gompertz.

Table 4.1. Growth parameters for length increment data from 30 populations; s.d. is the standard deviation. Three growth models, the von Bertalanffy, Gompertz and inverse logistic were fitted to 30 samples of tag-recapture data using maximum likelihood. Samples that differed in space and time were treated as separate samples.

site	latitude	longitude	year	von Bertalanffy			Gompertz			inverse logistic			
				L_∞	k	s.d.	L_∞	g	s.d.	MaxΔL	L_{50}	L_{95}	s.d.
59	-41.57	148.32	1994	151	0.46	5.4	148	0.59	5.4	24.2	118	157	5.4
59	-41.57	148.32	1995	141	0.58	3.5	140	0.66	3.5	31.6	105	145	3.3
59	-41.57	148.32	1996	157	0.45	5.3	153	0.58	5.3	28.7	117	167	5.3
159	-42.58	148.05	1994	160	0.36	3.8	158	0.44	3.8	20.8	126	168	3.8
159	-42.58	148.05	1996	175	0.30	6.8	169	0.41	6.7	18.4	139	169	6.6
170	-41.17	144.67	1995	141	0.32	3.1	140	0.38	3.1	14.2	116	146	3.1
272	-42.61	145.26	2001	162	0.36	3.6	161	0.42	3.7	26.3	120	163	3.4
297	-42.20	148.35	2003	152	0.39	4.9	147	0.53	4.8	24.0	115	152	4.6
300	-41.74	148.30	2003	164	0.48	5.7	157	0.68	5.4	30.0	123	157	4.9
313	-40.50	144.70	2001	128	0.29	3.4	127	0.35	3.6	17.9	92	128	3.3
314	-39.93	143.83	2001	147	0.35	4.4	145	0.44	4.5	21.1	112	149	4.3
315	-39.69	147.88	2001	121	0.35	2.9	119	0.43	3.1	20.0	87	121	2.7
316	-40.73	148.12	2001	139	0.35	4.1	136	0.46	4.2	25.7	96	147	4.1
337	-42.87	147.94	2003	141	0.29	4.5	136	0.41	4.3	17.1	108	138	4.1
458	-42.96	145.49	2003	172	0.26	4.1	164	0.39	3.7	19.9	131	167	3.5
459	-43.48	146.02	2003	155	0.32	2.5	155	0.37	2.6	15.4	128	155	2.4
460	-43.07	145.66	2003	164	0.36	4.6	162	0.44	4.6	19.9	131	160	4.3
461	-43.11	147.38	2003	173	0.35	4.6	162	0.54	4.4	29.5	122	173	4.3
470	-43.22	145.78	2003	171	0.28	4.1	168	0.38	4.1	22.1	127	167	3.8
478	-43.54	146.99	2003	145	0.36	3.9	140	0.50	3.7	22.3	110	146	3.6
480	-43.56	146.89	2003	136	0.48	4.2	134	0.61	4.3	30.0	97	137	3.9
482	-43.11	147.40	2003	150	0.58	4.3	148	0.70	4.3	27.6	118	154	4.2
588	-40.92	148.32	2003	171	0.28	4.3	163	0.41	4.1	20.6	127	162	3.8
662	-40.86	145.51	2006	102	0.23	2.9	102	0.28	2.9	10.1	78	97	2.8
663	-43.04	147.48	2007	128	0.51	4.3	127	0.62	4.5	32.2	88	134	4.0
702	-43.14	147.39	2006	163	0.40	5.0	160	0.51	5.0	31.8	115	178	5.0
764	-43.14	147.68	2006	166	0.38	3.9	159	0.53	3.9	27.2	123	174	3.9
813	-43.51	146.98	2008	141	0.23	3.0	140	0.30	2.8	13.2	112	132	2.6
815	-43.53	146.96	2008	144	0.34	3.3	143	0.41	3.3	18.4	113	151	3.3
819	-41.76	145.00	2008	141	0.32	2.9	141	0.38	3.0	21.1	105	141	2.7

Table 4.2. Information criteria associated with statistical model selection. Three growth models (von Bertalanffy (VB), Gompertz (Gz) and inverse logistic (IL)) were fitted to 30 samples of tag-recapture data. Samples that differed in space and time were treated as separate samples. Results of the likelihood ratio test (LRT) presented here compare the fit of the inverse logistic model to the 2-parameter model (either the von Bertalanffy or Gompertz) whichever had the lowest maximum likelihood.

site	year	log likelihood			AIC			minimum	LRT	Akaike weights		
		VB	Gz	IL	VB	Gz	IL	AIC	significance	VB	Gz	IL
59	1994	416	416	415	838	838	839	Gz	n.s	0.31	0.46	0.23
59	1995	93	94	92	193	194	191	IL	s	0.26	0.15	0.59
59	1996	1020	1020	1019	2046	2046	2047	Gz	n.s	0.34	0.37	0.29
159	1994	329	329	329	664	664	666	VB	s	0.49	0.36	0.15
159	1996	304	303	301	614	612	610	IL	s	0.08	0.27	0.65
170	1995	235	235	234	476	476	477	VB	n.s	0.4	0.33	0.27
272	2001	547	555	539	1100	1117	1087	IL	s	0	0	1
297	2003	815	808	798	1636	1622	1604	IL	s	0	0	1
300	2003	359	353	344	724	713	696	IL	s	0	0	1
313	2001	1033	1046	1022	2072	2098	2051	IL	s	0	0	1
314	2001	1263	1265	1246	2532	2536	2499	IL	s	0	0	1
315	2001	516	526	502	1038	1059	1011	IL	s	0	0	1
316	2001	656	660	654	1317	1325	1316	IL	s	0.3	0.01	0.69
337	2003	421	414	408	847	833	823	IL	s	0	0.01	0.99
458	2003	333	321	315	673	648	638	IL	s	0	0.01	0.99
459	2003	309	311	302	625	628	612	IL	s	0	0	1
460	2003	264	266	259	534	538	527	IL	s	0.02	0	0.97
461	2003	479	472	469	963	950	946	IL	s	0	0.09	0.91
470	2003	156	155	151	317	317	311	IL	s	0.04	0.04	0.92
478	2003	962	947	936	1930	1900	1880	IL	s	0	0	1
480	2003	432	436	420	871	878	848	IL	s	0	0	1
482	2003	388	388	384	782	783	776	IL	s	0.04	0.03	0.93
588	2003	339	335	326	684	675	660	IL	s	0	0	1
662	2006	278	279	275	562	564	558	IL	s	0.09	0.04	0.88
663	2007	327	332	320	661	671	649	IL	s	0	0	1
702	2006	777	778	776	1559	1562	1560	VB	n.s	0.52	0.11	0.37
764	2006	631	629	628	1268	1263	1264	Gz	n.s	0.06	0.5	0.44
813	2008	419	412	395	844	829	797	IL	s	0	0	1
815	2008	162	163	162	331	332	332	VB	n.s	0.5	0.28	0.22
819	2008	240	245	235	485	496	477	IL	s	0.01	0	0.99

The Akaike weights ranged between 0.37-0.52 for the von Bertalanffy and Gompertz collectively, and indicate more uncertainty for the best von Bertalanffy or best Gompertz in the presence of other candidate models. Associated with this, in all samples where the von Bertalanffy or Gompertz was the best statistical model the likelihood ratio tests (LRT, Table 4.2) revealed that the fit was not significantly better than the other candidate models (with the exception of site 159 in year 1994 where the von Bertalanffy was statistically better than the inverse logistic). In contrast where the inverse logistic model was the best model the likelihood ratio tests revealed that the fit was always a significant improvement over the other models (Table 4.2).

4.4.2 Biological plausibility

The estimated median shell lengths of catches were proximal to the L_{∞} parameters of the von Bertalanffy and Gompertz, and the L_{95} of the inverse logistic (Table 4.3). Overall the maximum difference between the median shell length and the parameter value (as a percentage of the parameter value) was within 20% of the parameter value (the percentage difference was calculated by: percent difference = 100*(P-M)/P, where P = estimated parameter and M is the median catch). For some sites there was strong agreement between the model parameters and the maximum length of catch (sites 170, 272, 460, and 482; Table 4.3). For other sites (159, 337, 461, 480, 663 and 819) the percent difference ranged from -15.4% to 14.5% for von Bertalanffy, -17.2% to 10.7% for Gompertz, and -14.6% to 16.9% for the inverse logistic. Even so, there were no significant differences between the

L_∞ and L_{95} parameters and the median shell length (Table 4.4). There was no significant difference between the L_{50} parameter of the inverse logistic and the size at maturity (SM_{50}) (Table 4.4). Given only eight pairs of observations there was a strong correlation between the L_{50} of the inverse logistic model and the SM_{50} ($r = 0.890$ $p<0.01$; Table 4.3, Figure 4.3, and Figure 4.4).

Table 4.3. Biological plausibility of model parameters for three growth models (VB -von Bertalanffy, Gz - Gompertz and IL - inverse logistic). Estimated values between median length of catches are tabulated against the relevant parameters of three growth models (L_∞ for both the von Bertalanffy and Gompertz and L_{95} for the inverse logistic). Estimated values of size at maturity are tabulated against the relevant parameter of the inverse logistic model (L_{50}). Each of the three growth models were fitted to tag-recapture data for 30 populations. The median length of catches represents the median length of adults in the population and were collected over a six year period between 2004-2009. Only the maximum values of the range collected over the six year period are presented.

site	VB L_∞ (mm)	Gz L_∞ (mm)	IL L_{95} (mm)	median length catch (mm)	IL L_{50} (mm)	size at maturity (mm)
59	151	148	157	-	118	
59	141	140	145	-	105	
59	157	153	167	-	117	107
159	160	158	168	150	126	
159	175	169	169	151	139	
170	141	140	146	145	116	
272	162	161	163	162	120	126
297	152	147	152	149	115	
300	164	157	157	-	123	
313	128	127	128	-	92	98
314	147	145	149	-	112	103
315	121	119	121	-	87	95
316	139	136	147	-	96	98
337	141	136	138	154	108	
458	172	164	167	162	131	128
459	155	155	155	163	128	
460	164	162	160	159	131	
461	173	162	173	148	122	
470	171	168	167	159	127	
478	145	140	146	157	110	
480	136	134	137	157	97	
482	150	148	154	148	118	
588	171	163	162	-	127	116
662	102	102	97	-	78	
663	128	127	134	146	88	
702	163	160	178	148	115	
764	166	159	174	147	123	
813	141	140	132	150	112	
815	144	143	151	157	113	
819	141	141	141	157	105	

Table 4.4. P values of significance for ANOVA of model parameters for three growth models (von Bertalanffy, Gompertz and inverse logistic) against their biological counterparts (n.s = not significant). Estimated values of median length of catches are biologically relevant to the parameters of three growth models that characterize the maximum shell length (L_∞ for both the von Bertalanffy and Gompertz and L_{95} for the inverse logistic, n = 30 for the median length comparisons). Estimated values of size at maturity are biologically relevant to the L_{50} parameter of the inverse logistic (n = 8 for the size at maturity comparisons). Median length of catches were collected over a six year period between 2004-2009. Only the maximum values of the range collected over the six year period are presented.

model parameters	median length	maturity SM_{50}
von Bertalanffy L_∞	0.3974 (n.s)	<0.001
Gompertz L_∞	0.07481 (n.s)	<0.001
inverse logistic L_{95}	0.5822 (n.s)	<0.001
inverse logistic L_{50}	<0.001	0.4422 (n.s)

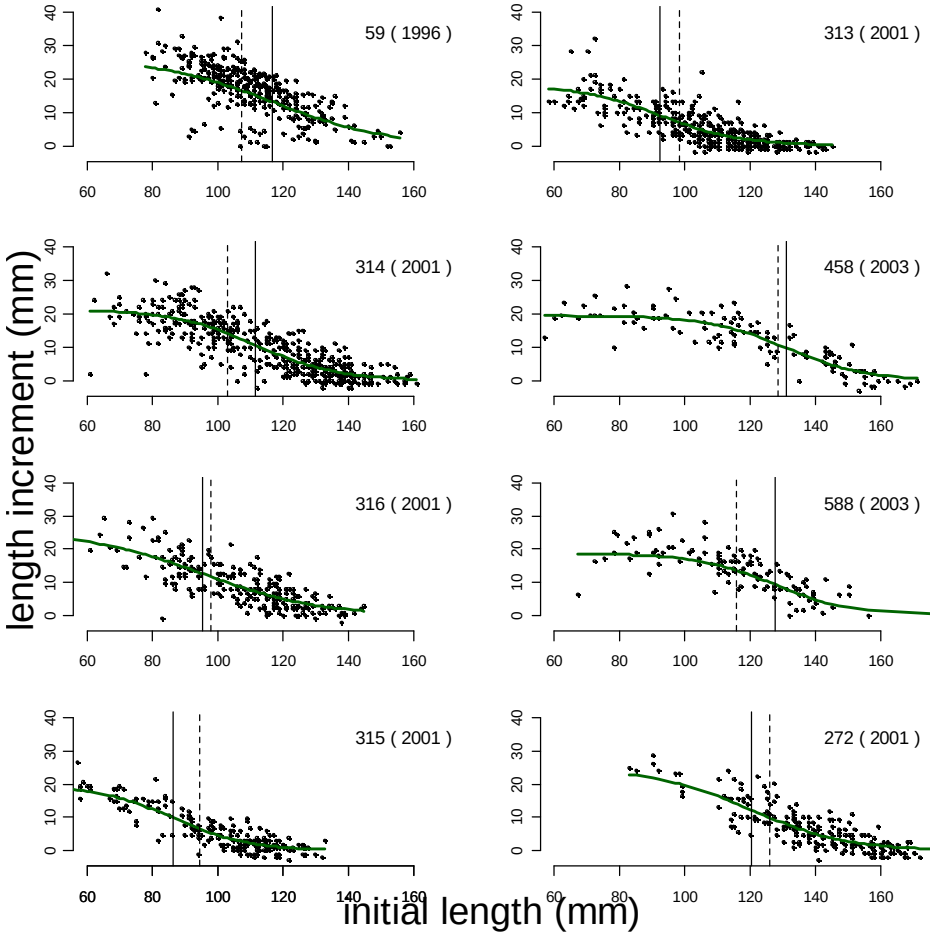

Figure 4.3. Relationship between the estimates of size at maturity (SM_{50} i.e. the initial shell length at which 50% of the population is mature, represented by the dotted vertical line) and the L_{50} parameter of the inverse logistic model (solid vertical line) for eight sites. For each site, growth and maturity data was collected in the same year. Sites numbers are shown on each plot alongside the year (in brackets) the data were collected.

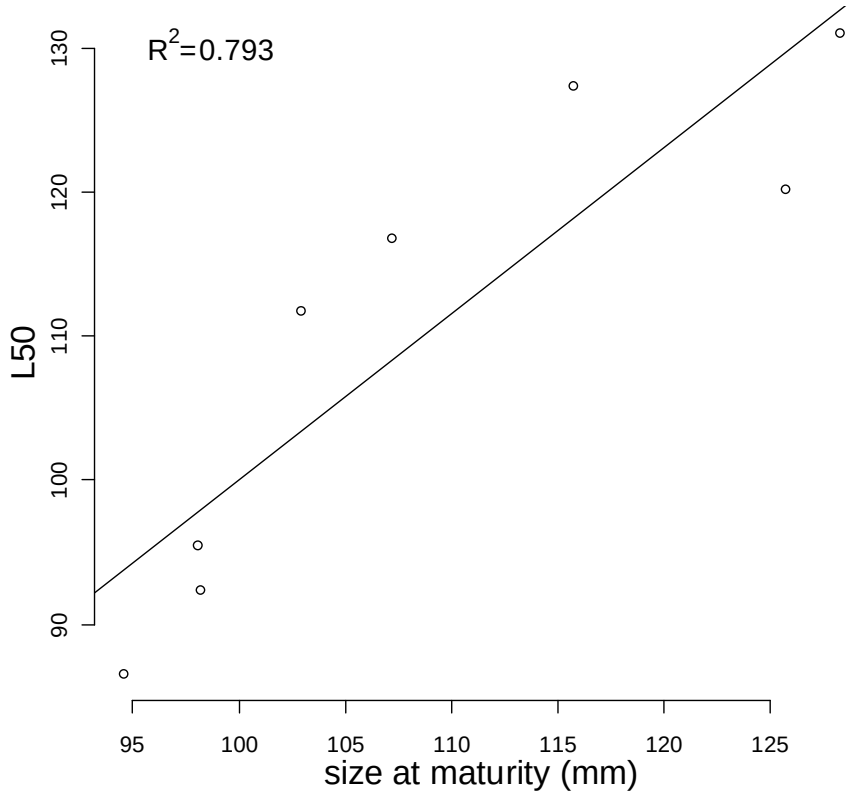

Figure 4.4. Correlation between size at maturity (SM_{50}) and the L_{50} of the inverse logistic fitted to tag recapture data for eight populations where growth and maturity data were collected in the same site and year. The correlation coefficient of r = 0.890 is significant at $p<0.01$ (n=8).

4.5 Discussion

This study offers a systematic approach to resolve ambiguity in model selection when formally selecting a model among plausible candidate models. Akaike weights in particular quantified the relative certainty in each fitted model given the data, and despite their

usefulness Akaike weights are surprisingly overlooked in statistical model selection. The growth models considered were simple low dimensional models described by only a few parameters. This made it straightforward to locate the global minimum of the negative log-likelihood for each model (Sorensen & Gianola 2002). Not only was the inverse logistic statistically the better fitting model for the majority of sites but the Akaike weights indicated that the inverse logistic was unambiguously the best model when it had the lowest AIC (Table 4.2). In contrast, the statistically optimal von Bertalanffy or Gompertz results remained relatively ambiguous; their likelihood ratio tests relative to the inverse logistic were generally not significant ($p>0.05$) and the Akaike weights were not much higher than the sub-optimal inverse logistic. Results suggest that their improvement over the inverse logistic for a given data set was marginal.

Biological validity is important in model selection because if the candidate set of models are biologically arbitrary (for example a polynomial could be used to describe mean growth increments) it is still possible to obtain a best-fit statistical model using AIC. Statistical model selection criteria only evaluate the relative plausibility of the candidate models presented (relative to each other). The best-fit statistical model, identified as the one with lowest relative AIC value, may still be biologically implausible in an absolute sense. Therefore every effort should be made to gain relevant biological knowledge of the models relative to the species in question before establishing an *a priori* set of candidate models (Burnham & Anderson 2002).

The biological plausibility of the three candidate models was considered in addition to their statistical goodness-of-fit (Burnham & Anderson 2002). Two biological qualities in particular were examined, median shell length and size at maturity. The L_∞ of the von Bertalanffy and Gompertz and the L_{95} of the inverse logistic were not statistically

significantly different to the median maximum shell length (Table 4.4). In addition, the L_{50} of the inverse logistic was not statistically significant to the size at maturity (SM_{50}) and the two were strongly correlated (Table 4.4). Given this high correlation, the L_{50} parameter of the inverse logistic may possibly be used as a proxy for size at maturity.

Recently the inverse logistic growth has been proposed as a candidate growth model for abalone populations (Haddon *et al.* 2008). In a study of *H. rufescens* in northern California the dose-response model (a growth model visually similar to the inverse logistic model) was statistically the best fitting model (Rogers-Bennett *et al.* 2007). However the dose-response model was rejected on the basis that the sharp transition in growth rate from constant juvenile growth to adult growth was not considered biologically plausible (Rogers-Bennett *et al.* 2007). The inverse logistic had a similar rapid transition and it was therefore considered important to investigate its biological validity. The transition appears to represent the size where growth increments are decreasing due to resources being allocated away from somatic growth and toward reproductive growth. It is possible that the onset of maturity may result in a rapid decrease in somatic growth rate (Lester *et al.* 2004). The strong correlation between the L_{50} parameter of the inverse logistic model and the SM_{50} in the present study clearly supports the biological validity of the inverse logistic model for blacklip abalone in Tasmania.

4.6 Conclusion

The inverse logistic adequately describes the growth of blacklip abalone populations over the geographic range of the species in Tasmania. The inverse logistic model was selected as

the best statistically fitting model for more sites than the von Bertalanffy or Gompertz. Akaike weights for the best fitting inverse logistic were also high leading to more confidence in the selection of this growth model. This finding is limited to models fitted to data with normal random errors. Nevertheless not only did the inverse logistic fit the data well but the model parameters were biologically valid. It is recommended that the inverse logistic be used in dynamic stock assessment modelling which includes a description of growth, because the von Bertalanffy or Gompertz growth models may introduce biases.

CHAPTER 5

Temperature gradients and population biology of *Haliotis rubra*

5.1 Abstract

Climate change is expected to realise relatively rapid warming of surface waters, especially along the east coast of Tasmania. What little is known about the influence of temperature on growth and maturity in wild abalone is confined to few populations or specific shell sizes. Ideally the entire juvenile phase, where most growth occurs, should be measured. In the present study, maximum shell length and somatic growth rate of 30 wild blacklip abalone populations and size at maturity of 252 populations were estimated in the presence of a natural temperature gradient. Maximum shell length significantly decreased with increasing temperature when mean maximum summer temperatures ranged between 16-21°C. The mean annual sea-surface temperatures across the 252 populations with maturity data ranged between 12-15 °C. Temperature had a significant effect on the size at maturity ($p< 0.001$) with a smaller size at maturity associated with higher temperatures. Measurements based on the growth residuals across the entire juvenile phase reveal a significant effect of temperature on the growth residuals over the entire juvenile phase ($p<0.001$). However, the decrease in growth rate may not be directly attributable to temperature but may be forced by the onset of maturity, which does appear to be directly influenced by temperature.

5.2 Introduction

5.2.1 Studying juvenile growth to detect impacts of climate change

Climate change is expected to realize rapid warming of surface waters in certain regions (IPCC 2007). Observations of water temperatures at abalone habitats along the coasts of eastern Australia, western USA and Normandy France have shown persistent increases throughout the time-frame of historical records (Ridgway 2007a; Rogers-Bennett 2007; Travers *et al.* 2009). Long term records along the south-east coast of Tasmania, spanning over 60 years, report an increase of 2.28^{o}C/century (Ridgway 2007a). With the exception of the North Pacific and North Atlantic, there is long term evidence of global ocean warming (Ridgway 2007a). Eastern Tasmania is a known major hotspot in the southern hemisphere, warming at 3.8 times the current global average (Ridgway 2007a).

Temperature is known to have an effect on biological traits within a species. One of the well known effects is known as Bergmann's rule where the meristic lengths of warm blooded vertebrates tend to be larger in cooler regions than in warmer regions within the same species (Mayr 1956). The trend associated with Bergmann's rule has also been demonstrated for several poikilothermic species (Ray 1960) including fish (Mayr 1956). Coastal fisheries consisting of sessile species are considered to be sensitive to increases in water temperature (Sharp 2003). The geographical ranges of temperature sensitive species are expected to contract towards cooler waters if temperatures exceed the thermal tolerance of a species (Rogers-Bennett 2007), which in Australia means a southwards contraction. In Australia, coastal fisheries in Tasmania are expected to decline since there is no continental shelf to contract to south of Tasmania, reducing the geographical range of

the species. This raises concerns about commercially valuable fish stocks in Tasmania where the effect of temperature upon biological traits is poorly understood.

Populations of blacklip abalone (*H. rubra*), around the coast of Tasmania and mainland Australia exhibit broadly varying population parameters and are subject to a range of temperature conditions. Being a poikilothermic and relatively sessile benthic invertebrate, blacklip abalone respond to local environmental conditions, integrating and expressing the recent history of these through their population biology (Miller *et al.* 2008; Saunders & Mayfield 2008). In Tasmania the mean shell length of harvested blacklip abalone is lower in the warmer waters of the north, and higher in the cooler waters of the south (Tarbath *et al.* 2008). This observation is currently only informally documented however, if true, a trend associated with Bergmann's rule may apply to abalone populations in Tasmania raising the possibility that ocean warming may lead to the mean size of individuals declining down the east coast, which would have marked economic consequences.

If it is assumed that the maximum shell length attained is associated with growth rate then it is also possible that warmer waters may be associated with lower growth rates, implying lower overall productivity. In a published controlled experiment, the optimum temperature for the growth of juvenile blacklip abalone was 17°C. Temperatures exceeding 21°C led to heat stress, which decreased growth rates (Gilroy & Edwards, 1998). Mean Tasmanian maximum summer water temperatures range between 16-21°C. The maximum of this range is at the upper limit of the stress free range of blacklip abalone under aquaria conditions. Temperature has also been shown to affect the size at maturity between populations. In New Zealand an observed decrease in size at maturity in wild populations of *Haliotis iris* was correlated with increasing water temperatures (Naylor *et al.* 2006). Similarly the size at the onset of maturity in wild populations of *Haliotis midae* in South

Africa was smaller in warmer waters compared to cooler waters (Newman 1969b). The impact of temperature on maximum shell length, growth rate and size at maturity on wild populations of blacklip abalone in Tasmania is presently unknown.

This study aims to characterize the maximum shell length, initial growth rate and size at maturity of abalone populations subject to a range of temperatures along the east and west coast of Tasmania. Unlike previous studies a large number of populations for each interaction was available; 30 populations for the interaction between temperature and maximum shell length, and for the interaction between temperature and initial growth rate, and 252 populations for the interaction between temperature and maturity. In addition, unlike previous studies, this study does not confine growth rate to few specific juvenile sizes. Instead the entire juvenile growth trajectory is used to examine the effect of temperature on growth over the entire juvenile size range. The study aims to quantify the relationship between temperature and the following three biological traits: maximum shell length, growth over the juvenile phase and size at maturity. A quantitative analysis of the effects of temperature on biological traits has the potential to be incorporated into the management and quantitative stock assessment of abalone populations and in forecasts of abalone yields under future climate change scenarios.

5.3 Methods

5.3.1 Data

A large database of field observations on abalone held at the Tasmanian Aquaculture and Fisheries Institute made it possible to conduct a large scale investigation of the biology of blacklip abalone under varying temperature conditions. All available growth and maturity data was used in the current study. Biological data for blacklip abalone used in the analyses were collected during fishery independent surveys conducted by research divers over a total period of 15 years from 1994-2008. Owing to different availability of samples, two subsets of the database were used: a subset for relating temperature to maximum shell length and growth rate which consisted of 30 samples and a subset for relating temperature to size at maturity, which consisted of 252 samples (Figure 5.1). The relationship between temperature and three biological traits was examined at the site spatial scale, being the finest spatial scale (Figure 5.1). Historically, the sites were selected on the advice of commercial divers who were actively harvesting and familiar with the region (Tarbath, Hodgson *et al.* 2001).

5.3.2 Sea temperature

Sea temperatures were collected from satellite data. However, coastal sea-surface temperature (satellite SST) data can be distorted by the proximal coastal landmass (Ling *et al.* 2009). Thus the validity of using satellite SST data to characterize the environment of

coastal populations was tested by determining the correlation between satellite SST and sea temperature data from available in-situ data-loggers (HOBO Water Temp Pro v2, accuracy of ±0.2°C over a 0° to 50°C temperature range, supplied by Onset Computer Corp., MA, USA). A large SST dataset was available that recorded daily temperatures derived from satellite SST readings from temporal (15 day) and spatial (0.042 º latitude and 0.036 º longitude degrees or 4 x 2-4.5km) composites (CSIRO 2004). To minimise interference from cloud cover, the 15 day (available every 6 days) median composite data set was chosen. The data has a spatial resolution of 4km in latitude and approx 4km in longitude. Satellite sea surface temperature values were extracted using Matlab 7.5 and the netcdf toolbox from UniDATA (University Corporation for Atmospheric Research). The satellite SST were first extracted at the nearest space and time locations to the data loggers and compared as a form of ground truthing the in-situ observations against the remote sensing estimates. The mean monthly satellite SST's were calculated and correlated against temperatures from data-loggers for the same location in space and time.

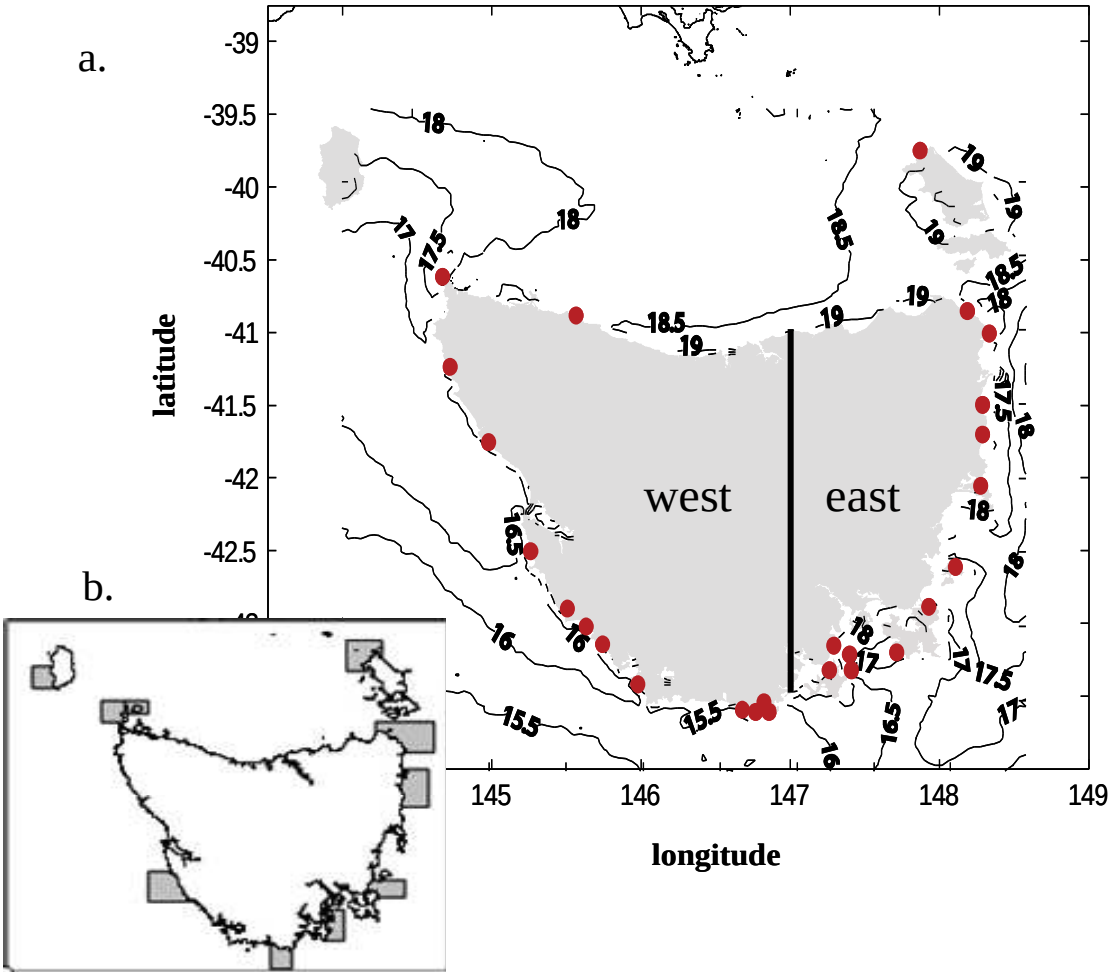

Figure 5.1. Schematic map of the distribution of sampling sites of tagged blacklip abalone around Tasmania illustrating two spatial scales; site spatial scale (Fig. a) and statistical block spatial scale (Fig. b). Analyses concerning temperature, (initial growth rate (MaxΔL), maturity (SM_{50}) and maximum shell length (L_{95})) were conducted at the site spatial scale (sites consisting of size at maturity data are too numerous to show here). The dataset, consisting of 30 tag-recapture samples (red dots), are presented in the context of water temperatures (℃) for the summ er month of February (Fig. a). Average February sea-surface temperature of the Tasmania region were derived from 15 day composite data averaged over the 1994-2008 period (CSIRO 2004). Samples are divided into east and west according to the southern boundaries of two ocean currents at 147℈ at the sou thern division (Ridgway 2007). The water temperature is represented by the contour plots. Temperature isobars are closer on the east coast than on the west coast indicating a greater temperature range along the east coast compared to the west. Analyses on correlations between biological traits (growth rate, maturity and maximum shell length) were conducted at spatial scale of statistical blocks and consisted of 10 samples (shaded in grey) (Fig. b).

SSTs were obtained in the same manner for each abalone sample considered in this study. Comparisons between temperature, maximum shell length, and growth rates were based on monthly mean SST data obtained over the year that tagged abalone were recovered. Similarly, comparisons between temperature and size at maturity were based on monthly mean SST data obtained over the year that field surveys were conducted. Data collected during surveys that differed in both time and spatial location were treated as separate samples. Owing to the presence of two major ocean current and the position of their boundaries (Ridgway 2007b) sites were deemed to be on the east coast if they had a longitude of greater than 147º, otherwise they were on the west coast.

5.3.3 Growth data

Individual growth rates of blacklip abalone were determined by fitting growth curves to length increment data obtained from tag-recapture studies. During the dives, the shell length of individual abalone were measured, allocated a numbered tag, and carefully returned to the same location, or at least proximal to where it was collected. Tagged abalone were then left at liberty for approximately one year before being removed and shell length measured. Growth increment data from different sites was accumulated in this way over a 15 year period, 1994-2008, from fishery independent surveys by the Tasmanian Aquaculture and Fisheries Institute (now part of the Institute for Marine and Antarctic Studies). Tagging data from each site was segregated according to the site and year of collection.

Five quality criteria were applied for data selection:

1) extreme negative growth increments, attributed to measurement or recording errors, were excluded i.e. data with length increments more negative than -3mm were excluded,
2) to define the full growth curve the sample needed to include juveniles i.e. less than 100 mm shell length, and,
3) initial lengths at release having a length increment of approximately 0 mm had to be included in the sample,
4) the time increment between mark and recapture was between 0.90 and 1.2 years,
5) The samples size of the samples was greater than n=90.

The effect of negative increments on model structure affected the model parameters of the Von Bertalanffy model (Chapter 3) and this formed criteria 1 for data selection. To minimize this effect, data with length increment < -3mm were removed (-3mm was selected to allow for some sampling error). Negative increments had negligible effects on model parameters fitted to the inverse logistic models (Chapter 3). It was shown in Chapter 3, that the inverse logistic assessment model successfully recovered the true growth trajectory if data included length increments close to zero, and this formed criteria 3 for data selection. Length increments were corrected for the time at liberty by dividing the observed length increment by the observed years at liberty (between 0.9 and 1.2 years) to normalize the length increments to one year.

In total there were 27 fishing sites with yearly tagging data. Three sites had multi-year data thus bringing the total to 30 samples that met the quality criteria above. These 30 samples of tag-recapture data represent locations that are frequently used as commercial fishing grounds (Figure 5.1). Two growth models, the von Bertalanffy and inverse logistic growth

models, were fitted to the 30 samples of annual tag-recapture data. The inverse logistic model was the best statistical model for modelling the growth of blacklip abalone populations in Tasmania (Chapter 4). The von Bertalanffy model was used to facilitate comparisons with external studies.

5.3.4 Growth model selection

The deterministic form of the von Bertalanffy model includes a size-based analogue re-parameterized for tag-recapture data, and used for estimating length increments from time increments. The inverse logistic is designed for tagging data and needed no transformation.

The von Bertalanffy (Fabens 1965; Haddon 2001):

$$\Delta L = \left(L_\infty - L_i\right)\left(1 - e^{-K\Delta t}\right) + \varepsilon \tag{5.1}$$

and the inverse logistic model (Haddon *et al.* 2008):

$$\Delta L = \frac{Max\Delta L}{1 + e^{Ln(19)\frac{\left(L_i - L_{50}^m\right)}{\left(L_{95}^m - L_{50}^m\right)}}} + \varepsilon \tag{5.2}$$

where ΔL is the expected length increment, L_∞ is the shell size where the mean length increment is zero (VB), L_i is the initial length when first tagged and released, K is the rate of change in length increment with increasing shell size, Δt is the time at liberty (as a fraction of a year), $Max\Delta L$ is the maximum length increment, L_{50}^m is the initial length at 0.5 times the difference between $Max\Delta L$ and lowest length increment and L_{95}^m is the initial length at 0.95 times the difference between $Max\Delta L$ and lowest length increment. The ε s

are independent additive normal random error terms. For simplicity, normal random errors were assumed for each growth model (Francis 1988b).

5.3.5 Size at maturity (SM_{50})

A large dataset existed within the Tasmanian Aquaculture and Fisheries Institute that consisted of maturity data obtained from 290 samples. Maturity data for blacklip abalone used in the analyses were collected during fishery independent surveys between 1996-2003 by the Tasmanian Aquaculture and Fisheries Institue (now part of the Institue for Marine and Antarctic Studies).

The method for determining maturity status was consistent for all samples in the database. Following is a brief account of how maturity was determined by previous technicians. Maturity was defined as the point at which gonad development matures to a state where the animal is capable of reproduction and can potentially contribute new recruits to the population. The state of maturity was determined by visual examination of gonad colour and size (Branden & Shepherd 1983; Tarbath 2003). Maturity data was classified into five groups: female, male, immature, undefined and trematode. Undefined included all data where the animals were mature but the sex was undefined. Trematodes included data where the capacity to reproduce was diminished due to the presence of trematodes in the gonads (Harrison & Grant 1971). Individuals where maturity was undefined or contained trematodes were omitted from analyses. Data consisted of shell lengths and associated counts of mature and immature individuals. The state of maturity was recorded alongside the shell length which was measured to the nearest 1 mm. Counts were stratified down to

site by year and males and females were combined. A logistic ogive was fitted to the proportional size at maturity data, using maximum likelihood methods and binomial residual errors (5.3) and (5.4) (Neter *et al.* 1990). The size at maturity (SM_{50}) value for each population was estimated as the length (l) at which 50% of the population are predicted to be mature (estimated as $-a/b$). The SM_{50} value is an approximation for a population.

$$\mu_l = \frac{e^{a+bl}}{1+e^{a+bl}} \tag{5.3}$$

$$-LL(a,b) = -\sum_{j=1}^{t}\left\{ Ln\left(\frac{N_j!}{n_j!(N_j!-n_j!)}\right) + n_j\left(a+bl_j\right) - N_j Ln\left(1+e^{a+bl_j}\right)\right\} \tag{5.4}$$

where μ_l is the predicted proportion of animals of length l expected to be mature, a and b are the parameters of the logistic curve, where b measures the rate of transition between immature and mature, l represents the t different length classes for which there are data, N_j is the total number of observations for length class l_j, n_j is the number of mature individuals in length class l_j and n_j/N_j is the observed proportion of mature animals observed in length class l_j.

Once the logistic function was fitted, samples were further excluded if they did not meet two data quality criteria concerning the coverage of the data across the sizes encompassing the size at maturity:

1) that the minimum observed proportion of mature animals was below 5%, and

2) that the maximum observed proportion of mature animals was greater than 95%.

5.3.6 Measuring the relative growth rate of populations

The relative growth rate of populations over the entire juvenile size range was determined using a technique modified from Morgan and Colbourne (1999) using a two step process. Firstly the inverse logistic model was fitted to tag-recapture data from each population. Secondly data from all 30 populations were pooled and the inverse logistic model was fitted to obtain increments to the pooled data. For all populations the juvenile portion was measured which included all individuals where initial length was below the inverse logistic L_{50} parameter. This parameter was used in lieu of size at maturity (SM_{50}, Chapter 4), owing to the absence of maturity data for some samples. The growth residuals for each population were obtained by subtracting the overall predicted mean length (of the pooled data) from predicted length increments (from each population). This value was divided by the number of juveniles to obtain the relative growth residuals of the juvenile portion of the population. The average residuals were calculated on the juvenile portion only. Populations with a mean residual greater than zero, indicated higher than average growth relative to the overall mean of all 30 samples combined (Morgan & Colbourne 1999). Likewise populations with a mean residual less than zero indicated below average growth relative to the all 30 samples combined. The values obtained from these growth residuals do not discern between growth patterns. For example, populations with a high growth residual may consist of either a very short period of fast growth which rapidly declines with size (as maturity commences) or the population may consist of moderately fast growing juveniles that maintain relatively high growth rates for a much longer period.

5.3.7 Statistical analyses

Data were subjected to ANCOVA tests. Where sites consisted of multiyear data, sample were segregated down to site by year and treated as a separate sample. Each site-by-year sample was considered to be independent therefore if one site consisted of data from two separate years the two dataset were treated as independent samples. The alternative option was to pool data from the two years. That would also entail having to pool together the SST data from the two years in which the biological data was measured. In addition for some samples the years may have differed by a considerable amount of time and as long as ten years in some samples. It was preferable to treat such temporally diverse samples as independent even though they came from the same site.

Temperature was analysed as continuous variable and coast was a factor with two levels: east and west. The maximal model for describing the effect of temperature for each biological trait for each coast was the most complex model.

Biological trait = temperature + coast + temperature:coast

Where the biological trait of interest included the following: Maximum shell length (L_{95} parameter of the inverse logistic model), initial growth rate (MaxΔL parameter of the inverse logistic model), size at maturity (L_{50} parameter of the inverse logistic model) and growth residuals.

The order of the terms (i.e. temperature and coast) has consequences to the final outcome (Crawley 2005). Temperatures differed between the two coasts, with higher mean temperatures on the east coast compared to the west coast. Therefore the coast term followed the temperature term in the maximal model. Model simplification was performed

if each term was insignificant ($p > 0.05$). The order of model simplification began by removal the interaction term (if it was insignificant), followed by removal of the coast effect (if it was insignificant).

5.4 Results

5.4.1 Ground-truthing satellite SST data

Satellite sea surface temperature measurements were obtained at the same location in space and time of each in situ datalogger site. In total 16 sites were sampled and 14 sites resulted in strong correlations in temperature between dataloggers and satellite SST measurements ($r > 0.8$) (Table 5.1). In the majority of sites (11) the correlation was very strong ($r > 0.9$).

The satellite SST temperatures tended to be shifted slightly higher than data logger temperatures at temperatures greater than 14 °C, which can be seen by comparing the observed values with a 1:1 temperature line (Figure 5.2).

Table 5.1. Correlations in monthly water temperatures between in situ data loggers and sea-surface temperature measurements (by satellite). The number of monthly readings for each datalogger is presented in the 'months' column. With the exception of one location where the r = 0.74, the mean monthly satellite SST temperatures strongly correlated with in-situ measurements (r > 0.9) at depths where abalone are found (n=16 sites).

sample	latitude	longitude	r	months
1	-40.76538	145.30817	0.98	15
2	-40.98667	148.34533	0.99	37
3	-41.87308	148.30950	0.97	31
4	-42.12547	148.09117	1.00	25
5	-42.19315	148.28300	0.99	21
6	-42.74470	148.01100	0.99	28
7	-42.74470	148.01100	0.92	31
8	-43.05453	147.41533	0.94	15
9	-43.11013	147.38500	0.91	36
10	-43.12883	147.67383	0.99	6
11	-43.12883	147.67383	0.99	24
12	-43.23388	148.00517	0.97	17
13	-43.50982	146.98150	0.86	42
14	-43.58752	148.04917	0.96	22
15	-43.59515	146.91850	0.96	8
16	-43.59515	146.91850	0.74	23

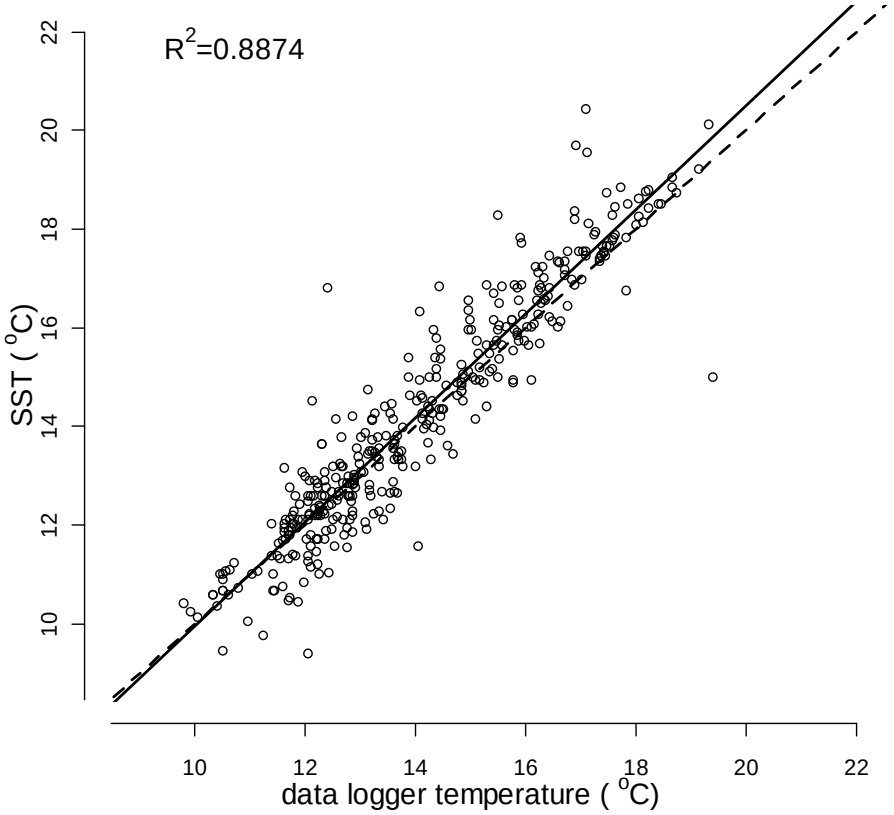

Figure 5.2. A correlation of mean monthly temperatures from satellite data (satellite SST) with mean monthly temperatures from 16 (in-situ) temperature dataloggers placed at locations and depths where abalone populations occur. The period of temperature readings for the dataloggers ranged from 6 - 42 months (see Table 5.1). SST was derived from 15 day composite satellite data (CSIRO 2004). The mean monthly satellite SST temperatures strongly correlated with in-situ measurements ($r = 0.942$, $R^2 = 0.8874$, for n=16 sites). Mean monthly satellite SST temperatures from the two devices were obtained in the exact point in time and geographical location. The dotted line represents a 1:1 correlation and the solid line represents the observed regression.

At 17°C, the optimal average temperature for juvenile abalone growth, the average satellite SST temperatures was 0.3 °C higher than the average datalogger. Many studies rely on satellite SST temperature and some other studies also report good agreement between satellite SST and actual in-situ measurements (Ridgway 2007b). Sample 16 of the datalogger readings had a moderate correlation ($r = 0.74$) despite it being at a identical

location to sample 15, which exhibited a very strong correlation between datalogger and satellite SST measurements ($r > 0.9$). The two samples differed in the datalogger instruments used. The two dataloggers were placed at the same location consecutively in time. The data logger used in sample 16 recorded a temperature of 19.4°C in February 2005 followed by a reading of 14.8°C in the following month. This reduction of 4.6°C in the timeframe of a month is not typical for the region in which it was collected. Therefore the source of the weak correlation is considered to be contributed by datalogger instrument error. Overall the strong correlation between the dataloggers and satellite SST measurements implies that using the satellite SST provides an accurate measurement of water temperature at depths where abalone are found. This validated the use of satellite SST for obtaining temperatures from sites with growth tagging data. Temperature data was collected in the year that tagged abalone samples were recaptured. In this way temperature data reflected the temperature conditions during the period at which tagged abalone were left at liberty. The mean annual average temperatures were determined for each location and year of the growth dataset used in this study.

5.4.2 Effect of temperature (satellite SST) on maximum shell length (L_{95})

The von Bertalanffy growth model is widely used to characterise the growth of marine populations, (Jákupsstovu & Haug 1988; McShane & Naylor 1995). To enable comparisons with other studies the von Bertalanffy is also used in the current study. However, here the inverse logistic model is used for all other analyses as it was shown to be statistically the best fitting model for abalone populations in Tasmania (Chapters 3 and 4). The L_{95} parameter of the inverse logistic model was used to characterise the distribution of

maximum shell size among abalone populations in Tasmania. The L_{95} represents the mean size at which 95% of the growth has occurred, nevertheless, for the purposes of this study the L_{95} parameter is considered to adequately represent differences in the mean maximum shell length between populations. The L_{95} ranged widely, (L_{95} ranged between between 97 – 178 mm, Table 5.2), and populations with the lowest maximum size in the State were located in the north, with five out of six populations having an L_{95} less than 150mm. Overall there was a latitudinal gradient in maximum abalone shell length, with northern populations having a lower mean maximum shell length size (mean L_{95} = 134mm, s.d = 23.6) than the central populations (mean L_{95} = 157mm, s.d=10.4) and southern populations (mean L_{95} =155 mm, s.d =15.8, Table 5.2). with the highest L_{95} of 178 mm recorded in a southern population.

Table 5.2. Growth parameters for 30 samples of length increment data. Two growth models, the von Bertalanffy, and inverse logistic are presented here. The best fitting model for each population was determined by a combination of AIC followed by a likelihood ratio test. The inverse logistic model was the best statistical model. The von Bertalanffy parameters are presented to enable comparisons with other published studies.

	site	latitude	longitude	year	von Bertalanffy			inverse logistic			
					Linf	k	s.d	MaxΔL	L_{50}	L_{95}	s.d
NORTHERN	315	-39.69	147.88	2001	121	0.338	2.869	19.6	87	121	2.678
	314	-39.93	143.83	2001	147	0.352	4.487	21.3	112	149	4.311
	313	-40.50	144.70	2001	128	0.289	3.480	18.1	92	128	3.377
	316	-40.73	148.12	2001	139	0.340	4.004	25.2	96	147	3.973
	662	-40.86	145.51	2006	102	0.202	2.567	9.0	78	97	2.492
	588	-40.92	148.32	2003	171	0.253	3.893	18.7	127	162	3.486
CENTRAL	170	-41.17	144.67	1995	141	0.266	2.679	12.3	116	146	2.662
	59	-41.57	148.32	1994	151	0.444	5.203	23.7	118	158	5.184
	59	-41.57	148.32	1995	141	0.475	3.022	27.6	105	145	2.871
	59	-41.57	148.32	1996	158	0.391	4.969	26.2	117	168	4.955
	300	-41.74	148.30	2003	164	0.524	6.014	31.9	123	157	5.264
	819	-41.76	145.00	2008	141	0.313	2.809	20.6	105	141	2.662
	297	-42.20	148.35	2003	152	0.423	5.263	25.8	115	152	4.942
	159	-42.58	148.05	1994	160	0.321	3.487	19.5	125	169	3.500
	159	-42.58	148.05	1996	175	0.344	7.578	20.4	139	169	7.328
	272	-42.61	145.26	2001	162	0.330	3.347	24.6	120	163	3.223
SOUTHERN	337	-42.87	147.94	2003	141	0.298	4.581	17.4	108	138	4.190
	458	-42.96	145.49	2003	172	0.255	3.998	19.5	131	167	3.423
	663	-43.04	147.48	2007	128	0.569	4.658	34.9	88	134	4.384
	460	-43.07	145.66	2003	164	0.345	4.423	19.3	131	160	4.193
	482	-43.11	147.40	2003	150	0.546	4.122	26.5	118	154	4.000
	461	-43.11	147.38	2003	173	0.332	4.344	28.1	122	173	4.090
	764	-43.14	147.68	2006	166	0.355	3.723	25.7	123	174	3.673
	702	-43.14	147.39	2006	163	0.398	4.967	31.8	115	178	4.954
	470	-43.22	145.78	2003	171	0.283	4.131	22.3	127	167	3.826
	459	-43.48	146.02	2003	155	0.337	2.597	15.9	128	155	2.459
	813	-43.51	146.98	2008	141	0.215	2.869	12.7	112	132	2.488
	815	-43.53	146.96	2008	144	0.295	2.936	16.3	113	151	2.928
	478	-43.54	146.99	2003	145	0.357	3.872	22.3	110	146	3.589
	480	-43.56	146.89	2003	136	0.479	4.242	30.0	97	137	3.910

ANCOVA results between L_{95} parameter (of inverse logistic) and mean annual SST temperature (Figure 5.3) indicate a significant effect on maximum shell length ($p<0.05$), where maximum shell length decreased as temperature increased. However it should be noted that small and large maximum shell length occurred at all temperatures and the correlation between temperature and maximum shell length may need further work.

There was a significant difference in maximum shell length between east and west coasts ($p<0.05$) with the west coast being 17 mm lower than the east coast (correcting for temperature). The regression equation on the west coast was

$$\text{Maximum shell length } (L_{95}) = -5.56 * \text{SST} + 240.06 \quad (5.5)$$

The regression equation on the east coast was

$$\text{Maximum shell length } (L_{95}) = -5.56 * \text{SST} + 257.04 \quad (5.6)$$

Blacklip abalone populations in the warmer northern regions of Tasmania are smaller than the cooler southern waters indicating that the trend associated with Bergman's rule may also apply to this poikilothermic species.

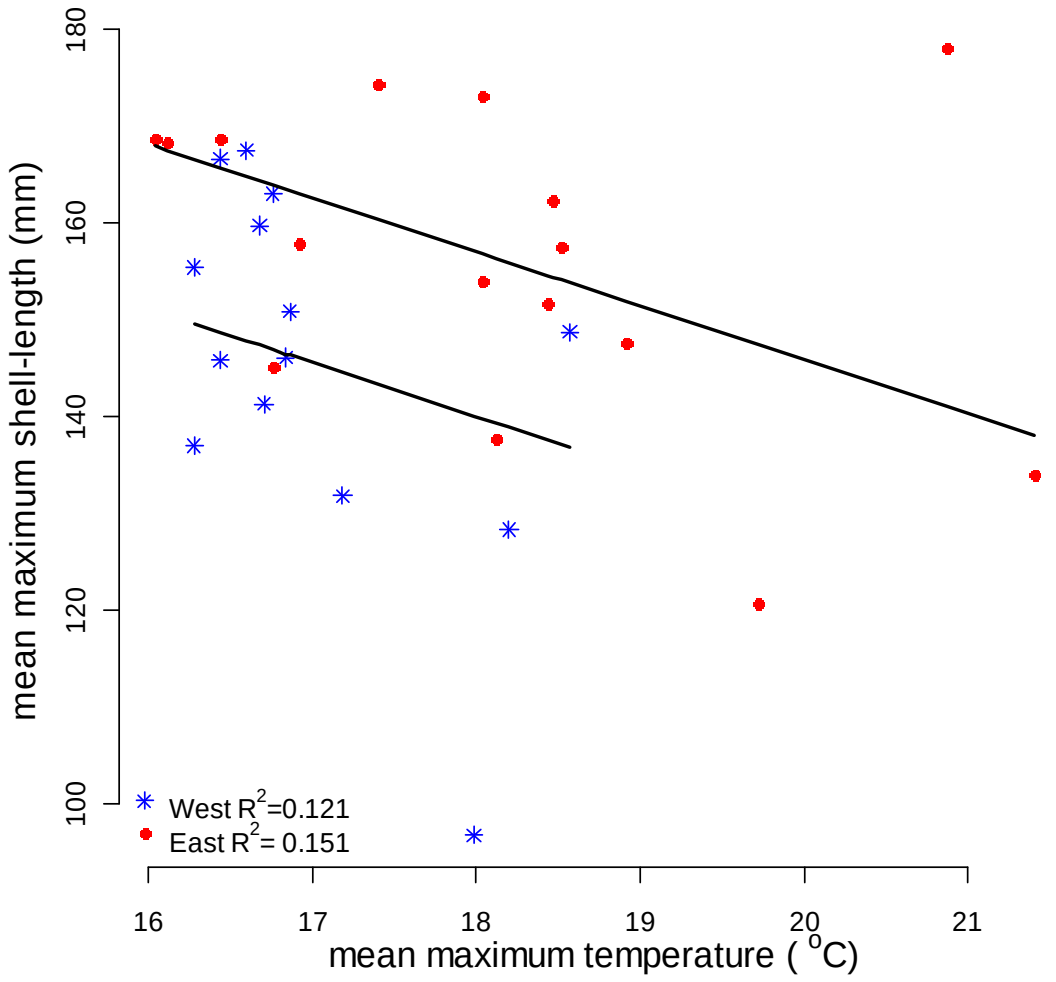

Figure 5.3. Correlation between temperature and maximum shell size using the L_{95} parameter of the inverse logistic model to obtain mean maximum shell length. Mean maximum (February) temperatures were used because higher temperatures (>21°C) were found to have an observed decrease upon growth rate in cultured adult abalone (Gilroy & Edwards 1998). Sea-surface temperatures were obtained at each site of the 30 tag-recapture samples in the year that the abalone in that sample were recaptured. Samples are divided into east and west at a latitude of 147°E

5.4.3 Effect of temperature (satellite SST) and size at maturity (SM_{50})

A second data set from 215 sites was used to determine the effect of sea temperature on size at maturity. Of the 215 sites, 28 consisted of multi-year data bringing the total to 252 populations (samples which differed in space or time were considered separate populations). Size at maturity for the 252 samples ranged between 72 – 130 mm. It is not likely that the size range in maturity considered here is representative of the entire population of blacklip in Tasmania however correlation values here will only be applied to the 72 – 130 mm size range. Across both coasts there was a negative correlation between size at maturity and mean annual temperature (Figure 5.4). Temperature had a significant influence on size at maturity for blacklip abalone populations considered in the current study ($p < 0.001$), indicating that populations in warmer temperatures matured at smaller sizes. However, there was no significant difference in the influence of temperature between east and west coast populations ($p=0.727$). In contrast, the difference in size at maturity between coasts was significant ($p < 0.05$) with size at maturity on the west coast being 3.6 mm larger than the east coast. This result is plausible given that temperatures on the east coast are generally higher than the west coast.

The final regression equation of size at maturity as a function of temperature for each coast was determined for both east and west coast populations (Figure 5.4)

east coast: size at maturity (SM_{50}) = - 5.7562 * satellite SST + 182.757 (5.7)

west coast: size at maturity (SM_{50}) = - 5.7562 * satellite SST +186.400 (5.8)

On both coasts a 1ºC increase in water temperature may result in a 5.76mm/yr decrease in size at maturity when mean annual temperatures range between 10-16°C.

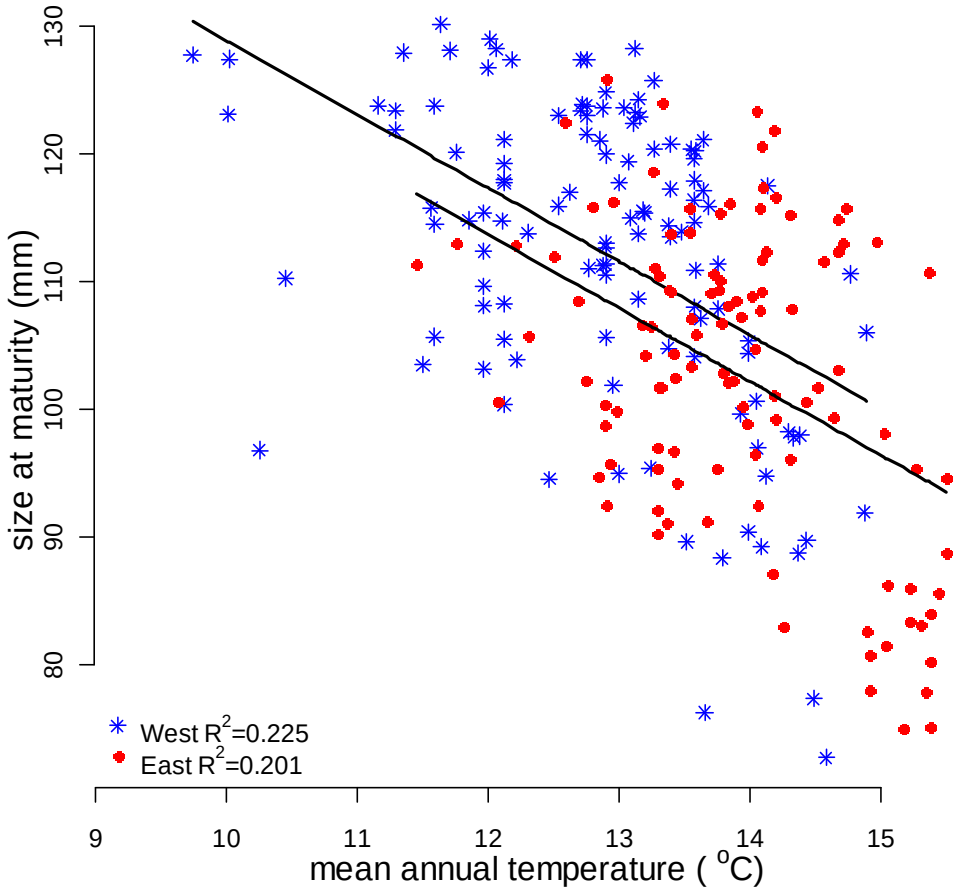

Figure 5.4. Correlations of mean annual temperature with size at maturity (SM_{50}). Sea-surface temperatures were obtained for a total of 252 samples divided into east and west at a latitude of 147°E (Figure 5.1). Regression lines shown were determined by ANCOVA.

5.4.4 Correlating growth residuals to water temperature (SST)

Populations with negative growth residuals, implying slower relative growth, were distributed all around Tasmania, although not evenly (Table 5.3). In the north of the state 50% of populations had negative growth residuals whereas in the south only 14% had

negative growth residuals. Overall the spatial distribution of growth residuals reveals a latitudinal gradient with low growth residuals more likely in the north, (Table 5.3). The occurrence of relatively slow growing populations in the north of the State has been reported since at least 1998 (Gilroy & Edwards 1998). The distribution of fast and slow growing populations around the State using growth residual analyses agrees with published reports and observations from experienced abalone divers but also provides a quantitative relative index.

Table 5.3. The relative growth residuals of 30 populations distributed around Tasmania exposed to varying temperature conditions. Samples are ordered according to latitude. The more negative the growth residual the slower the relative growth rate for that population, the more positive the growth residual the higher the growth rate. 'Year' relates to the year that the tagged abalone were recaptured. Mean annual temperature refers to the mean for the year of recapture. Maximum temperature refers to maximum February temperature in the year of recapture.

	site	latitude	longitude	year	growth residual	Temperature mean annual (°C)	Temperature maximum (°C)
NORTHERN	315	-39.69	147.88	2001	-3.8	15.5	19.7
	314	-39.93	143.83	2001	0.5	15.3	18.6
	313	-40.50	144.70	2001	-5.5	14.3	18.2
	316	-40.73	148.12	2001	-1.3	15.0	18.9
	662	-40.86	145.51	2006	-11.5	14.3	18.0
	588	-40.92	148.32	2003	3.8	14.7	18.5
CENTRAL	170	-41.17	144.67	1995	-3.3	11.8	16.8
	59	-41.57	148.32	1994	3.9	13.7	16.9
	59	-41.57	148.32	1995	3.8	13.7	16.8
	59	-41.57	148.32	1996	5.4	13.6	16.1
	300	-41.74	148.30	2003	10.3	14.0	18.5
	819	-41.76	145.00	2008	-1.6	14.0	16.7
	297	-42.20	148.35	2003	3.2	14.7	18.4
	159	-42.58	148.05	1994	3.4	13.6	16.4
	159	-42.58	148.05	1996	5.9	13.2	16.0
	272	-42.61	145.26	2001	4.6	13.3	16.8
SOUTHERN	337	-42.87	147.94	2003	-2.7	14.4	18.1
	458	-42.96	145.49	2003	3.4	13.1	16.4
	663	-43.04	147.48	2007	1.3	14.7	21.4
	460	-43.07	145.66	2003	5.4	12.8	16.7
	482	-43.11	147.40	2003	6.6	13.6	18.0
	461	-43.11	147.38	2003	7.7	13.6	18.0
	702	-43.14	147.39	2006	5.6	14.4	20.9
	764	-43.14	147.68	2006	6.2	13.6	17.4
	470	-43.22	145.78	2003	4.9	12.8	16.6
	459	-43.48	146.02	2003	1.5	12.7	16.3
	813	-43.51	146.98	2008	-4.7	13.7	17.2
	815	-43.53	146.96	2008	-2.0	13.7	16.9
	478	-43.54	146.99	2003	1.1	13.6	16.4
	480	-43.56	146.89	2003	5.8	11.8	16.3

Juvenile populations with relatively low growth residuals occurred along both the east and west coasts of Tasmania (Figure 5.5). A previous study (Chapter 2) using modal progression analysis characterized the growth of juvenile between 10 - 75 mm. The growth rate of wild population of juveniles increased with increase in temperature (Figure 5.6). However the relative growth residuals of 30 populations distributed around Tasmania, and exposed to varying temperature conditions, indicates a negative correlation between growth residual and temperature demonstrating that juvenile populations with relatively slow growth occur in warmer temperatures (Table 5.3, Figure 5.5) The effect of temperature on growth residual was significant on both east and west coast ($p<0.01$). The correlation between growth residual and average annual temperature is stronger on the east coast ($r = 0.555$) than on the west coast ($r = 0.4$). However, there was no significant difference in the effect of temperature on growth residual between coasts ($p= 0.52$).

The regression equation of the growth residual as a function of water temperature was determined for both east and west coast populations (Figure 5.5),

west coast: growth residual= -2.469 * satellite SST + 32.25 (5.9)

east coast: growth residual = -2.469 * satellite SST + 38.20 (5.10)

There was a significant difference in growth residuals between east and west ($p<0.01$) with the east coast being 5.947mm/yr greater than the west coast. From the regression equations a 1ºC increase in water temperature resulted in a 2.469 mm/yr decrease in relative growth residuals on both the east and west coast.

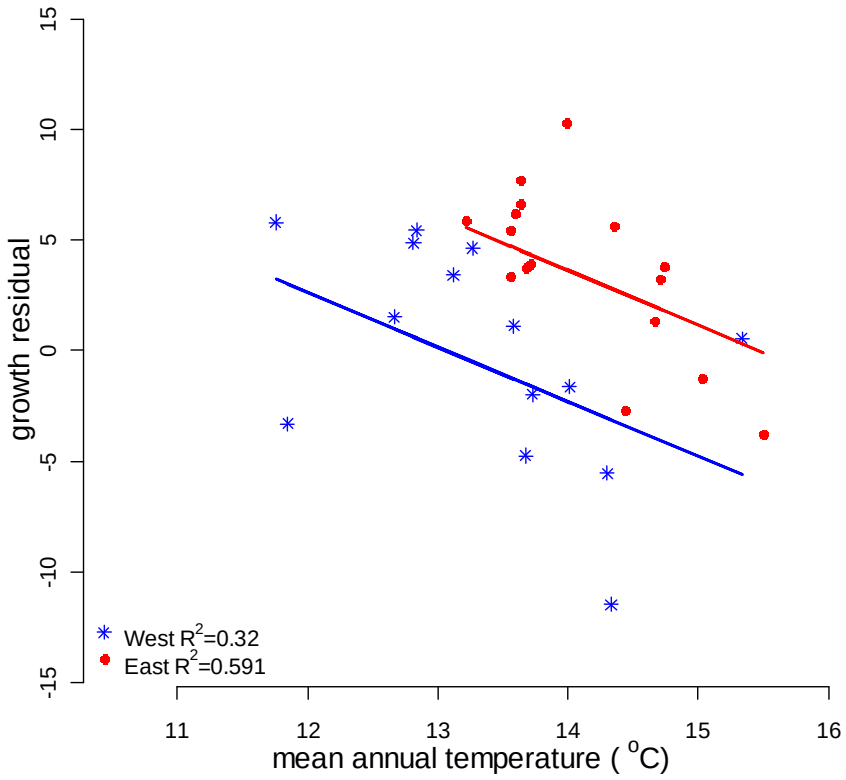

Figure 5.5. A correlation of mean annual satellite SST temperature and growth residuals for 30 abalone populations in Tasmania showing a negative correlation between temperature and growth residuals. A total of 30 populations were distributed around Tasmania and divided into east and west at a latitude of 147°E (Figure 5.1). Regression lines shown were determined by ANCOVA. Temperature specific growth residuals were lower on the west coast (n=14) compared to the east coast (n=16).

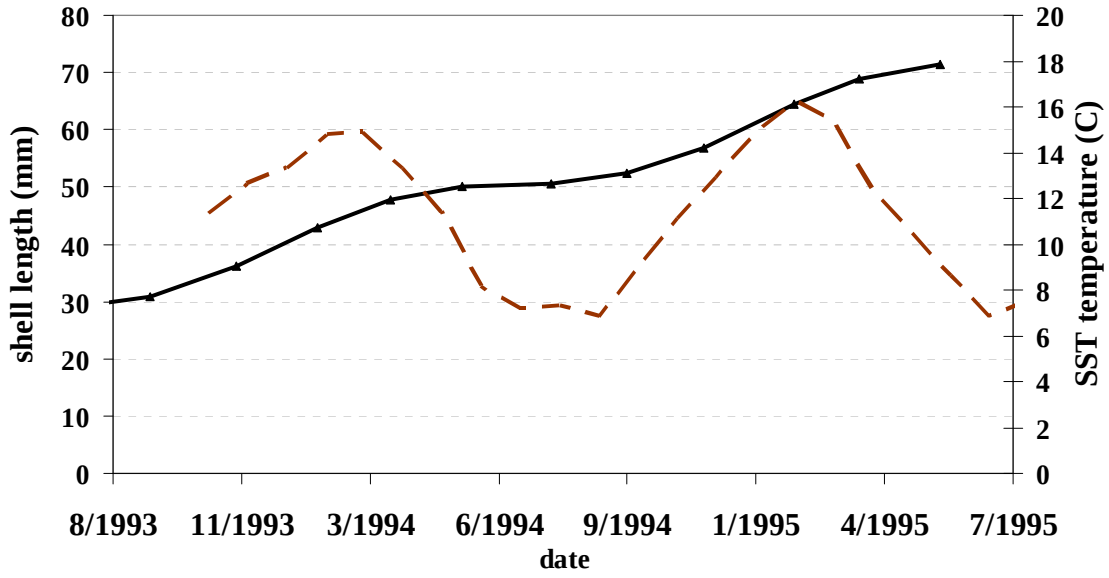

Figure 5.6. The relationship between the growth of juveniles (30mm - 70mm) and temperature. The solid line represents the growth of juveniles determined by modal progression analysis from a cohort at Hope Island Tasmania (43.20°S, 147.05°E) on the east coast of Tasmania between August 1993 – May 1995 (Chapter 2). The subdivision of data into cohorts came from the optimum modal analysis (Chapter 2). The solid black line represents monthly mean temperature (satellite SST) at Hope Island.

5.5 Discussion

A wealth of knowledge exists on the optimum temperature conditions for the growth rate of juvenile abalone (Gilroy & Edwards 1998) under controlled conditions. Information that reconciles controlled experiments with wild populations facilitates research into the effect of water temperature on stock productivity. Therefore Haliotids, are excellent candidate species for studying the effects of climate change on biological traits, particularly blacklip abalone which prefers cooler waters. Information about the effects of climate change on commercially valuable species are often constrained by limited biological knowledge. However, the effect of temperature on biological characteristics in Haliotids is studied

more extensively under controlled conditions than in wild populations owing to the rapidly expanding aquaculture industry driving this research. Nevertheless results from controlled experiments contribute to the understanding of temperature effects on the more difficult to study wild populations.

5.5.1 Temperature and maximum shell length

Observations from 30 wild abalone populations considered in the present study, indicate that the mean asymptotic shell length decreased as mean temperatures increase. Accordingly, abalone populations in Tasmania seem to conform to the size-temperature trend associated with Bergmann's rule. The trend may possibly apply to all abalone populations in Australia which incorporates the entire geographic range of the species. Water temperatures are warmer in regions north of Tasmania, and the asymptotic shell length is generally lower than Tasmanian populations; 115-138 mm in New South Wales (Worthington & Andrew 1998), 117 – 142 mm in Victoria (McShane *et al.* 1988) and 138 – 144 mm in South Australia (Shepherd & Hearn 1983) compared to an observed maximum of 178 mm in Tasmania (Table 5.2). The maximum shell length range of 97 – 178 mm observed in abalone populations considered in the current study is consistent with values reported previously for this species in Tasmania (124-172 mm) (Nash 1992). Similar length-temperature trends are documented for a range of abalone species. In South Africa, *H.midae* attains a smaller asymptotic shell length (approximately 155 mm) in warmer waters (maximum temperature 20.9^{o}C) compared to cooler waters (163-210 mm in 14.4-17.1^{o}C), (Tarr 1995) echoing a trend observed previously for that species (Newman 1969a).

Similarly in New Zealand, the asymptotic shell length of *H.iris* declined in warmer waters above 18^{o}C (Naylor *et al.* 2006).

The application of Bergman's rule for abalone populations in Tasmania is defined solely in an empirical sense; as a simple observation correlating shell length size with temperature. Admittedly the physiological mechanism that underlies Bergmann's rule is not considered, and questions are raised in the literature regarding the appropriateness of ascribing Bergman's rule in the absence of any causal mechanisms (Ray 1960). Nevertheless it has been put forth that the rule is a fundamental phenomenon in the animal kingdom (Ray 1960). Studying Bergman's rule with the above consideration in mind, the size-temperature trend observed, is a valid generalization for blacklip abalone populations in Tasmania.

5.5.2 Temperature and maturity

An important finding in the present study is that observations from 252 abalone populations reveal that size at maturity decreases as temperatures increase. Similarly the size at maturity of *H.iris* decreased with an increase in temperature (Naylor *et al.* 2006). It is possible that for blacklip abalone in Tasmania a 'maturity rule' similar to Bergmann's rule for maximum shell length may apply to size at maturity and temperature. That is, within the species, individuals that mature at smaller sizes occur in warmer regions and individuals that mature at larger sizes occur in cooler regions.

The decrease in size at maturity may be due to one of two possibilities. Either juvenile growth rates decline as a result of warmer temperatures leading to smaller size at maturity

or the onset of maturity is brought about earlier by warmer temperatures leading to an associated decline in growth rate of larger juveniles that are approaching maturity.

5.5.3 Temperature and growth rate

For the large part, the growth of juveniles is exclusively somatic during the juvenile stage and differs from adult growth, which is a combination of somatic and reproductive growth. The juvenile phase is pertinent because it is where growth occurs most rapidly (Godø & Haug 1999; Morgan & Colbourne 1999).

Aquaria studies report variable responses of the growth of blacklip abalone with incremental increases in water temperature. The water temperature at which growth was maximal ranged between 16.4-17.3 ^{o}C (Gilroy & Edwards 1998; Harris *et al.* 2005). Above 21^{o}C abalone exhibited physiological stress, reduced growth rates, and sporadic movement (Gilroy & Edwards 1998). At 24.4^{o}C abalone begin to dislodge from the substrata eventually resulting in mortality (Gilroy & Edwards 1998). The critical thermal maximum occurs at 26.9^{o}C, where 50% of the population dislodge from the substrata (Gilroy & Edwards 1998). The temperatures at which blacklip abalone exhibited stress under aquaria conditions (i.e. >21^{o}C) are well above the average temperatures that occur in Tasmanian waters. On a seasonal time scale, growth increments over the winter period are lower than the summer period (Shepherd & Hearn 1983) and this was observed in a juvenile population at Hope Island Tasmania (Figure 5.6). Therefore the mean temperatures reported in natural conditions for the 30 samples of tag-recapture data were within the thermal tolerance of the species and were optimal for rapid growth. Mean temperatures are

used as an indication of the coldest and warmest areas. In reality, fluctuating temperatures affect abalone growth rates differently than simple averages of fluctuation conditions. However average temperatures have been successful in measuring the effect of temperature on meristic developments in fish (Ray 1960).

This leads to another major shortcoming in the study of water temperature and its effect upon growth rate in wild populations: a lack of prior knowledge about the thermal tolerance and thermal optimum range of the species. Studies into the effect of temperature on growth for south African *H.midae* (Tarr 1995) indicate that although growth rates varied, summer temperature maxima, which ranged between 14.4 – 20.9^{o}C, did not affect growth rate. However controlled aquaria experiments later indicated that temperatures between 12 - 20^{o}C were optimal for growth of *H.midae* (Britz *et al.* 1997). Considering the aquaria findings in conjunction with wild populations, it is reasonable to assume that wild populations of *H.midae* were located at temperatures that aquaria studies later revealed were optimal for the growth of the species and may explain why there was no correlation between growth rate and temperature in wild populations (Tarr 1995). Food availability has been suggested to contribute to the variability of growth rates between populations (Day & Fleming 1992; Tarr 1995). This suggests that to some degree temperature and nutrients may be independent in their influence on abalone growth. Aquaculture studies for many Haliotid species also suggest that this may be the case. However it has also been reported that temperatures above the thermal tolerance can decrease growth rate of juveniles even though feed is provided to excess (Britz *et al.* 1997; Grubert 2002; Steinarsson & Imsland 2003). Aquaria studies have therefore established that temperature plays a key role in controlling the physiological processes affecting initial growth rate. Studies suggest that increasing the temperature increases the metabolic rate. This increase in metabolic rate may

lead to an increase in growth (Searle *et al.* 2006), however this also increases the oxygen demands, possibly beyond the capacity of the surrounding waters (Searle *et al.* 2006). For this reason optimal temperatures have been observed to be size specific (Steinarsson & Imsland 2003; Searle *et al.* 2006): the larger the abalone the lower the optimal temperature for growth. Therefore temperatures need to decrease with increasing abalone shell length to sustain optimal growth rates throughout the juvenile period (Steinarsson & Imsland 2003; Searle *et al.* 2006), possibly as oxygen demand among larger juvenile becomes a limiting factor to growth.

In Tasmania, east coast populations generally have higher juvenile growth residuals than west coast populations at the same latitude (Figure 5.5). There may be two possible reasons for this. Firstly waters on the east coast of Tasmania tend to be warmer than the west coast at the same latitude. Wild populations that experience a greater accumulation of days with optimal temperature conditions (i.e. 17^{o}C, (Gilroy & Edwards 1998)) may have a greater growth advantage over populations in colder or much warmer regions. It is likely that east coast populations experienced more days of optimal temperatures over the juvenile period than west coast populations thereby enabling them to grow faster during the juvenile growth period. Secondly, if there are differences in temperature specific nutrient loads between the two coasts, then the slightly higher initial growth rates on the east coast may also reflect higher nutrient levels on the east compared to the west. This is currently speculative. Nevertheless the east coast has higher temperature anomalies and this is indicative of higher replenishment of nutrient loads (Ridgway 2007a).

Growth rate and age or size at maturity are two important population biology parameters that are often studied in combination and found to be correlated (Shepherd & Laws 1974; Belk 1995; Saunders & Mayfield 2008). The size at which blacklip abalone mature has

previously been claimed to correspond with their emergence out of crypsis (Peck *et al.* 1987; Prince *et al.* 1988b; Nash *et al.* 1994). The growth of individuals in South African populations of *H. midae* was reported to be affected by internal physiological processes, such as the onset of maturity (Newman 1968). Growth declines at that stage are commensurate with the onset of maturity as energy is transferred from somatic growth toward reproductive growth with a reduction in shell growth rate being expected (Lester *et al.* 2004).

The method of using growth residuals to distinguish between relatively fast and slow growing populations has not previously been attempted for blacklip abalone. Studies on influence of growth and temperature usually examine size specific growth rate rather than the entire juvenile phase (Naylor *et al.* 2006). The growth rate of juveniles slows down as they approach maturity and selecting particular size class to measure growth rate can introduce confounding effects with the onset of maturity, especially given that different populations mature at different sizes. For example, size at maturity (SM_{50}) in Tasmanian populations ranged between 72 -130 mm. The difference in size at maturity between populations may lead to an unequal influence of the growth rate of say 100 mm abalone. It has been suggested in published studies that the K parameter of the von Bertalanffy be used to describe growth rate (Francis 1996). However the K parameter is not a parameter for growth rate in term of size increments per unit of time (i.e. mm/yr). Instead the parameter measures the rate of decrease in growth rate per size class unit (i.e. mm/yr/mm). For all these reasons the K parameter was considered inappropriate for describing the growth of the juvenile portion of abalone growth and instead growth residuals were used.

The trend observed in this chapter is that abalone populations with relatively lower overall growth in the juvenile stage also had relatively lower size at maturity. Quantifying the

relative growth residual over the entire juvenile period, using a modified version of the average residual technique from Morgan and Colbourne (1999), simultaneously captures the effect of temperature upon the growth rate of small and large juveniles and the size at maturity. There appeared to be a noticeable decline in growth residuals over the juvenile period in response to increases in water temperature (Figure 5.5), indicating that growth over the entire juvenile stage was relatively slower at locations where temperatures were warmer. Given that energy is partitioned away from somatic growth toward reproductive growth in large juveniles, it is possible that the decrease in growth residuals was partly driven by the onset of maturity, which in turn was driven by an increase in temperature (Newman 1969a).

Temperature aside, growth rates of blacklip abalone in Australia vary considerably over small spatial scales (10's km) (Worthington & Andrew 1998). Nevertheless a latitudinal cline in growth rates was previously reported for blacklip abalone populations in Tasmania (Nash 1992). Populations in the cooler waters of the south were considered to have faster growth rates compared to the warmer waters of the north. This trend is partly supported by the findings in the current study where northern warm water populations had slower growth residuals than cooler southern populations. One possible reason may be evident in the temperature-maturity observations in the current study. Here the onset of maturity occurred at smaller size in the north compared to the south. With the associated reallocations of energy away from somatic growth toward reproductive growth, it is valid to suggest that size specific somatic growth of larger juvenile abalone is slower in the north compared to the south.

It is reasonable to associate asymptotic shell length with growth rate: the greater the asymptotic shell length the higher the growth rate must have been. However observations

of northern populations of blacklip are anomalous. Relatively low maximum sizes in the north consisted of initial growth rate estimates (MaxΔL) that were as high as southern populations (Table 5.2). Maximum initial growth rates (MaxΔL) greater than 20 mm/yr occurred in both warmer waters in the north (sites 314, 315, 316) and cooler water of the south (n = 9 sites Table 5.2), however the populations in the cooler water of the south had a maximum shell length (L_{95}) approximately 20 mm greater than population in the north for the same juvenile growth rate. This apparently anomalous result was also reported in *H.midae* in South Africa where populations with fast juvenile growth had smaller maximum shell length in warmer waters (Newman 1969a). A possible explanation is that northern populations occur in temperatures that are likely to accumulate a greater number of days at warmer temperatures. Warmer temperatures may be driving the relative early onset of maturity causing populations in warmer temperatures to mature at smaller sizes compared to populations in cooler temperatures. Once maturity commences energy is reallocated away from somatic growth and hence the asymptotic shell length is lower in warmer populations. Although individuals from populations at cooler temperatures grow at a slower growth rate during the juvenile phase, the growth period is maintained for a longer period because the onset of maturity occurs later in cooler temperatures. The implication is that the onset of maturity may not only be driven by a time clock or a size clock but may also be driven by a 'temperature clock'. Therefore the resulting growth residual over the entire juvenile phase may be a compromise between the optimal temperature for maturity (which slows somatic growth rate) and the optimal temperature for growth (which increase growth rate).

5.6 Implications to fisheries management

The causes of global warming are expected to persist into the future and climate model simulations project an associated increase in water temperature over the next few decades both in Australia and globally (IPCC 2007; Poloczanska *et al.* 2007). Quantifying relative differences in growth and maturity between populations enables stock assessments to be tailored to individual populations. Satellite SST data has successfully predicted trends in biological traits and provide a practical means for modelling the effects of increasing temperatures upon yields making it practical for stock predictions. The extensive surface coverage provided by Satellite SST makes it possible to describe the environmental effect at a spatial scale larger than the biological heterogeneity of blacklip abalone but finer than the larger spatial scale of the fisheries management zones. Size at maturity declined with increasing mean annual water temperature and the effect upon the productivity of populations is not as straightforward as previously suggested in the literature, meaning that increasing water temperatures may act in opposite directions with respect to growth rates and size at maturity (i.e. growth rates increase but the size at maturity decreases). For example, temperatures around 17°C are optimum for growth of juvenile blacklip but these temperatures are also likely to initiate the onset of maturity (Newman 1969a). Providing that populations have had a substantial period of optimal growth at approximately 17°C the size at maturity may be slightly higher than population that have fewer days of optimal growth temperature but warm enough to initiate the onset of maturity. Knowledge of the effect of temperature (and its associated factors) upon growth and maturity will enable future biomass predictions and stock assessments to incorporate the potential effects of

elevated temperature (with its associated factors) predicted to occur if the current trends of climate change persist.

CHAPTER 6

The effectiveness of broad-scale Legal Minimum Lengths for protecting spawning biomass

6.1 Abstract

It is widely recognized that broad-scale Legal Minimum Length (LML) limits may fail to protect the spawning stock of exploited populations. Data that can define growth and maturity are often lacking at a fine spatial scale and this can limit the estimation of LML on a regional basis. A method is introduced for generating growth parameters from size at maturity data. Fine-scale theoretical LML estimates could then be obtained in the absence of empirical growth data. The method was scaled up to obtain theoretical LML estimates for 252 blacklip abalone populations in Tasmania, Australia, at a spatial scale not previously possible. In total, 106 sites appeared to be adequately protected. These sites were mostly to the north west of Tasmania, in regions that were not economically valuable. In contrast 46 out of the 252 populations were considered under-protected, potentially placing those populations at risk of over-fishing. The majority of the unprotected sites were in the south west, a region that is economically valuable. The LML setting in the economically valuable south west region must be increased in order to achieve the management goals of the LML rule.

6.2 Introduction

Legal Minimum Length rules (LML) are commonly used worldwide to help conserve fish stocks and meet economic objectives in the presence of environmental challenges (Martin & Maceina 2004; Stewart 2008). The LML is one the oldest and most broadly used management tool, adopted to protect spawning stocks against recruitment overfishing (Haddon 2001; Stewart 2008). Despite their extensive use, the performance of LMLs in meeting management objectives is rarely assessed (Stewart 2008). A successful LML is achieved if the set minimum harvestable size protects the population's reproductive potential by allowing the mature portion to undergo a sufficient number of breeding cycles. The consequent recruitment should then be able maintain the stock at acceptable biomass levels (Hilborn & Walters 1992; Martin & Maceina 2004; Stergiou *et al.* 2009). The LML setting commonly consists of two population parameters; growth-rates and size at maturity. Without population specific details of growth rates the proportion of the mature population protected by the LML will remain unknown. Clearly, if the LML settings are too low, the population is at risk of overfishing and therefore failing to meet management objectives. Conversely, if the LML is too high, stocks may be over-protected increasing the risk of opportunity costs through foregone catch and the decline in the quality of legal sized product.

The LML was the first management rule implemented when the fishery was first established in 1962. One of the current Management Plan objectives is to allow mature abalone two breeding cycles before harvesting (Tarbath, Haddon *et al.* 2001). Assuming one breeding cycle occurs annually, the length increment corresponding to two years growth past the size at maturity (SM_{50}) needs to be determined. The SM_{50} is an estimate of

the shell length at which 50% of the population is mature. LML size-limits for blacklip abalone in Tasmania are thus determined by adding the predicted two year growth increment to the size (shell length) at maturity (SM_{50}) (Tarbath, Haddon *et al.* 2001). The growth increment added to SM_{50}, to attain the LML setting, provides a buffer between strong and weak reproductive events in species with unpredictable recruitment patterns (Francis & Shotton 1997; Martin & Maceina 2004).

Ideally the LML should be set so that all mature individuals in a population are afforded enough time after maturity to produce young and sustain the population indefinitely. While there are numerous size at maturity samples collected from a broad geographical distribution around Tasmania, the main limitation in calculating the LML is paucity of growth data available (Tarbath, Haddon *et al.* 2001). Ideally population specific growth data is important in generating growth parameters and determining the LML. However in the absence of empirical data growth needs to be estimated theoretically, in order to determine the suitable length increment that factors in the time taken to produce young and adequately sustain the population.

Abalone populations in Tasmania are generally self sustaining closed populations with only minor exchange of recruits between populations (Temby *et al.* 2007). An LML setting may provide protection in one area but not confer protection on populations in neighbouring areas (approx > 100 m apart) (Prince *et al.* 1988b; Temby *et al.* 2007). It is thus inevitable that some populations will be over-protected while other populations remain under-protected by broad-scale LML limits (Martin & Maceina 2004; Saunders *et al.* 2008). In Tasmania, seven LML limits are applied over relatively large geographical areas (Figure 6.1). These LMLs attempt to protect a sufficient proportion of the mature population in each zone. In reality, the LML is a compromise relative to the heterogeneous nature of

populations at a fine spatial scale. Under-protection suggests a risk of an excessive reduction in spawning biomass with the consequent possibility of recruitment overfishing. While the intent of using a LML is to provide protection to the mature biomass, the number of populations that are sufficiently protected and the proportion of the spawning stock protected by the present LMLs in the different zones around Tasmania is not known. As the SM_{50} is the size at which 50% of a population is mature, the LML, being set as the SM_{50} plus two years growth, will still lead to a substantial proportion of the population having less than two breeding cycles prior to harvesting.

Despite the ongoing debate within the Tasmanian abalone fishery, the degree of protection afforded to abalone in any zone remains to be formally quantified. This study introduces a method for overcoming the relative paucity of growth data, thereby obtaining population specific theoretical estimates of LML. The purpose of this study was to identify and quantify any mismatch in spatial scale between the imposed management LML and the biological heterogeneity of abalone populations. The aims of the present study were fivefold as follows. First, to develop a method for inferring the theoretical growth parameters for populations, using only size at maturity data. Second, to assess the predictive power of this method, using leave-one-out cross-validation procedure. Third, to obtain fine-scale, population specific, theoretical estimates of LML. Fourth, to compare the fine-scale theoretical LML to the broad-scale management LML and identify populations that are theoretically under protected. Finally, to quantify the proportion of stock that is theoretically protected by the broad-scale management LML size limit, i.e. the proportion that has had two years growth post maturity before being fished at the LML size.

6.3 Methods

6.3.1 Site selection

The sites sampled represented areas in the Tasmanian abalone fishery where abalone are commercially harvested. The sites selected were generally chosen on the advice of commercial divers who were actively harvesting and familiar with the region (Tarbath, Hodgson *et al.* 2001) (Figure 6.1).

6.3.2 Data

A database of field observations held at the Tasmanian Aquaculture and Fisheries Institute (TAFI) was used. Two subsets of the database were used: one for relating size at maturity and growth parameters of the inverse logistic growth model, and the second for calculating theoretical estimates of LML that are population specific.

The first subset consisted of eight samples (Figure 6.1), and only included sites that had both maturity and growth collected at the same location in time and space. The eight sites provided a baseline data set for generating regression equations between maturity and the three growth parameters of the inverse logistic model. The second subset consisted of 252 samples which represented all the samples in the database with adequate maturity data. This dataset was used to generate fine-scale theoretical LML estimates for each of 252 populations. Biological data for blacklip abalone used in the analyses were collected during fishery independent surveys conducted by research divers.

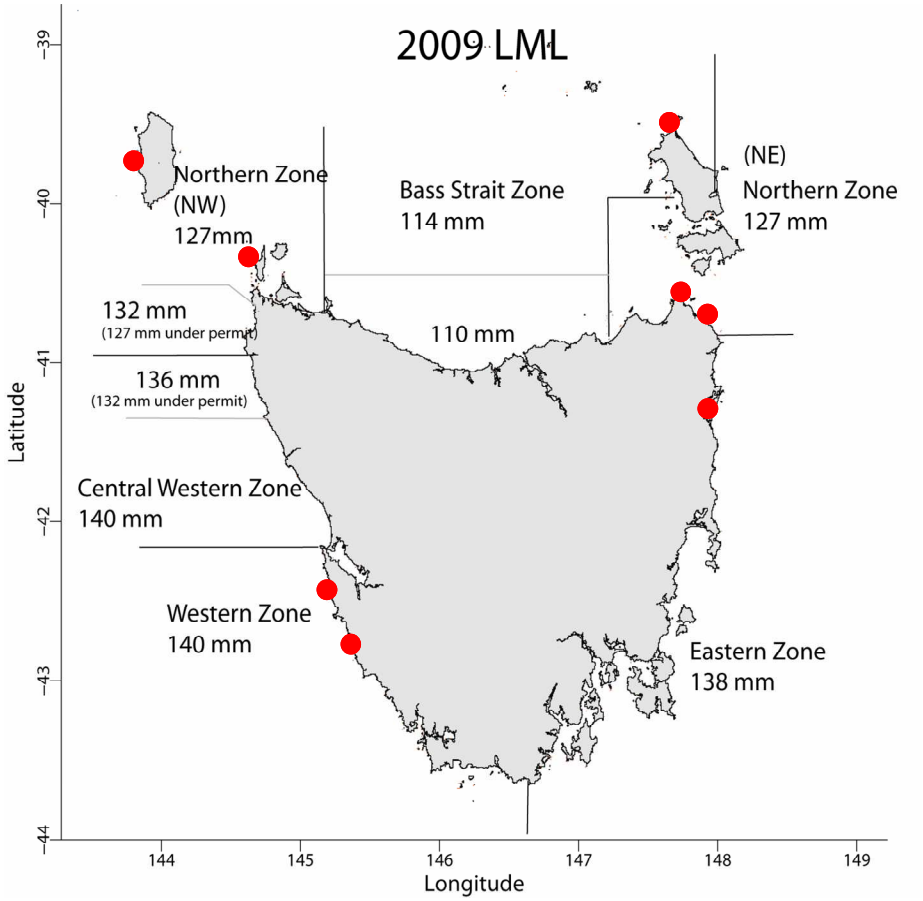

Figure 6.1. Map of current management Legal Minimum Lengths (LML) in Tasmania showing sites where both maturity and growth data was collected within the same location in time and space. In the Northern Zone (NW) and Central Western Zone two LMLs apply, the estimates in bracket are provisional LML that apply to divers under a special permit.

6.3.3 Estimating growth

Individual growth rates of blacklip abalone were determined by fitting the inverse logistic growth model to length increment data obtained from tag-recapture studies (Haddon *et al.* 2008). Chapters 3 and 4 showed that the inverse logistic model was the best statistical model for modelling the growth of blacklip abalone populations in Tasmania.

$$\Delta L = \frac{MaxL}{1+e^{Ln(19)\frac{(L_i - L_{50}^m)}{(L_{95}^m - L_{50}^m)}}} + \varepsilon \quad (6.1)$$

where ΔL is the expected length increment, L_i is the initial length when first tagged, $MaxL$ is the maximum length increment, L_{50}^m is the initial length at 0.5 times the difference between $MaxL$ and lowest length increment and L_{95}^m is the initial length at 0.95 times the difference between $MaxL$ and lowest length increment. The constant ε's are independent additive normal random error terms.

During the fishery independent sampling, the shell length of individual abalone were measured, allocated a numbered tag, and returned to the same location, or at least proximal to where it was collected. Tagged abalone were then left at liberty for approximately one year before being recaptured and the shell length re-measured. Growth increment data from different sites were accumulated in this way over a 14 year period, 1994-2008. Tagging data from each site was analysed according to the site and year of collection.

Five quality criteria were applied for data selection:

1) extreme negative growth increments, attributed to measurement and other data errors, i.e. data with length increments more negative than -3mm were excluded,

2) the minimum initial length at release consisted of individuals of less than 100 mm shell length,

3) initial lengths at release that exhibited a length increment of approximately 0 mm were included in the sample,

4) the time increment between mark and recapture was between 0.90 and 1.2 years,

5) The samples size were greater than n=90.

6) Where growth data were accompanied by size at maturity data, the data was collected from the same location in time and space.

Data with length increments more negative than -3mm were removed (-3mm was selected to allow for some sampling error), although negative increments had negligible affects on model parameters fitted to the inverse logistic model (Chapter 3). Growth rates were calculated by dividing the length increments by the observed years at liberty (between 0.9 and 1.2 years). In total eight samples of mark-recapture data accompanied by maturity data from the same location in space and time (year) were extracted from the database (Figure 6.1).

6.3.4 Estimating size at maturity

A large dataset of size at maturity data existed at the Tasmanian Aquaculture and Fisheries Institute. For the purpose of this study, maturity data collected from the same location but from different years was considered to be a separate sample. Maturity ogives based on length were calculated from data collected from fishery independent surveys during the period 1987-2006. The method for determining maturity was consistent for all samples. Maturity was defined as the point at which gonad development matured to a state where

the animal is capable of reproduction and can potentially contribute new recruits to the population. In practice, the state of maturity was determined by visual examination of gonad colour and size (Branden & Shepherd 1983; Tarbath 2003). Maturity data consisted of shell lengths and associated counts of mature and immature individuals. Data were classified into five groups: female, male, immature, undefined and trematode. Undefined included all data where the animals were mature but the sex was undefined. Trematodes included data where the capacity to reproduce was assumed to be diminished due to the presence of trematodes in the gonads (Harrison & Grant 1971). Individuals categorised as undefined or trematode were omitted from analyses. The state of maturity was recorded alongside the shell length which was measured to the nearest 1 mm.

Counts were stratified down to site by year and males and females were combined. A logistic ogive was used to fit the proportional size at maturity data, using maximum likelihood methods and binomial residual errors, equations (6.2) and (6.3) (Neter *et al.* 1990). The size at maturity (SM_{50}) value for each population was estimated as the length (l) at which 50% of the population are predicted to be mature (estimated as $-a/b$).

$$\mu_l = \frac{e^{a+bl}}{1+e^{a+bl}} . \tag{6.2}$$

The log-likelihood is given by,

$$-LL(a,b) = -\sum_{j=1}^{t}\left\{ Ln\left(\frac{N_j!}{n_j!(N_j!-n_j!)}\right) + n_j\left(a+bl_j\right) - N_j Ln\left(1+e^{a+bl_j}\right)\right\} \tag{6.3}$$

where μ_l is the predicted proportion of animals of length l expected to be mature, a and b are the parameters of the logistic curve (where b measures the rate of transition between

immature and mature), l represents the t different length classes for which there are data, N_j is the total number of observations for length class l_j, n_j is the number of mature individuals in length class l_j and n_j/N_j is the observed proportion of mature animals observed in length class l_j.

Once the logistic function was fitted, samples of size at maturity were further excluded if they did not meet two data quality criteria concerning the coverage of the data across the sizes encompassing the size at maturity. Samples were excluded if:

1) the minimum observed proportion of mature animals was below 5%, and

2) the maximum observed proportion of mature animals was greater than 95%.

In total 252 populations were extracted from the database that met these criteria.

6.3.5 Theoretical estimates of growth model parameters

The time and financial constraints of obtaining growth parameters directly through tag-recapture studies limit the number of samples collected (Proudfoot *et al.* 2008). Owing to the large number of samples with maturity data, the advantage of obtaining growth parameters indirectly through maturity data was explored. The aim was to seek a cost effective method to parameterise the growth of populations that would not be otherwise possible. If a significant relationship exists between the growth parameters and the parameters of the size at maturity then there is the potential to use such relationships to generate theoretical growth parameters to overcome the limited number of growth data.

A baseline dataset of eight samples was available that consisted of populations with both tag-recapture and maturity data in the same location in space and time. This baseline dataset was used to test for correlations between growth and maturity parameters. The inverse logistic growth model, equation (6.1), was fitted to the eight samples of tag-recapture data using maximum likelihood methods with normal random errors. The growth parameters obtained represented the empirical estimates of growth. The size at maturity (SM_{50}) from the eight samples was estimated using the logistic equation (6.2) and equation (6.3).

The relationships between the SM_{50} and estimates of the MaxΔL, L_{50} and L_{95} parameters of the inverse logistic model were examined using linear regression. Linear regression models were fitted where the SM_{50} was treated as the explanatory variable and the growth parameters as the response variables (Neter *et al.* 1996),

$$Y = a + bSM_{50} \qquad (6.4)$$

where Y is either MaxΔL or L_{50} or L_{95}.

Any regression equation that showed a significant correlation ($p<0.05$) between each growth parameter of the inverse logistic and the SM_{50} for the eight populations was used to generate mathematically derived or theoretical growth parameters for the inverse logistic model. This made it possible to obtain growth parameters for populations where growth data was not available and to subsequently calculate the two year growth increment post maturity and the population specific LML.

6.3.6 Method validation

The adequacy of estimating growth parameters for abalone populations using the regression between SM_{50} and the growth parameters of the inverse logistic of the baseline dataset of eight populations was examined using cross-validation. Cross validation is a procedure that is useful for determining the predictive power of a baseline dataset. Generally, cross validation consists of dividing the dataset into two subsamples, where one is used as the statistical predictor which will be referred to in this study as the training subsample, and the other, termed the validation subsample, is used to test the predictive performance of the training subsample (Stone 1974). The leave-one-out cross validation procedure is considered an appropriate testing method for small baseline datasets, especially where it is possible that each observation may influence the parameters of the regression models (Lae 1999). In this case, the leave-one-out cross-validation consists of splitting the baseline dataset (n= 8) into two subsets such that one observation of the sample is set aside (n=1 population) and the remaining subsample (n=7 populations) is used as a training subsample. The omitted subsample (n=1) forms the validation set (Stone 1974). The regression model is fitted to the training subsample (n=7). The training set regressions obtained are then used to predict estimates of $Max\Delta L$, L_{50}, and L_{95} for the "validation" subsample (n=1). This division of the dataset is repeated in all (n) possible ways (Stone 1974) obtaining predicted estimates of $Max\Delta L$, L_{50} and L_{95} for the "validation" subsample each time. The predicted values generated by each of the eight leave-one-out iterations are plotted against their respective observed values and a final regression line is fitted to determine the predictive power.

6.3.7 Obtaining theoretical LML estimates.

Theoretical growth parameter estimates were obtained from significant regressions between SM_{50} and growth parameters of the inverse logistic model. The two year growth increment was calculated by substituting the theoretical parameter estimates and the observed size at maturity estimates into equation (6.1) in two time steps where each time step represent 1 year, where

ΔL is the theoretical length increment after 1 time step (1 year growth)

L_i is the observed SM_{50} in the first time step and the ($SM_{50} + \Delta L$) in the second time step

A theoretical LML (LML_T) for each of the eight populations was calculated by adding the two year growth increment obtained theoretically using equation (6.4) to the observed size at maturity estimate. The accuracy of the theoretical LML was ground-truthed against eight populations that each consisted of both empirical growth and maturity data. The LML for those eight populations were firstly estimate empirically using observed growth and maturity data. The empirical LML (LML_E) was obtained by directly fitting the inverse logistic model to the tag-recapture data obtained from the eight population samples and calculating the growth increment after two years. This was then added to the observed size at maturity. The theoretical LML was also estimated and compared to the empirical LML using the following regression model.

$$\text{Theoretical LML } (LML_T) = b^* \text{empirical LML } (LML_E) + a \qquad (6.5)$$

This regression equation was rearranged so as to correct the theoretical LML (LML_T) estimates towards the empirical estimates

$$\text{Corrected theoretical LML} = (LML_T - a)/b \quad (6.6)$$

6.3.8 Calculating the theoretical LML of 252 populations

Theoretical growth parameters for the inverse logistic model were estimated from the regression equations against SM_{50} for each population and using these growth model parameter estimates in each case, the theoretical two year growth increment was calculated for all 252 populations. Thus, the theoretical LML for 252 populations was calculated using the (empirical) SM_{50} and the theoretical two year growth increment. The theoretical LML was corrected for any potential bias using equation (6.6).

6.3.9 Measuring the percentage of stock protected by the LML currently used by management

For simplicity, the percentage of stock protected was determined as the proportion of the populations that had a minimum of two years of growth post maturity before being available for harvest. In this study the percentage of stock protected was determined for 252 samples, each with an empirically estimated SM_{50}, combined with theoretical growth parameters, and the LML currently used by management. Size transition matrices were used to determine what proportion of the population growing forward from the SM_{50} size

class would be below the management LML size class after two years of growth. A size transition matrix (STM), using 2 mm size classes from 2 mm up to 210 mm, was generated for each of the 252 sites in turn using the theoretical growth parameters for each site. The probabilities of growing from one size class into larger size classes were calculated by using a normal distribution to represent the distribution of growth increments expected from each size class over a one year interval. Therefore, the proportions expected to grow into each larger size class were estimated by calculating the cumulative normal distribution from the upper limit of each size class and for all size classes, except the smallest and largest, subtracting the cumulative normal distribution from the lower limit of each size class. For the largest size class the calculation was 1.0 minus the cumulative normal distribution from the lower limit of the size class in equation (6.7).

In the equation:

$$G_{i,j} = \int_{-\infty}^{L_i+\frac{LW}{2}} \frac{1}{\sqrt{2\pi}\sigma_{L_i}^{j}} e^{-\left[\frac{\left(L_i-\bar{L}_{i,j}\right)^2}{2\left(\sigma_{L_i}^{j}\right)^2}\right]} dL \qquad L_i = L_{Min}$$

$$G_{i,j} = \int_{L_i-\frac{LW}{2}}^{L_i+\frac{LW}{2}} \frac{1}{\sqrt{2\pi}\sigma_{L_i}^{j}} e^{-\left[\frac{\left(L_i-\bar{L}_{i,j}\right)^2}{2\left(\sigma_{L_i}^{j}\right)^2}\right]} dL \qquad L_{Min} < L_i < L_{Max}$$

$$G_{i,j} = \int_{L_i-\frac{LW}{2}}^{+\infty} \frac{1}{\sqrt{2\pi}\sigma_{L_i}^{j}} e^{-\left[\frac{\left(L_i-\bar{L}_{i,j}\right)^2}{2\left(\sigma_{L_i}^{j}\right)^2}\right]} dL \qquad L_i = L_{Max} \tag{6.7}$$

The central term relating to $L_{Min} < L_i < L_{Max}$ can be re-written:

$$G_{i,j} = \left(\int_{-\infty}^{L_i+\frac{LW}{2}} \frac{1}{\sqrt{2\pi}\sigma_{L_i}^{j}} e^{-\left[\frac{\left(L_i-\bar{L}_{i,j}\right)^2}{2\left(\sigma_{L_i}^{j}\right)^2}\right]} dL \right) - \left(\int_{-\infty}^{L_i-\frac{LW}{2}} \frac{1}{\sqrt{2\pi}\sigma_{L_i}^{j}} e^{-\left[\frac{\left(L_i-\bar{L}_{i,j}\right)^2}{2\left(\sigma_{L_i}^{j}\right)^2}\right]} dL \right) \tag{6.8}$$

where $G_{i,j}$ is the transition probability of an abalone growing from size class j into size class i, L_i is the mid-size of size class i, LW is the size class width, $\sigma_{L_i}^{j}$ is the standard deviation of the normal distribution of growth increments for the initial size class j. $\bar{L}_{i,j}$ is the expected average final size for initial size class j, which equals $L_j + \Delta\hat{L}_{i,j}$, where $\Delta\hat{L}_{i,j}$ is the average expected growth increment for initial size class j. It is necessary to ensure that L_{Min} and L_{Max} encompass the range of all likely size classes. The two terms are the cumulative normal distribution from the top of the particular size class and from the bottom of the particular size class. The subtraction of the smaller cumulative normal distribution from the

larger is explicit in (6.8). If the minimum and maximum size classes are treated as in the equation then the sum of the transition probabilities for all *n* size classes into which animals may grow will automatically equal one (Haddon *et al.* 2008).

At each site, the size transition matrix was used to project two years growth for a vector of numbers at size that started as 1000 animals in the SM_{50} size class.

$$N_{t+2} = G(GN_t) \tag{6.9}$$

where for each given site N_t is the vector of numbers at size at time *t* and G is the size transition matrix. The percentage of the stock at each site that is protected was calculated from the proportion of the population below the management LML after two years of growth from the SM_{50} size class. The raw numbers below the LML were expressed as percentages which were then divided by two to account for the fact that at the SM_{50} only 50% of the population is mature. The proportion only consists of that fraction which had a minimum of two full years as mature individuals below the LML size.

$$P_s = \left(\left(\sum_{L=SM_{50}}^{LML} N_{L,t+2} \right) / 10 \right) / 2 \tag{6.10}$$

where P_s is the percent protection and $N_{L,t+2}$ is the vector of numbers at size *L* after two years growth.

6.4 Results

6.4.1 Biological heterogeneity

Of the eight populations considered the two year growth increment was more heterogeneous than the SM_{50} (CV is 0.30 for growth increment and 0.12 for SM_{50}) (Table 6.1). Throughout the geographic range of the species in Tasmania, the size at maturity obtained from 252 samples ranged between 72 - 130 mm, a difference of 58 mm. For the eight samples considered in the baseline dataset, the size at maturity ranged between 94 – 128 mm, a difference of 34 mm. Although the eight samples only represent 3% of the 252 samples considered, the range in size at maturity among the eight samples is 57% of the range covered by the 252 samples. This implies that despite the small sample size of n=8 the samples adequately represented the range in size at maturity that occurs in the Tasmanian abalone fishery.

6.4.2 Obtaining the theoretical growth parameters

There was strong correlation between SM_{50} and L_{50} at a fine spatial scale ($r = 0.891$, significant at $p=0.01$ at degrees of freedom (d.f) = 6 (see Fowler & Cohen 1990), (Figure 6.2 Table 6.2). The regression equation defining the relationship between L_{50} and SM_{50} is used to obtain theoretical estimates for L_{50}, which is henceforth referred to as $L50_T$

$$L50_T = 1.1539 * SM_{50} - 15.335. \quad (6.11)$$

In addition, there was a strong correlation between SM_{50} and L_{95} (r = 0.783, significant at p=0.05 at d.f = 6, (Figure 6.2, Table 6.2). The regression equation defining the relationship between L_{95} and SM_{50} is used to obtain theoretical estimates for L_{95}, which is henceforth referred to as $L95_T$

$$L95_T = 1.0862 * SM_{50} + 32.461. \quad (6.12)$$

Given these significant correlations, it was possible to theoretically obtain growth model parameters for the L_{50} and L_{95} parameters of the inverse logistic model in the absence of tag-recapture data by using the regression equations based on maturity data equation (6.11) for $L50_T$ and equation (6.12) for $L95_T$

Table 6.1. Size at maturity and two year growth increments of mature populations at eight sites within the Tasmanian fishery, showing the heterogeneous nature of these biological properties. The empirical LML presented here was simply calculated by adding the two year growth increment to the size at maturity obtained empirically. The theoretical LML presented here was calculated by adding the two year growth increment obtained theoretically, to the size at maturity estimate obtained empirically.

statistical block	site	latitude	longitude	year	SM_{50}	2yr increment (mm)		LML (mm)	
					(mm)	empirical	theoretical	empirical	theoretical
37	315	-39.69	147.88	2001	95	10.9	17.2	106	112
3	314	-39.93	143.83	2001	103	22.7	17.9	126	121
49	313	-40.5	144.7	2001	98	11.6	17.5	110	116
31	316	-40.73	148.12	2001	98	19.4	17.5	117	116
31	588	-40.92	148.32	2003	116	22.2	19.0	138	135
29	59	-41.57	148.32	1996	107	27.2	18.3	134	125
10	272	-42.61	145.26	2001	126	16.3	19.9	142	146
10	458	-42.96	145.49	2003	128	17.5	20.1	146	148
				CV	0.12	0.30			

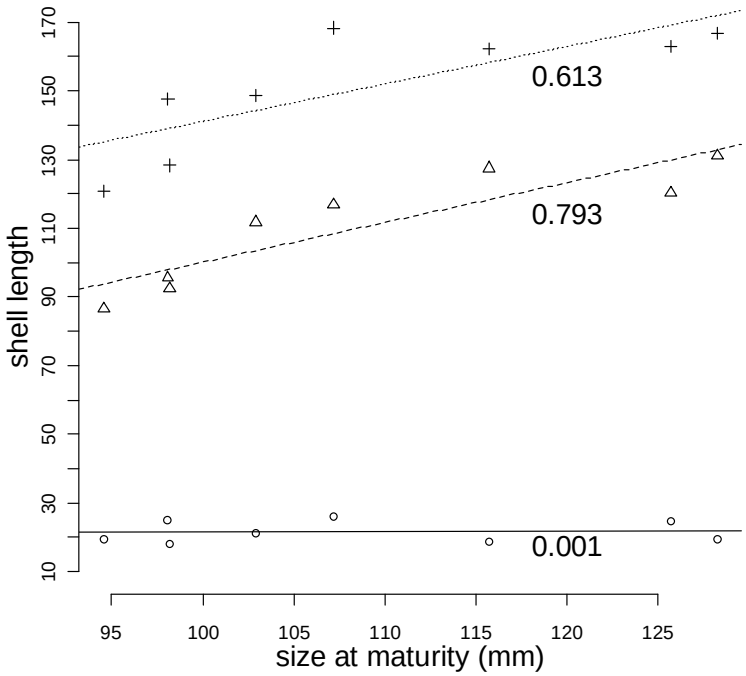

Figure 6.2. Regression of size at maturity and three parameters of the inverse logistic model; MaxΔL (solid line; data are circles), L_{50} (dashed line; data are triangles), and L_{95} (dotted line; data are crosses). Also shown is the variation accounted for by the relationship (R^2) for each regression line. Data are based on eight populations with growth and maturity data from the same location in space and time.

Table 6.2. Summary of correlation results from regression analysis and significance: a) observed size at maturity (SM_{50}) with the two parameters of the inverse logistic model fitted to tag recapture data, b) cross validation of two of the inverse logistic parameters; $L50_T$ is the L_{50} obtained theoretically (L_{50} is derived from the fitted model), similarly for $L95_T$ and L_{95} and c) the theoretical LML (LML_T) and the LML obtained empirically (LML_E).

	Comparison	R^2	r	p-value
a) size at maturity and growth model parameters	SM_{50} and L_{50}	0.793	0.891	<0.01
	SM_{50} and L_{95}	0.613	0.783	<0.05
b) cross validation	$L50_T$ and L_{50}	0.66	0.812	<0.05
	$L95_T$ and L_{95}	0.4	0.632	>0.05
c) assessing LML	LML_T and LML_E	0.898	0.948	<0.001

The correlation between SM_{50} and MaxΔL parameter was poor (Figure 6.2). As such, an investigation into the relationship between the MaxΔL and L_{50} and L_{95} was considered, with the ultimate aim of generating theoretical estimates of MaxΔL using the $L50_T$ and $L95_T$ parameters estimated in the regression with SM_{50} (equations (6.11) and (6.12)). A dataset consisting of growth recapture data from 30 populations was used to determine if the observed L_{50} and L_{95} parameters of the inverse logistic growth model can be used to estimate the MaxΔL parameter. The strongest correlation between MaxΔL and any

combination of the other two parameters of the inverse logistic model occurred between the MaxΔL and the L_{95} and L_{50} combined (r = 0.7263, significant at p=0.001). The theoretical MaxΔL parameter of the inverse logistic ($MaxΔL_T$) can thus be obtained from L_{50} and L_{95} (or $L50_T$ and $L95_T$) values using,

$$MaxΔL_T = 0.46095* L95_T \ -0.46856* L50_T + 5.58943. \quad (6.13)$$

Thus all required growth model parameters were obtained theoretically in the absence of tagging data using empirical size at maturity data.

6.4.3 Cross-model validation

For the leave one out cross validation procedure the predictive performance of the baseline data in predicting growth model parameters from SM_{50} data is shown in Figure 6.3. The $L50_T$ parameter of the inverse logistic estimated from size at maturity was significantly correlated to the L_{50} parameter obtained from empirical growth data. This implies that the baseline data and the regression equation of the relationship between the two variables was able to be used to reliably predict the L_{50} parameter. The correlation of r = 0.812 was significant at p=0.05 (Table 6.2). Relative to the 1:1 regression line, five values for $L50_T$ were over-estimated particularly at the upper and lower range of the empirical L_{50} (Figure 6.3), while three values in the mid-range were underestimated.

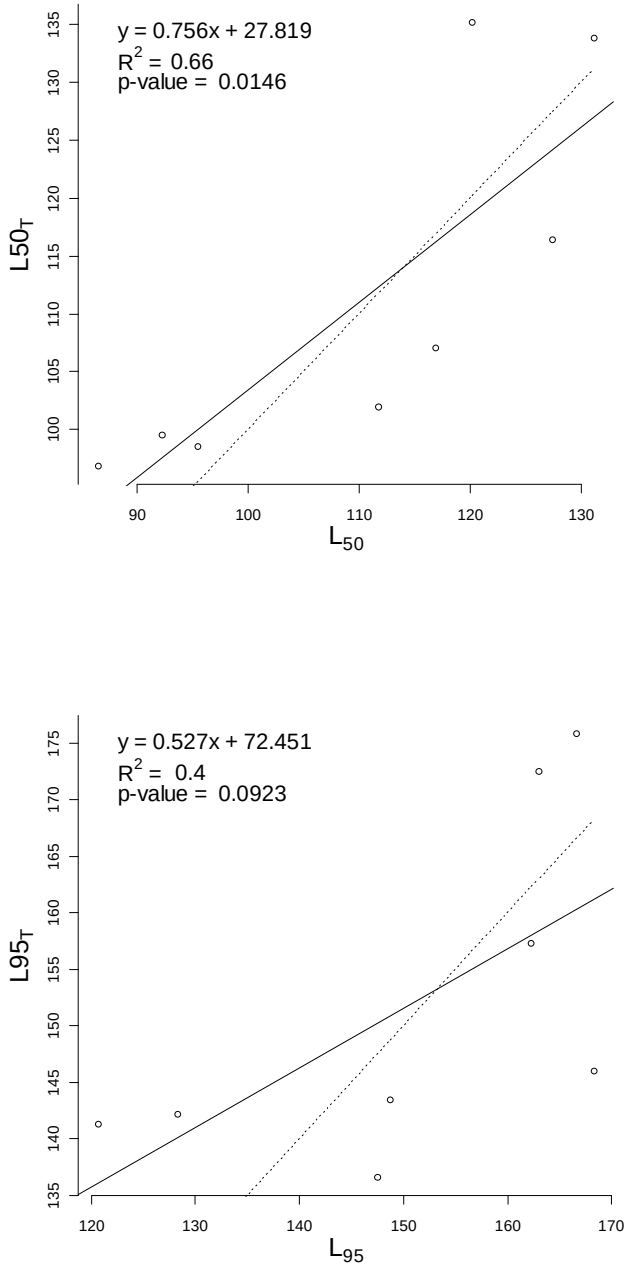

Figure 6.3. Results of leave one out cross validation with eight populations assessing the validity of obtaining $L50_T$ and $L95_T$ parameters from SM_{50} estimates. All values are in mm. Growth and maturity data were collected from the same location in time and space for the eight populations. The scatter plot of predicted values (y-axis) against the observed values (x-axis) is shown for the two parameters of the inverse logistic model (L_{50} and L_{95}) which had a significant correlation with size at maturity (SM_{50}). The solid line indicates the regression and the dotted line represent the perfect fit - a 1:1 slope of the empirical parameters. Fig. a) is the cross-validation of $L50_T$ and Fig. b) is the cross-validation of $L95_T$.

the $L95_T$ parameter of the inverse logistic estimated from size at maturity was moderately correlated to the L_{95} obtained from empirical growth data. The correlation of $r = 0.632$ was not significant at $p<0.05$ (however it was significant at $p < 0.1$) (Table 6.2). This implies that the baseline data was only moderately reliable in predicting the $L95_T$ parameter. In comparing with exact correspondence (namely the 1:1 line) as a reference (Figure 6.3), the trend of under or overestimation was similar to that obtained for L_{50}. Four values for $L95_T$ were over-estimated, particularly at the upper and lower range of the empirical L_{95} (Figure 6.3). Values that were underestimated also appeared in the mid-range, again similar to the L_{50}.

The parameter values L_{50} and L_{95} obtained from the eight samples were evenly distributed throughout the range of the empirical estimates. Despite the scarcity of observations in the database (eight observations) the power to predict the L_{50} value from SM_{50} estimates was considered adequate, whereas the power to predict the L_{95} was slightly less powerful.

6.4.4 Assessing the accuracy of the theoretical LML

A theoretical LML (LML_T) was calculated using the theoretical growth parameters for each of the eight samples - to obtain theoretical estimates of two years growth increments - and then adding this to the associated SM_{50} obtained empirically for each of the eight samples. The empirical LML (LML_E) was calculated using the available empirical data for each of the eight samples. The LML_T was compared to the LML_E using regression statistics and there was a strong correlation between the two ($r = 0.947$, $p<0.001$) (Table 6.2) for the

eight populations. The following regression equation between the empirical and the theoretical LML was obtained,

$$\text{Theoretical LML } (LML_T) = 0.8946 * LML_E + 16.8868. \quad (6.14)$$

The LML_T was approximately 4 – 9 mm higher than the LML_E (Figure 6.4) and therefore the LML_T was corrected by rearranging the above regression equation to obtain the following

$$\text{Corrected theoretical LML} = (LML_T - 16.8868)/ 0.8946. \quad (6.15)$$

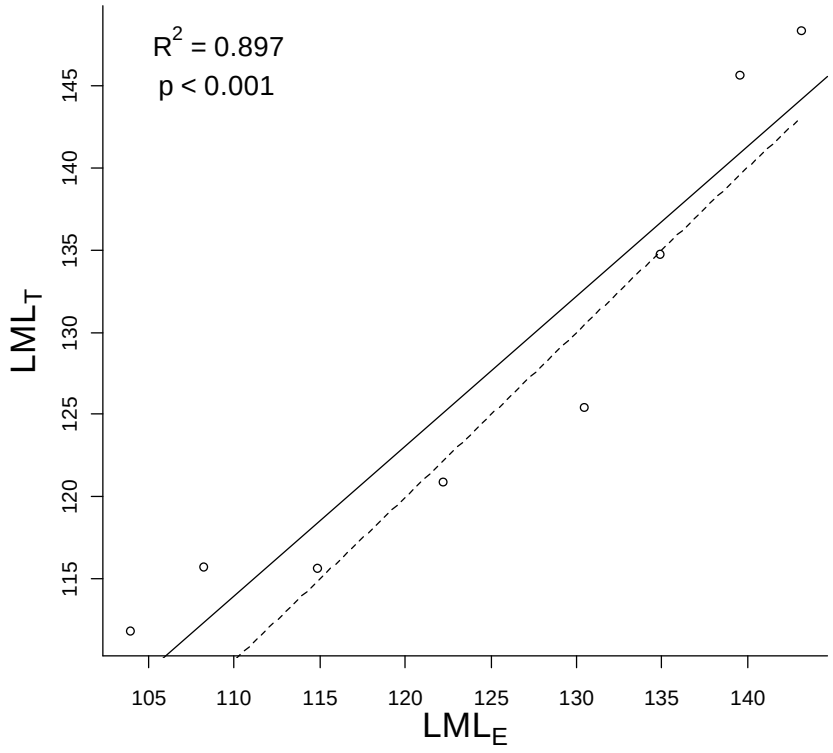

Figure 6.4. Comparison of the theoretical LML (LML_T) and the LML obtained empirically (LML_E) for eight populations with growth and maturity data from the same site and year. The solid line represents the observed regression of the LML_T to the LML_E and the dashed line represents what would be a 1:1 correlation between the LML_T and the LML_E to illustrate the deviation between the two LML estimates. The LML_E is derived from growth parameters obtained from empirical growth data while the LML_T is derived theoretically from theoretical growth parameters mathematically derived from empirical SM_{50} data.

6.4.5 Theoretical LML of 252 populations

Using the correlations described, it was possible to formulate growth model parameters for all 252 samples. The $Max\Delta L_T$ was obtained by substituting the theoretical estimates of $L50_T$ and $L50_T$ into equation (6.13). Formulated parameters of the inverse logistic growth model (i.e. $Max\Delta L_T$, $L50_T$ and $L95_T$) were used to calculate the theoretical two year

increment (see section 6.3.7). The theoretical LML (LML_T) of each of the 252 populations was the estimated by adding the theoretical two year growth to the empirical SM_{50} estimate and corrected according to equation (6.15). Each of the 252 populations was assigned the corrected theoretical LML.

6.4.6 Quantifying any mismatch between the theoretical LML and management LML

Differences between the corrected theoretical LML and the management LML are illustrated in Figure 6.5. The disparity in spatial scales between the corrected theoretical LML and the management LML is particularly clear in the south west of Tasmania where most populations were under protected. The majority of sites in the south west had a theoretical LML greater than the management LML thereby exposing those populations to recruitment and growth overfishing (Figure 6.5). Along the central and southern east coast the mismatch in spatial scales for the LML was variable.

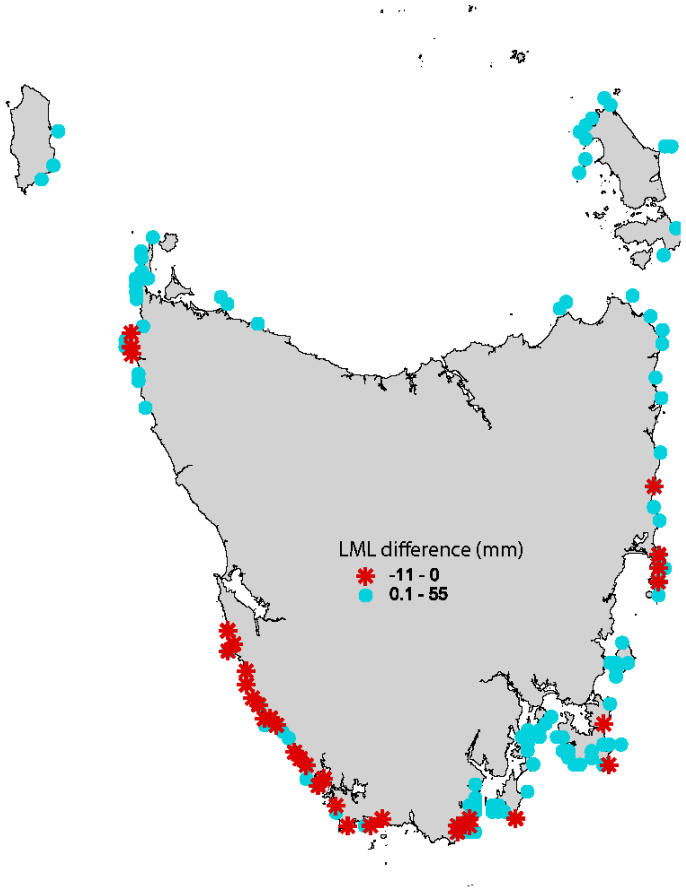

Figure 6.5. Map showing the difference between the corrected theoretical LML and the management LML for 252 populations. The LML difference is obtained by subtracting the corrected theoretical LML from the management LML. A negative result (red asterisk) indicates that the management LML is theoretically set too low and populations might not undergo the required two year breeding cycle before entering the fishery. The red asterisk therefore indicates populations that are at risk of recruitment overfishing.

6.4.7 Proportion of stock protected

The proportion of stock that has had two or more breeding cycles between SM_{50} size and management LML size is indicative of how adequately the stock is protected (Figure 6.6). This can be used to quantify the success of the LML management goal at a fine spatial scale. Within the framework of this study an estimate of 50% implies that the LML is

ideal. This accounts for the fact that at that LML a small portion of the stock will have had more than 2 years protection possibly 3 or 4 years. This is because at the size at maturity a small portion will have reached maturity at a size smaller than the SM_{50}, and will have had 3 or 4 years protection at the LML size.

With the exception of the Tasmanian Western Zone, the typical trend within a zone was that for the majority of sites, 50% of the population completed two full breeding cycles before reaching the management LML after two years growth post SM_{50} size (Figure 6.6). In contrast, the trend in the Western Zone was that for the majority of sites, less than 20% of the population had the full two breeding cycles before reaching the management LML. The trend in the Western Zone quantifies the extent of stock protection for populations identified in Figure 6.5 where the adjusted theoretical LML was greater than the management LML, theoretically exposing the populations to overfishing.

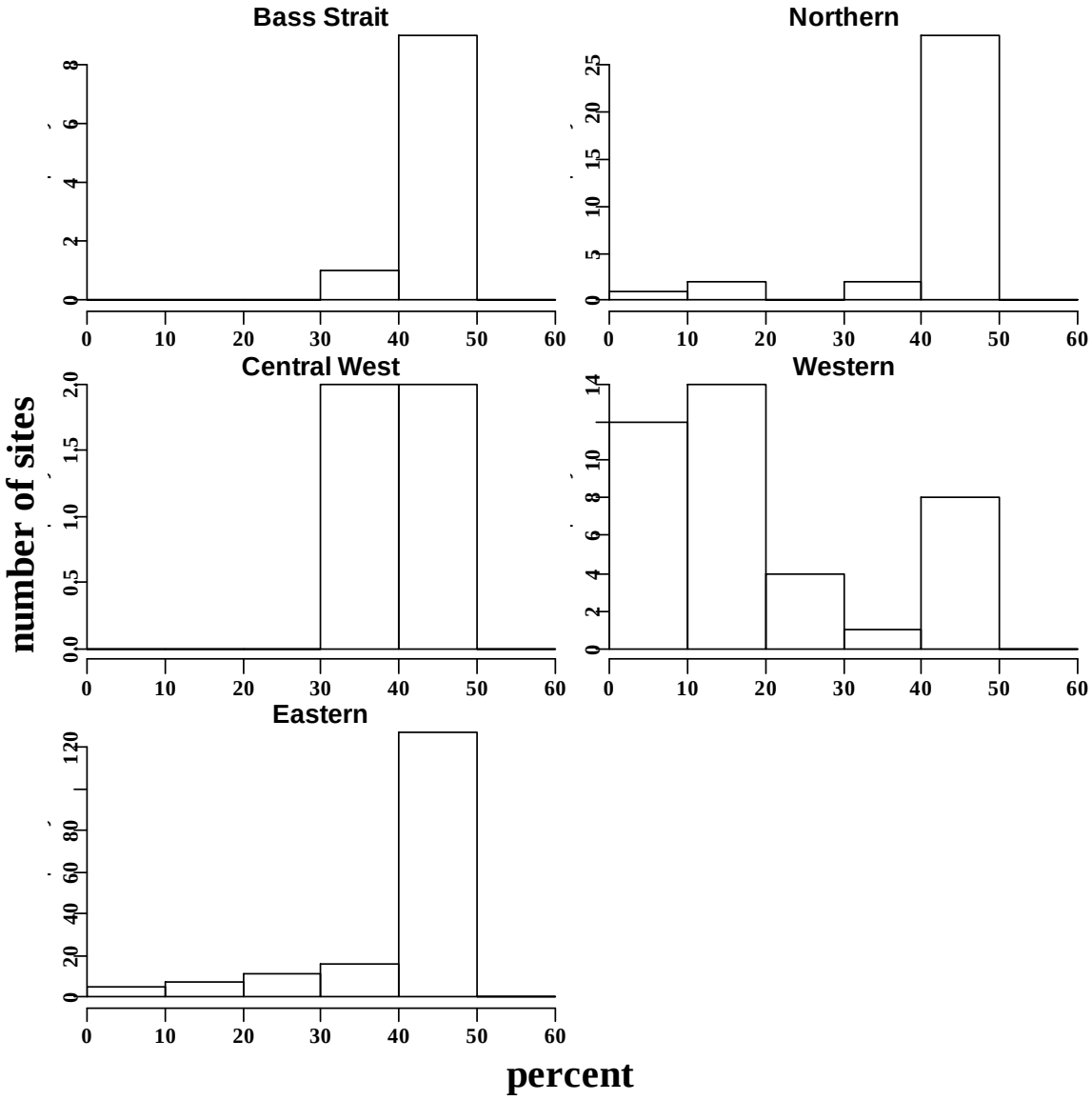

Figure 6.6. Proportion (%) of stock that has had two full breeding cycles before reaching the management LML (i.e. two years of growth post size at maturity (SM_{50})). Proportions are generated from site-specific size transition matrices. Results are segregated according to the five management zones used in the Tasmanian fishery; 1) Bass Strait, 2) Northern, 3) Eastern, 4) Western and 5) Central West (see Figure 6.1). For the purpose of this study, an estimate of 50% stock protection is used to imply that the stock is adequately protected.

6.5 Discussion

One of the major challenges for the management of fisheries with length-based assessments is deciding appropriate spatial scales for describing population dynamics and applying management rules based upon LML. Defining an optimum resource unit in a formal way has proven to be elusive not only for blacklip abalone in Australia but for many fisheries worldwide (Stergiou *et al.* 2009). Delineating a stock with similar population dynamics would require small unit sizes that will ideally encompass homogenous biological characteristics. For abalone this would require knowledge of the variation in growth rate because even at a fine spatial scale, growth was found to be more heterogeneous than size at maturity (Table 6.1). Initially a single LML setting of 127 mm was applied throughout the state between 1962 – 1989, encompassing the entire geographic range of the species (Tarbath *et al.* 2008). Presently, seven different LML settings are applied across the State that attempt to capture both population dynamics and management objectives (Figure 6.1).

6.5.1 Biological variability

Growth of adult blacklip abalone seems much more variable than maturity, as the coefficient of variation for growth was higher (CV = 0.30) than maturity (CV = 0.12) (Table 6.1). This may reflect different responses to productivity of the environment, and other local conditions including food availability, temperature and habitat complexity (Gilroy & Edwards 1998; Casselman 2007). Growth rates can have a large inheritable component (Hara & Kikuchi 1992) and aquaculture studies confirm that there are distinct genetic traits of blacklip abalone that can be phenotypically expressed in growth rate

(Baranski *et al.* 2008). That growth varies at a small spatial scale between sites has been known but the cost of obtaining data at fine spatial scales is the major factor prohibiting the estimation and application of fine scale LMLs. Even though the number of sites with tagging data providing information on growth is limited relative to the number of sites with maturity data, the variation in growth remains much greater. Without fine scale growth data, it is not possible to determine if the abalone fishery can be managed successfully by implementing LML rules at a broad spatial scale.

6.5.2 Method validation

The cross validation revealed the relative power of the predictive models. Good correlations were obtained for the theoretical estimates of the L_{50} and L_{95} estimate of the inverse logistic growth model and those obtained using observed tag-recapture data (Figure 6.2). This enabled theoretical parameters to be predicted from SM_{50} that closely approximated those obtained from using observed tag-recapture data. In contrast there was a poor correlation between the theoretical $Max\Delta L_T$ parameter and the $Max\Delta L$ obtained from fitting the model to observed tag-recapture data (not presented). This is not surprising since the $Max\Delta L$ parameter is difficult to estimate accurately given typical tagging data (Chapter 3). A small dataset consisting of only eight sites with both growth and maturity data will result in a greater difference between baseline and validation sets than a larger baseline dataset. Additional growth data may strengthen the ability to validate the method. Within small datasets it is likely that each observation contributes influential 'unique information' that is of relevance to the model (Lae 1999).

6.5.3 The usefulness of theoretical parameter estimates and theoretical LML's

The usefulness of obtaining theoretical parameter values is that their estimation is not necessarily intended to provide concrete site specific growth estimates, but instead offers a preliminary assessment of the quantity and location of under-protected stocks. The aim was to identify potential sites of interest for consideration into a strategic selection of sampling for future field work.

The ultimate aim was to obtain theoretical LML that are biologically valid and for this reason a comparison was made between the theoretical LML and the empirical LML using regression statistics. Despite the use of linear regression equations, which collapse any variation around relationships between SM_{50} and growth parameters and the limited data that were used to generate the necessary relationships, the correlation between the (theoretical) LML_T and the (empirical) LML_E was strong. The correlation between the two LML estimates ($r=0.948$), and the regression relationship, was used to correct the theoretical LML_T to more closely mimic the LML_E. The corrected theoretical LML ranged between 81-150 mm. Before correction, there was a tendency for the LML_T to overestimate the LML_E. There are several factors that may contribute to the deviations between the two estimates. These include 1) the small training data set consisting of eight samples 2) the difficulty in obtaining theoretical MaxΔL estimates and 3) the high variability in growth around the State. Additional empirical growth data is required and depending on the sites, may also be used to monitor for temporal variability in growth.

6.5.4 Stock protection

The mismatch between setting the management LML and the biological heterogeneity of growth and maturity at a fine spatial scale remains a problem. Some stocks will continue to receive less protection and others more protection than intended; in all zones the current management LML will remain a compromise. The intention of generating site specific theoretical LML's is to identify regions where the level of protection to the spawning stock may fall short of the management goal. In this chapter this has been achieved by quantifying the extent of any mismatch between spatial scales in theoretical and management LML. Corrected theoretical LML's may improve awareness on how the resource is fished by identifying populations that are knowingly under protected (potentially over fished) and populations that are overprotected (large proportions of the available population remain unfished). Importantly the method allows theoretical estimates of LML to be reviewed against qualitative assessments into the extent of stock protection which can often be subjective.

6.5.5 Implications of under-protecting stocks

The procedure of adding two years growth to the size at maturity to estimate the LML is a simplistic method that assumes abalone spawn successfully on an annual basis and all individuals are equally fecund after reaching maturity. Studies based on gamete production in blacklip abalone indicate that few gametes are produced in the first year of maturity and these are not likely to lead to substantial spawning. Furthermore, such spawning events may not occur for at least another year (Shepherd & Laws 1974). Recruitment strength is

the most stochastic of all population processes (Francis & Shotton 1997). Rather than being consistent on an annual basis, recruitment processes occur unpredictably among many fish populations, varying both spatially and temporally, making estimates of recruitment highly uncertain (Francis & Shotton 1997).

In addition to the current two year growth component of the LML setting, the estimate of size at maturity is measured at the length at which 50% of the population is mature. Accordingly, at this shell length size, a substantial proportion of the population (~50%) is immature and this portion of the population will not have undergone two breeding cycles at the LML shell size. Therefore the time increment, post maturity, may potentially be adjusted to account for the immature proportion at size at maturity. The time increment following maturity is therefore an important aspect of ensuring that abalone reach their full reproductive potential before being harvested. The calculation of the growth increment relies on an accurate description of growth. Although a theoretical description of growth, as proposed in the present study, may not be as accurate as empirical data, it is considered an improvement on a complete absence of growth data without which a preliminary evaluation into the success of LML at a fine spatial scale would not be possible.

6.6 Conclusion

The method of obtaining theoretical estimates of growth parameters partly overcomes the limitation of insufficient growth data and is designed to provide an approximate spatial description on the distribution of growth rates. By refining size at maturity at small spatial scales, and correlating it to growth parameters it was possible to derive theoretical estimate

of growth and develop site specific LML's. This was then used to evaluate the success of the current broadscale LML rule in Tasmania. The method of obtaining growth parameters in the absence of growth data is dependent on two provisions. Firstly, it only applies to populations where the average growth can be described using an inverse logistic growth function. Secondly, a large database of fine-scale size at maturity data is required. The method was useful in obtaining fine scale LML estimates for the purpose of estimating the number of populations and identifying regions that are under-protected and at risk of overfishing.

CHAPTER 7

General Discussion

Careful estimates of growth are essential for many studies on fish productivity (Summerfelt 1987). For example estimates of growth are necessary for studies on fish ecology (Neuheimer & Taggart 2007), life history characteristics (Grover 2005) and calculating sustainable yields. These factors may vary spatially and temporally between spatially segregated populations and these ultimately influence decisions in fisheries management (Hilborn & Walters 1992). Carefully determined growth estimates are therefore important for more accurate stock assessments and biological predictions (Arce & León 1997).

Accurate growth estimates are possible through the selection of a growth model that is statistically and biologically plausible for the species in question. Furthermore methods used to estimate growth need to be periodically evaluated and assessed for shortcomings and progress (Summerfelt 1987). In my research the selection of an appropriate growth model was examined foremost (Chapters 2-4) to allow for accurate estimates of the effect of temperature and fishing effects on stock productivity (Chapters 5 and 6).

7.1 Key findings

7.1.1 Modelling growth using the inverse logistic model

It is has long been recognized that the Tasmanian abalone fishery consists of hundreds of spatially explicit stocks which are ecologically similar on a small scale of tens or hundreds of metres (Prince *et al.* 1987; Nash 1992; Temby *et al.* 2007). Determining the growth of these populations requires careful consideration into the growth model used. Furthermore, with many populations to sample, it was anticipated that lapses in sampling consistency may mislead the selection of the most appropriate growth model. For example, in Chapter 2 model selection remained ambiguous. Two cohorts of juveniles sampled from the same population resulted in the selection of two different growth models. Furthermore, when the Gompertz growth model was used to estimate growth there was high variability in parameter estimates between two cohorts (Chapter 2). It might be argued that the Gompertz is sensitive to real, but subtle, differences in the growth of the two cohorts which may confer an advantage for detecting growth related differences between samples. However it is important to also consider that the differences might be artificial and may be associated with observation or measurement error (Francis & Shotton 1997) as was shown in Chapter 3.

Results in Chapter 3 show that relative to the von Bertalanffy and the Gompertz models, the inverse logistic model is the most statistically and biologically robust growth model for blacklip abalone populations in Tasmania and is sufficiently robust to tag-recapture data with sampling error. The two main characteristics of sampling error that had the greatest influence on model outcomes were limited initial size range of tagged animals and low

sample size, with the size range of tagged animals being more influential on parameter estimates than sample size. These two criteria combined were used for screening tag-recapture data in subsequent chapters. In Chapter 3 I demonstrated that when the inverse logistic was statistically sub-optimal, it was more accurate biologically than the statistically sub-optimal von Bertalanffy or Gompertz. This suggests greater confidence in the inverse logistic in accurately describing growth even if it is (unknowingly) the incorrect model.

In Chapter 4 customary model selection methods were applied to identify the best statistical model when fitted to numerous samples of tag-recapture data. After applying data screening criteria identified in Chapter 3, 30 samples were selected to test the statistical fit of growth models and to select the most appropriate model. The inverse logistic was the best fitting model for the majority of populations, being statistically optimum for 27 (90%) of the samples (Chapter 4).

It is recommended that, the inverse logistic be used in stock assessment modelling which includes a description of growth, because the von Bertalanffy or Gompertz growth models may introduce biases. The inverse logistic model is suitable for all abalone species including *H. rufescens* in the USA. The inverse logistic may also be suitable for any species that are difficult to age including rock lobster and sea urchins (Ling *et al.* 2009). In addition, the inverse logistic model can be used in the absence of growth data for the above-mentioned species, provided that size at maturity and maximum shell length measurements (collected by fishing industry) are available.

7.1.2 Seasonal growth and temperature

Results from the modal progression analysis of two cohorts from a population at Hope Island reveal that somatic growth of the juveniles (10 – 75 mm shell length) is seasonal (Chapter 2). Results clearly indicate that growth rate increased during the austral spring and summer months (September to March) as mean monthly temperatures increased from ~11 to ~16°C. Seasonal growth has been reported for many abalone species, with fastest growth in summer also reported for some (Troynikov *et al.* 1998) but not other blacklip abalone populations in Victoria (Day & Fleming 1992).

Seasonal variation in growth is caused by a combination of many extrinsic and intrinsic factors (Day & Fleming 1992). Temperature has a physiological effect on the growth of poikilotherms, influencing the metabolic rate, gas exchange and oxygen supply (Atkinson 1994). This processes involved are complex, however the physiological response to temperature can be simplified as one where growth is optimum within a certain temperature range and then decreases outside this range (Sharpe & DeMichele 1977). In addition, the absorption of growth enhancing lipids is seasonal and is reported to be higher in warmer temperatures, although this was mainly applicable to adult abalone (Su *et al.* 2006).

Although results in Chapter 2 revealed temperature related seasonal changes in growth rate of juveniles and that growth rate was optimal during the spring/summer months, results in Chapter 5 did not reveal any trend between maximum initial growth rates where maximum water temperatures varied between 16 – 21°C. It is therefore possible that this range is optimal for growth in juveniles. This supports an earlier study where abalone (*H.rubra*) behaviour was assessed under a temperature gradient and found that the preferred

temperatures for growth were below 21°C and that 17°C is optimal for growth in this species (Gilroy & Edwards 1998). The combination of findings from Chapter 2 and 5 confirm what many studies have previously reported for many fish species: that growth is fastest within a given temperature range and outside this range growth decreases (Sharpe & DeMichele 1977; Neuheimer & Taggart 2007).

A study of *H. midae* in South Africa did not find any relationship between temperature and growth rate (Tarr 1995). It is worth noting that the temperatures of the study sites considered in that study were within the thermal tolerance for growth for *H. midae*, as was later reported by a South African study for that same species under controlled conditions (Britz *et al.* 1997).

In Chapter 2 the temporal resolution was at 2 monthly intervals, enabling a seasonal signal to be detected whereas in Chapter 5 the temporal resolution of growth residuals was annual and the calculation of growth residuals incoporated estimates of the MaxΔL parameter of the inverse logistic. It was previously established in Chapter 3 that the MaxΔL is sensitive to sampling error and may lead to implausible parameter values particularly if the size range of tagged abalone is low. Although sampling error may obscure trends between temperature and MaxΔL, the characteristics of sampling error were identified in Chapter 3 and data were screened accordingly. Therefore the MaxΔL paramter estimates in the samples used were considered a robust measure of initial growth rate.

While there was no evidence of any trend between maximum water temperature and initial growth rates across sites (Chapter 5), a latitudinal gradient in growth rate was previously been reported for blacklip abalone in Tasmania (Nash 1992) implying that growth rate may decrease with increasing temperature. However, close inspection of the data presented in

Nash (1992), similarly shows no latitudinal gradient in the growth rates of juveniles, however there is evidence of a latitudinal gradient in the growth of adult sized abalone in that study. It is therefore important to distinguish between growth rate of juveniles measured directly and the growth rate inferred by the final shell size. This distinction is important because growth potential is best indicated by growth of juveniles (Morgan & Colbourne 1999), while adult size reflects both growth rates and size at maturity given that growth decreases once maturity is reached. Ignoring this distinction may lead to misleading comparisons of the life history characteristics of different populations.

7.1.3 Variability in growth among populations

For many abalone species growth is reported to be highly variable at small spatial scales (Tarr 1995; Worthington *et al.* 1995; Naylor *et al.* 2006). In Tasmania, the scale and structure of unit stocks, and the nature of the relationships between catch rate and stock abundance is unknown, making it difficult to spatially model abalone populations. Results in Chapter 3 indicate that when negative growth data are included in the von Bertalanffy model, K increases and L_∞ decreases. This result clearly demonstrates that any heterogeneity reported between samples may be an artifact of the data. To characterise growth reliably, the inverse logistic was selected as the most appropriate growth model. Growth parameters obtained from fitting the inverse logistic to 30 samples of tag-recapture data from populations distributed around the State indicate that growth is highly variable (Chapter 4). The asymptotic shell length of populations in Tasmania exceeds that of other Australian regions; 118 – 151 mm in NSW (Worthington & Andrew 1997, 1998), 117 – 142 mm in Victoria (McShane *et al.* 1988) and 138 – 144 mm in South Australia (Shepherd &

Hearn 1983). Fine scale spatial heterogeneity in growth is also greater in Tasmania and presents a clear challenge in the management of the fishery.

7.1.4 Growth rate and maximum shell length

Life history parameters involving growth rate, maturity and maximum shell length have been extensively studied in marine species in order to optimise the exploitation of fished stocks (Alm 1959; Caswell 2001). In a review of life history studies by Alm (1959) it was reported that rapid growth rate leads to early size at maturity. However in the same review many other studies report otherwise, even within the same species (Alm 1959).

Within a geographic range of a species it is generally assumed that large abalone have fast growth rates and occur in relatively cooler waters. Studies into effects of temperature on life history characteristics occasionally report enigmatic combinations where relatively small sized abalone that are found in warmer temperatures have relatively fast growth rates (Newman 1969a). Similarly, there was no relationship between growth rate of juveniles and maximum shell length in Nash's (1992) data, although it was reported otherwise. The methods used by Nash (1992) relied on ageing techniques which are no longer considered reliable for abalone (McShane & Smith 1992). Nevertheless rapid growth of juveniles did not lead to larger abalone, although Nash (1992) did not report this explicitly. Similarly, (Newman 1969a) reported a combination of fast initial growth but relatively small final shell lengths for *H. midae* in South Africa between Cape Agulhas and Qora river, an area with the highest mean annual temperatures of all the study sites examined. The small final

size of abalone in that region had led to the expectation that juvenile growth rates should also be low.

Results in this thesis offer an explanation for the apparently enigmatic combination of relatively rapid maximum growth rate but relatively low maximum shell length. High growth rates in juvenile abalone at sites around Tasmania occur at sites where water temperatures are both relatively warm and cool. However fast growth rates in warmer waters do not necessarily lead to a larger maximum shell size because the onset of maturity occurs earlier in warmer waters and this causes a reduction in growth (Chapters 4 and 5). The size at maturity, rather than growth rate of juveniles, has a greater effect on maximum size in that maximum shell length is positively correlated with size at maturity, i.e. maximum shell length decreases with decreasing size at maturity (Chapter 4). In a study of *Haliotis kamtschatkana*, smaller size adult abalone also matured at smaller sizes (Campbell *et al.* 2003). Observations of decrease in size at maturity with increasing water temperatures suggests that maturation occurs sooner in warmer waters than in cooler waters, i.e. the age at maturity is lower in warmer than in cooler waters. Since the juvenile phase is the period of relatively rapid growth, the duration of this rapid growth phase is therefore reduced in warmer waters due to the earlier onset of maturity. As abalone mature, energy is partitioned away from somatic growth and toward reproductive growth and therefore somatic growth rate typically decreases dramatically (Lester *et al.* 2004). Therefore observations of fast growth and small maximum shell length may reflect both the growth rate of juveniles and the duration of the juvenile phase as determined by the onset of maturity, i.e. the age at maturity.

7.1.5 Economically valuable populations are at risk of overfishing

The Legal Minimum Length (LML) rule is an important management tool that provides some protection to the spawning biomass (Martin & Maceina 2004; Stewart 2008). The LML rule in Tasmania allows stocks to undergo two breeding cycles after the onset of maturity (Tarbath, Haddon *et al.* 2001). The goal is to ensure that all stocks, especially those in highly productive areas, remain sustainable. However, previous to the study in Chapter 6, it was difficult to quantify the extent of stock protection or identify which populations are at risk of overfishing because knowledge of both growth and maturity is required at a fine spatial scale. Unlike maturity data, growth data is unavailable at a fine spatial scale and this makes it difficult to measure the success of the current broadscale LML settings applied across the State.

Results in Chapter 6 show that the important south west region, a region of high yield to the fishery, was potentially at risk of over-fishing. For some populations in the region the risk is great because juveniles grow to larger sizes and the current management LML is set below the size at maturity. Therefore a proportion of the population is likely to be harvested as juveniles – before they mature – with little chance of the protection of two breeding cycles before being harvested.

Size at maturity is driven by temperature (Chapter 5) with high size at maturity at cooler temperatures (Chapter 5), so it is appropriate that LML settings are higher in the south of the State where water temperatures are cooler. However, variability in observed two year growth increments between populations was greater than the variability in observed size at maturity. Therefore, it is important to consider that adjusting the LML according to

temperature or size at maturity may be a solution but may not take into account the variability in growth rates because growth rates do not follow a temperature trend.

Nevertheless, knowledge of site specific growth rates and size at maturity also has implications for future LML settings under climate change predictions. Firstly, as global warming is expected to realize increases in water temperature, it may be necessary to continue to evaluate associated changes in the growth rate of adults and size at maturity. Although maturity was not the central focus of this thesis it can be noted that the spatial trend in size at maturity follows a temperature gradient and therefore adjusting LML settings according to size at maturity may be sufficient to account for some spatial variability in productivity and the effect of temperature on stock productivity. Ideally, this would be associated with updates to the LML settings, particularly in the south west region, however populations along the east coast need to be especially monitored as relatively rapid increases in water temperature are predicted (Ridgway 2007a).

7.2 Distinctive attributes of this thesis

The number of populations considered in this thesis are numerous relative to many studies on wild abalone. Once samples were screened for data quality, a total of 30 populations from 27 sites were selected which were distributed throughout the geographic range of blacklip abalone in Tasmania. The geographical scale of the analyses presented in this thesis captures the naturally high levels of variation in growth in spatially explicit abalone populations, under widely varying conditions of temperature and size at maturity. The only other study of comparable scale was conducted in New Zealand, where 30 sites were also

examined for growth (Naylor *et al.* 2006). Other similar Australian studies consist of fewer sites, e.g. 16 sites in South Australia (Saunders & Mayfield 2008) and seven sites in NSW (Worthington *et al.* 1995). Overseas studies have far fewer populations owing to a relatively small geographical extent of these fisheries, e.g. six sites in a study of *H. midae* in South Africa (Tarr 1995) and only one population in a growth study from California USA (Rogers-Bennett *et al.* 2007). With fewer sites there is a greater potential for sampling more adequately, however if left unchecked there is also the possibility that biological conclusions may be biased by data that misrepresent the biology through sampling error due to low size range or low sample size. The problem of low size range was anticipated and addressed in the Californian study in which tag-recapture data (50 – 100 mm shell length) were supplemented by a sample of juveniles ranging from 5 – 30 mm in shell length (Rogers-Bennett *et al.* 2007).

By considering all the available data on size at maturity (252 populations) it was possible to get the full natural range of size at maturity within the fishery. Studies that are limited to smaller regional areas may under-estimate the range of natural variation and the consequences are that the findings are not representative of the entire fishery. Trends based on subsections of the full range may not capture the full biological contrast. For example in a study determining whether maturity is age related, size at maturity ranged from 91 – 112 mm (Nash 1990). This represents only a fraction of the range evident in the dataset considered in this thesis where size at maturity ranged between 55 – 157 mm (for n = 252 populations). With such an intrinsically variable species the larger the number of separate populations sampled the more likely it is that the full range of variation will be established.

An important thread common to all chapters is that biological knowledge contributes to model selection. Biological plausibility in parameter estimates is an important consideration when evaluating the choice of model and fitting methods used (Laslett *et al.* 2003). Throughout Chapters 2 and 5 findings from published aquaculture studies were important as they were used to assess the validity of the outcomes. For example, results from controlled experimental studies were important in assessing the biological validity of three candidate models studied in Chapter 2 by comparing their predictions on growth rate with the expectations of growth rates of juveniles from the controlled studies. Aquaculture studies were also useful in determining the thermal tolerance of abalone which was prerequisite knowledge for understanding temperatures likely to affect growth rates (Chapter 5).

Another distinctive feature of this thesis was the investigation of the implications of negative growth increments on growth model outcomes. Although negative increments are common, their effect on model fitting and outcomes has not previously been statistically tested. The data in Chapter 3 reveal that negative growth increments are typical in tag-recapture surveys. It is possible that negative growth increments are real. As there are no data or methods available that enable real negative growth to be distinguished from the measurement errors, an arbitrary 'rule' was used and declared in the methods. In line with previous practice (at least in some areas in Australia), all measurements to minus 3mm are assumed to reflect potentially real growth dynamics, and measurements more negative than -3 mm are assumed to be measurement or recording errors. Negative growth increments, indicative of measurement error and/or shell chipping, should be minimised to improve the accuracy of biological findings. Some negative increments in the data can be avoided by noting down any evidence of shell chipping when shells are measured. Other negative

increments will be purely and simply measurement error, and cannot be avoided. The use of electronic measuring boards may potentially decrease measurement error and may likely reduced the time taken to measure the shell length of abalone. Any extra time gained in this manner should perhaps be used to improve the quality of tag-recapture data.

7.3 Recommendations for future research related to growth and productivity

Blacklip abalone is a good candidate species for the study of environmental conditions on growth and related biology because populations have a wide geographic range. It is a cool temperate species but juveniles can tolerate temperature of up to 21°C (Gilroy & Edwards 1998). Future research can improve the resolution and an understanding of the relationship between growth rate and productivity can be improved by developing a more formal field sampling design. In terms of biological sampling, it is recommended that samples for size at maturity should always be taken at the same time as tagging surveys, so that data on growth and maturity are from the same location in time and space. Such data were rare in the current thesis because the data used was based on opportunistic sampling. If a study of productivity could proceed along these lines, it would need to focus on selected populations with similar and contrasting growth rates and sizes at maturity under similar and contrasting environmental conditions (within the same year). The location of samples could continue to be placed in areas of commercial interest so that the estimates of relative biological productivity could be related to fishery dependent statistics of catches, catch rates, and catch length frequencies.

Another possibility for future research could focus on the inter-annual variation in productivity within populations. This would have value because in most stock assessment models the notion of stationarity is assumed, i.e. the parameters describing growth and maturity are assumed to remain constant through time. Quantifying temporal variability in productivity of selected populations would enable a better understanding of the extent and effect of natural fluctuations in growth rate on productivity. Most Australian studies on abalone span timescales of a few years. There are fisheries in the USA and Canada that have studied population biology for decades, although trends can be detected over the course of 10 years (Beacham 1983; Bowering 1989; Morgan 1999; Morgan & Colbourne 1999; Sigourney *et al.* 2006). Nevertheless, longer time spans may be required to study the effect of temperature on growth rate, size at maturity and maximum shell length in blacklip abalone in Tasmania.

Other areas of future research include examination of the relationship between temperature and size at maturity. Reproductive cycles are often driven by temperature cues where continual exposure above a temperature threshold may trigger the onset of maturity. In blacklip abalone this temperature minimum for mature abalone occurs at 7.8°C (Grubert 2002). It would be useful to determine the details of whether exposure to different temperatures regimes would induce the onset of maturity at different sizes for the same population. Examining the interactions between size at maturity, temperature, growth rate and maximum shell length attained in experimental situations may help to elucidate the mechanism underlying the inverse association between growth rate and maximum shell length that is sometimes encountered in warmer waters.

These recommendations are based on extensive field sampling which can be very costly and may outweigh the benefits gained by improved understanding of the biology (Punt

2006). The scale of data collection required to provide sufficient and appropriate advice for management, extends beyond the financial scope of scientific programmes. A viable alternative, currently under consideration, is to allow commercial divers to collect samples for scientific programmes under permit. This would reduce the costs of scientific programmes and would enable data to be collected from isolated places where commercial divers are already operating. This will help answer some of the questions raised about variability in growth in populations dispersed around Tasmania and south-east Australia in a more cost effective manner. Such a scheme would also allow scientific programmes to benefit from the field expertise and field operations of industry divers.

Although this thesis has started to reveal some findings about growth related productivity one major drawback in quantifying productivity of stocks is that the actual area of habitat occupied by the stock is not quantified. The abalone fishery is divided into statistical reporting blocks and each block differs in the area of reef habitat which blacklip occupy. Therefore the high yield reported from one statistical block may be a result of larger reef area in that statistical block relative to another statistical block. This thesis did not address this issue but improving knowledge of the extent of productive reef in each area would have great value in improving the management of this valuable resource.

7.4 Future research for monitoring the effects of temperature related climate change on productivity

The effects of climate change on marine biota is becoming an important topic, with an increasing number of studies modelling bioenergetics based on the relationship between

temperature and growth rate, e.g. in lobsters (Pecl *et al.* 2009) and octopus (Andre *et al.* 2009). However this would not be useful or informative for abalone because the elevated temperatures that reduce growth rates are also temperatures where abalone mortalities occur (Gilroy & Edwards 1998). If a program was to be set up to monitor the effect of temperature change on abalone stocks it would be better to monitor the interaction between size at maturity and temperature because, unlike growth studies, the influence of temperature on productivity is detected at temperatures well below those that cause mortalities (Chapter 5) (Grubert 2002). Examining interactions between the two important biological traits of growth and size at maturity would be necessary for developing a more complete picture of the effects of climate change on productivity.

REFERENCES

ABARE 2007, *Australian Fisheries Statistics 2006*, ABARE and FRDC.

ABS 2009, *Tasmania's international exports 2005-06, 2006-07, 2007-08*, viewed http://www.development.tas.gov.au/__data/assets/pdf_file/0010/3979/Exports2008.pdf>.

Alm, G. 1959, 'Connection between maturity, size and age in fishes. ' *Report / Institute of Freshwater Research, Drottningholm*, vol. 40, pp. 5–145.

Andre, J., Pecl, G.T., Grist, E.P.M., Semmens, J.M., Haddon, M. & Leporati, S.C. 2009, 'Modelling size-at-age in wild immature female octopus: a bioenergetic approach', *Marine Ecology Progress Series*, vol. 384, pp. 159-174.

Arce, A.M. & León, M.E.d. 1997, *Report on the FAO/DANIDA/CFRAMP/WECAFC Regional Workshops on the Assessment of the Caribbean Spiny Lobster (Panulirus argus). FAO Fisheries Report*, 619, FAO, Rome.

Atkinson, D. 1994, 'Temperature and organism size: A biological law for ectotherms?' *Adv. Ecol. Res.* , vol. 25, pp. 1-58.

Baranski, M., Rourke, M., Loughnan, S., Hayes, B., Austin, C. & Robinson, N. 2008, 'Detection of QTL for growth rate in the blacklip abalone (Haliotis rubra Leach) using selective DNA pooling', *Animal Genetics*, vol. 39, no. 6, pp. 606-614.

Basson, M., Rosenberg, A.A. & Beddington, J.R. 1988, 'The accuracy and reliability of two new methods for estimating growth parameters from length-frequency data', *ICES J. Mar. Sci.*, vol. 44, no. 3, pp. 277-285.

Beacham, T.D. 1983, 'Variability in size and age at sexual maturity of argentine, *Argentina silus*, on the Scotian Shelf in the Northwest Atlantic ocean', *Env. Biol. Fish.* , vol. 8, pp. 67-72.

Belk, M.C. 1995, 'Variation in growth and age at maturity in bluegill sunfish:genetic or environmental effects?' *Journal of Fish Biology* vol. 47, pp. 237-247.

Bowering, W.R. 1989, 'Witch flounder distribution off Southern Newfoundland, and changes in age, growth, and sexual maturity patterns with commercial exploitation', *Transactions of the American Fisheries Society*, vol. 118, pp. 659-669.

Branden, K.L. & Shepherd, S.A. 1983, *A survey of stocks of the abalone Haliotis roei Gray on the western coast of Spencer Gulf, South Australia. Parts 1 and 2*, 4, Department of Fisheries South Australia, Adelaide.

Britton, J.R. & Harper, D.M. 2008, 'Juvenile growth of two tilapia species in lakes Naivasha and Baringo, Kenya', *Ecology of Freshwater Fish*, vol. 17, no. 3, pp. 481-488.

Britz, P.J., Hecht, T. & Mangold, S. 1997, 'Effect of temperature on growth, feed consumption and nutritional indices of Haliotis midae fed a formulated diet', *Aquaculture*, vol. 152, no. 1-4, pp. 191-203.

Burnham, K.P. & Anderson, D.R. 2002, *Model selection and multimodel inference: a practical information-theoretic approach.*, Springer-Verlag., New York, NY.

Butterworth, D.S., Cochrane, K.L. & De Oliveira, J.A.A. 1997, 'Management procedures: a better way to manage fisheries? The South African experience. ' paper presented to Global trends: fisheries management. American Fisheries Society Symposium, Bethesda, Maryland.

Campbell, A., Lessard, J. & Jamieson, G.S. 2003, *Fecundity and seasonal reproduction of northern abalone, Haliotis kamtschatkana, in Barkley Sound, Canada.*

Casselman, J.M. 2007, 'Determining minimum ultimate size, setting size limits, and developing trophy standards and indices of comparable size for maintaining quality muskellunge (Esox masquinongy) populations and sports fisheries', *Environmental Biology of Fishes*, vol. 79, no. 1-2, pp. 137-154.

Caswell, H. 2001, *Matrix Population Models: construction, analysis and interpretation*, Sinauer Associates, Inc., Sunderland, Massachusetts.

Catchpole, E.A., Freeman, S.N., Morgan, B.J.T. & Nash, W.J. 2001, 'Abalone I: analyzing mark-recapture-recovery data incorporating growth and delayed recovery', *Biometrics*, vol. 57, pp. 469-477.

Chatzinikolaou, E. & Richardson, C.A. 2008, 'Population dynamics and growth of Nassarius reticulatus (Gastropoda: Nassariidae) in Rhosneigr (Anglesey, UK)', *Marine Biology*, vol. 153, no. 4, pp. 605-619.

Cox, L.A. 2002, *Risk Analysis: Foundations, Models, and Methods*, Springer.

Crawley, M.J. 2005, The R Book.

Cropp, R. 1989, *Abalone culture in Tasmania*, 37, Department of Sea Fisheries, Tasmania, Hobart.

CSIRO 2004, *A Decade of SST Satellite Data:The Remote Sensing Project of The Marine and Atmospheric labs of CSIRO*, CSIRO.

Daume, S. 2003, *Early life history of abalone (Haliotis rubra, H. laevigata): settlement, survival and early growth*, Project 1998/306.

Day, R.W. & Fleming, A.E. 1992, 'The determinants and measurement of abalone growth', in S.A. Shepherd, M.J. Tegner & S.A. Guzmán del Próo (eds), *Abalone of the world: biology, fisheries and culture*, Blackwell, Oxford, pp. 141-164.

Day, T. & Taylor, P.D. 1997, 'Von Bertalanffy's growth equation should not be used to model age and size at maturity.' *American Naturalist (Am. Nat.)*, vol. 149, pp. 381–393.

Dick, E.J. 2004, 'Beyond 'logormal versus gamma':discriminating among error distributions for generalized linear models', *Fisheries Research*, vol. 70, pp. 351-366.

Efron, B. & Tibshirani, R. 1993, *An introduction to the bootstrap*, vol. 57, Monographs on statistics and applied probability 57, Chapman & Hall, New York.

Fabens, A.J. 1965, 'Properties and fitting of the von Bertalanffy growth curve', *Growth*, vol. 29, pp. 265-289.

FAO 2006, *FAO Fishery Information, Data and Statistics Unit. 2006. Total production 1950-2004.*, FISHSTAT Plus edn, Food and Agriculture Organization of the United Nations, <Available at: http://www.fao.org/fi/statist/FISOFT/FISHPLUS.asp>.

Fowler, J. & Cohen, L. 1990, *Practical statistics for field biology*, John Wiley & Sons Ltd., Chichester, West Sussex.

Francis, R.I.C.C. 1988a, 'Are growth parameters estimated from tagging and age-length data comparable?' *Canadian Journal of Fisheries and Aquatic Sciences*, vol. 45, pp. 936-942.

---- 1988b, 'Maximum likelihood estimation of growth and growth variability from tagging data', *New Zealand Journal of Marine and Freshwater Research*, vol. 22, pp. 42-51.

---- 1995, 'An alternative mark-recapture analogue of Schnute's growth model', *Fisheries Research*, vol. 23, pp. 95-111.

---- 1996, 'Do herring grow faster than orange roughy', *Fishery Bulletin*, vol. 94, no. 4, pp. 783 - 786.

Francis, R.I.C.C. & Shotton, R. 1997, '"Risk" in fisheries management: a review', *Canadian Journal of Fisheries and Aquatic Sciences*, vol. 54, pp. 1699-1715.

Gilroy, A. & Edwards, S.J. 1998, 'Optimum temperature for growth of Australian abalone: preferred temperature and critical thermal maximum for blacklip abalone, *Haliotis rubra* (Leach), and greenlip abalone, *Haliotis laevigata* (Leach)', *Aquaculture Research*, vol. 29, pp. 481-485.

Godø, O.R. & Haug, T. 1999, 'Growth Rate and Sexual Maturity in Cod (Gadus morhua) and Atlantic Halibut (Hippoglossus hippoglossus)', *Journal of Northwest Atlantic Fishery Science*, vol. 25, pp. 115–123.

Gompertz, B. 1825, 'On the nature of the function expressive of the law of human mortality, and on a new model of determining the value of life contingencies.' *Philosophical Transactions of the Royal Society*, vol. 115, pp. 513-585.

Grover, M.C. 2005, 'Changes in size and age at maturity in a population of kokanee *Oncorhynchus nerka* during a period of declining growth conditions', *Journal of Fish Biology* vol. 66, pp. 122–134.

Grubert, M.A. 2002, 'Estimation of the Biological Zero Point of blacklip (*Haliotis rubra*) and greenlip (*H.laevigata*) abalone', paper presented to Proceedings of the 9th Annual Abalone Aquaculture workshop, Queenscliff, Victoria.

Gulland, J.A. & Rosenberg, A.A. 1992, *A review of length-based approaches to assessing fish stocks.*, 323, FAO, Rome.

Haaker, P.L., Parker, D.O., Barsky, K.C. & Chun, C.S.Y. 1998, 'Growth of red abalone, *Haliotis rufescens* (Swainson), at Johnsons Lee, Santa Rosa Island, California', *Journal of Shellfish Research*, vol. 17, no. 3, pp. 747-753.

Haddon, M. 2001, *Modelling and Quantitative Methods in Fisheries*, 1 edn, Chapman and Hall/CRC, Boca Raton.

Haddon, M., Mundy, C. & Tarbath, D. 2008, 'Using an inverse-logistic model to describe growth increments of blacklip abalone (Haliotis rubra) in Tasmania', *Fishery Bulletin*, vol. 106, pp. 58–71.

Hamilton, G., McVinish, R. & Mengersen, K. 2007, 'Using a Bayesian Net to aid in the selection of candidate variables ', paper presented to Society for Risk Analysis (SRA) 2007 (Australian & New Zealand Regional Organisation).

Hara, M. & Kikuchi, S. 1992, 'Increasing the growth rate of abalone, Haliotis discus hannai, using selection techniques', *NOAA Technical Report NMFS*, vol. 106, pp. 21-26.

Harris, J.O., Burke, C., Edwards, S. & Johns, D. 2005, 'Effects of oxygen supersaturation and temperature on juvenile greenlip, Haliotis laevigata Donovan, and blacklip, Haliotis rubra Leach, abalone', *Aquaculture Research*, vol. 36, pp. 1400-1407.

Harrison, A.J. 2006, *The Tasmanina abalone fishery: a personal history*, <http://members.trump.net.au/ahvem/Fisheries/Abalone/abalone1.html>.

Harrison, A.J. & Grant, J.F. 1971, 'Progress in abalone research', *Tasmanian Fisheries Research*, vol. 5, pp. 1-10.

Hilborn, R. & Mangel, M. 1997, *The Ecological Detective: Confronting Models with Data*, Princeton University Press, Princeton, New Jersey.

Hilborn, R. & Walters, C.J. 1992, *Quantitative fisheries stock assessment: choice, dynamics and uncertainty*, 1st edn, Chapman and Hall, London.

Huchette, S.M.H., Koh, C.S. & Day, R.W. 2003, 'Growth of juvenile blacklip abalone (Haliotis rubra) in aquaculture tanks: effects of density and ammonia', *Aquaculture*, vol. 219, no. 1-4, pp. 457-470.

IPCC 2007, *Climate Change 2007: Synthesis Report. An Assessment of the Intergovernmental Panel on Climate Change*.

Jákupsstovu, S.H. & Haug, T. 1988, 'Growth, sexual maturation, and spawning season of Atlantic halibut, *Hippoglossus hippoglossus*, in Faroese waters', *Fisheries Research*, vol. 6, no. 3, pp. 201-215.

Katsanevakis, S. & Maravelias, D. 2008, 'Modelling fish growth: multi model inference as a better alternative to *a priori* using von Bertalanffy equation', *Fish and Fisheries*, vol. 9, pp. 178-187.

Lae, R. 1999, 'Predicting fish yield of African lakes using neural networks', *Ecological modelling* vol. 120, no. 2-3 p. 325

Laslett, G.M., Eveson, J.P. & Polacheck, L. 2003, *Correspondance*, Biometrics.

Lester, N.P., Shuter, B.J. & Abrams, P.A. 2004, 'Interpreting the von Bertalanffy model of somatic growth in fishes: the cost of reproduction', *Proceedings of the Royal Society B: Biological Sciences*, vol. 271, no. 1548, pp. 1625-1631.

Ling, S.D., Johnson, C.R., Ridgway, K., Hobday, A.J. & Haddon, M. 2009, 'Climate-driven range extension of a sea urchin: inferring future trends by analysis of recent population dynamics', *Global Change Biology*, vol. 15, no. 3, pp. 719-731.

Martin, A.D. & Maceina, M.J. 2004, 'Assessment of detecting minimum length limit changes for crappie in two Alabama reservoirs', *Fisheries Research*, vol. 68, no. 1-3, pp. 293-303.

Mayr, E. 1956, 'Geographical Character Gradients and Climatic Adaptation', *Evolution*, vol. 10, no. 1, pp. 105-108.

McShane, P.E. & Naylor, J.R. 1995, 'Small-scale spatial variation in growth, size at maturity, and yield- and egg-per-recruit relations in the New Zealand abalone *Haliotis iris*', *New Zealand Journal of Marine and Freshwater Research*, vol. 29, pp. 603-612.

McShane, P.E. & Smith, M.G. 1992, 'Shell growth checks are unreliable indicators of age of the abalone *Haliotis rubra* (Mollusca, Gastropoda)', *Australian Journal of Marine and Freshwater Research*, vol. 43, pp. 1215-1219.

McShane, P.E., Smith, M.G. & Beinssen, K. 1988, 'Growth and morphometry in abalone (*Haliotis rubra* Leach) from Victoria', *Australian Journal of Marine and Freshwater Research*, vol. 39, pp. 161-166.

Miller, K.J., Maynard, B.T. & Mundy, C.N. 2008, 'Genetic diversity and gene flow in collapsed and healthy abalone fisheries', *Molecular Ecology*

Morgan, M.J. 1999, 'The Effect of a Change in Perception of Length Distribution of a Population on Maturity-at-age, Weight-at-age and Spawning Stock Biomass', *J. Northw. Atl. Fish. Sci.*, vol. 25, pp. 141–150.

Morgan, M.J. & Colbourne, E.B. 1999, 'Variation in maturity-at-age and size in three populations of American plaice', *ICES Journal of Marine Science*, vol. 56, pp. 673–688.

Nash, W.J. 1990, 'Abalone mature with age not size', *Fishing Today*, vol. 3, no. 2, pp. 38-39.

---- 1992, 'An evaluation of egg-per-recruit analysis as a means of assessing size limits for blacklip abalone (*Haliotis rubra*) in Tasmania', in S.A. Shepherd, M.J. Tegner & S.A. Guzmán del Próo (eds), *Abalone of the world: biology, fisheries and culture*, Blackwell Scientific, Oxford, pp. 318-340.

Nash, W.J., Sanderson, J.C., Bridley, J., Dickson, S. & Hislop, B. 1995, 'Post-larval recruitment of blacklip abalone (*Haliotis rubra*) on artificial collectors in southern Tasmania', *Marine and Freshwater Research*, vol. 46, no. 3, pp. 531-538.

Nash, W.J., Sellers, T.L., Talbot, S.R., Cawthorn, A.J. & Ford, W.B. 1994, *The population biology of abalone (Haliotis species) in Tasmania. 1: Blacklip abalone (H. rubra) from the North Coast and the islands of Bass Strait*, 48, Department of Primary Industry and Fisheries, Tasmania, Hobart.

Naylor, J.R., Andrew, N.L. & Kim, S. 2003, *Fishery independant surveys of the relative abundance, size-structure, and growth of paua (Haliotis iris) in PAU 4.*, Ministry of Fisheries, Wellington.

Naylor, J.R., Andrew, N.L. & Kim, S.W. 2006, 'Demographic variation in the New Zealand abalone *Haliotis iris*', *Marine and Freshwater Research*, vol. 57, pp. 215-224.

Neter, J., Kutner, M.H. & Wasserman, W. 1990, *Applied linear statistical models : regression, analysis of variance, and experimental designs*, R.D. Irwin, Homewood.

Neter, J., Nachtschiem, C.J., Kutner, M.H. & Wasserman, W. 1996, *Applied linear statistical models 4th Edition* Richard d Irwin, Chicago.

Neuheimer, A.B. & Taggart, C.T. 2007, 'The growing degree-day and fish size-at-age: the overlooked metric.' *Can. J. Fish. Aquat. Sci.*, vol. 64, pp. 375-385.

Newman, G.G. 1968, 'Growth of the South African abalone, *Haliotis midae*', *Union South Africa Div. Fish. Invest. Rep.*, vol. 67, p. 24 pp.

---- 1969a, 'Distribution of the abalone (*Haliotis midae*) and the effect of temperature on productivity', *Invest. Rep. Div. Sea Fish and Rep. South Africa*, vol. 74, pp. 1-8.

---- 1969b, 'Distribution of the abalone (*Haliotis midae*) and the effect of temperature on productivity.' *Investl Rep. Div. Fish. Un. S. Afr.*, vol. 74.

Peck, L.S., Culley, M.B. & Helm, M.M. 1987, 'A laboratory energy budget for the ormer Haliotis tuberculata L', *Journal of Experimental Marine Biology and Ecology*, vol. 106, pp. 103-123.

Pecl, G., Frusher, S., Gardner, C., Haward, M., Hobday, A., Jennings, S., Nursey-Bray, M., Punt, A., Revill, H. & van Putten, I. 2009, *The east coast Tasmanian rock lobster fishery – vulnerability to climate change impacts and adaptation response options. Report to the Department of Climate Change, Australia.*, Department of Climate Change.

Pitcher, T.J. & MacDonald, P.D.M. 1973, 'Two models of seasonal growth in fishes', *Journal of Applied Ecology*, vol. 10, pp. 599-606.

Polacheck, T., Hilborn, R. & Punt, A.E. 1993, 'Fitting surplus production models: comparing methods and measuring uncertainty', *Canadian Journal of Fisheries and Aquatic Sciences*, vol. 50, pp. 2597-2607.

Poloczanska, E.S., Babcock, R.C., Butler, A., Hobday, A., Hoegh-Guldberg, O., Kunz, T.J., Matear, R., Milton, D.A., Okey, T.A. & Richardson, A.J. 2007, 'Climate change and Australian marine life', in *Oceanography and Marine Biology, Vol 45*, Crc Press-Taylor & Francis Group, Boca Raton, vol. 45, pp. 407-478.

Prince, J.D. 1991, 'A new technique for tagging abalone', *Australian Journal of Marine and Freshwater Research*, vol. 42, pp. 101-106.

Prince, J.D., Sellers, T.L., Ford, W.B. & Talbot, S.R. 1987, 'Experimental evidence for limited dispersal of *Haliotid* larvae (genus *Haliotis*: Mollusca: Gastropoda)', *Journal of Experimental Marine Biology and Ecology*, vol. 106, pp. 243-263.

---- 1988a, 'A method for ageing the abalone *Haliotis rubra* (Mollusca: Gastropoda)', *Australian Journal of Marine and Freshwater Research*, vol. 39, pp. 167-175.

---- 1988b, 'Recruitment, growth, mortality and population structure in a southern Australian population of *Haliotis rubra* (Mollusca, Gastropoda)', *Marine Biology*, vol. 100, pp. 75-82.

Proudfoot, L.A., Kaehler, S. & McQuaid, C.D. 2008, 'Using growth band autofluorescence to investigate large-scale variation in growth of the abalone Haliotis midae', *Marine Biology*, vol. 153, no. 5, pp. 789-796.

Punt, A.E. 2006, 'The FAO Precautionary Approach after almost 10 years: have we progressed towards implementing simulation-tested feedback-control management systems for fisheries management', *Natural Resource Modeling*, vol. 19, no. 4, pp. 441-464.

Quinn II, T.J. & Deriso, R.B. 1999, *Quantitative Fish Dynamics*, Oxford University Press, New York.

R Development Core Team 2008, *R: A language and environment for statistical computing.*, R Foundation for Statistical Computing., Vienna, Austria., 3-900051-07-0.

Ratkowsky, D.A. 1986, 'Statistical properties of alternative parameterizations of the von Bertalanffy growth curve', *Canadian Journal of Fisheries and Aquatic Sciences*, vol. 43.

Ray, C. 1960, 'The application of Bergmann's and Allen's rules to the poikilotherms', *J. Morph.*, vol. 106, pp. 85-108.

Ricker, W.E. 1975, 'Computation and interpretation of biological statistics of fish populations', *Bulletin of the Fisheries Research Board of Canada*, vol. 191.

Ridgway, K.R. 2007a, 'Long-term trend and decadal variability of the southward penetration of the East Australian Current', *Geophys. Res. Lett.*, vol. 34.

---- 2007b, 'Seasonal circulation around Tasmania: An interface between eastern and western boundary dynamics', *Journal of Geophysical Research, C - Oceans*, vol. 112.

Rogers-Bennett, L. 2007, 'Is climate change contributing to range reductions and localized extinctions in northern (*Haliotis kamtschatkana*) and flat (*Haliotis walallensis*) abalones?' *Bulletin of Marine Science*, vol. 81, pp. 283-296.

Rogers-Bennett, L., Rogers, D. & Schultz, S.A. 2007, 'Modeling growth and mortality of red abalone (*Haliotis rufescens*) in northern California', *Journal of Shellfish Research*, vol. 26, no. 3, pp. 719-727.

Sainsbury, K.J. 1980, 'Effect of individual variability on the von Bertalanffy growth equation', *Canadian Journal of Fishery and Aquatic Sciences*, vol. 37, pp. 241-247.

Sainsbury, K.J., Punt, A.E. & Smith, A.D.M. 2000, 'Design of operational management strategies for achieving fishery ecosystem objectives', *ICES J. Mar. Sci.*, vol. 57, pp. 731-741.

Saunders, T. & Mayfield, S. 2008, 'Predicting biological variation using a simple 'morphometric marker' in a sedentary marine invertebrate (*Haliotis rubra*).' *Marine Ecology Progress Series.*

Saunders, T.M., Mayfield, S. & Hogg, A.A. 2008, 'A simple, cost-effective, morphometric marker for characterising abalone populations at multiple spatial scales', *Marine and Freshwater Research*, vol. 59, pp. 32-40.

Scandol, J.P. 2004, *A framework for the assessment of harvested fish resources in NSW*, 15, NSW Department of Primary Industries, Sydney.

Schnute, J. 1981, 'A versatile growth model with statistically stable parameters', *Canadian Journal of Fishery and Aquatic Sciences*, vol. 38, pp. 1128-1140.

Schnute, J.T. 1991, 'The importance of noise in fish population models', *Fisheries Research*, vol. 11, pp. 197-223.

Searle, T., Roberts, R.D. & Lokman, P.M. 2006, 'Effects of temperature on growth of juvenile blackfoot abalone, Haliotis iris Gmelin', *Aquaculture Research*, vol. 37, no. 14, pp. 1441-1449.

Sharp, G.D. 2003, *Future climate change and regional fisheries: a collaborative analysis*, Food and Agrictulture Organization of the United Nations, Rome.

Sharpe, P.J.H. & DeMichele, D.W. 1977, 'Reaction kinetics of poikilotherm development', *J. Theor. Biol.*, vol. 64, no. 649-670.

Shepherd, S.A. & Hearn, W.S. 1983, 'Studies on southern Australian abalone (genus *Haliotis*) IV. Growth of *H. laevigata* and *H. ruber*', *Australian Journal of Marine and Freshwater Research*, vol. 34, pp. 461-475.

Shepherd, S.A. & Laws, H.M. 1974, 'Studies on southern Australian abalone (genus *Haliotis*) II. Reproduction of five species', *Australian Journal of Marine and Freshwater Research*, vol. 25, pp. 49-62.

Shono, H. 2000, 'Efficiency of the finite correction of Akaike's Information Criteria', *Fisheries Science*, vol. 66, pp. 608-610.

Sigourney, D.B., Ross, M.R., Brodziak, J. & Burnett, J. 2006, 'Length at age, sexual maturity and distribution of Atlantic Halibut, *Hippoglossus hippoglossus* L., off the Northeast USA', *J. Northw.Atl.Fish.Sci.*, vol. 36, pp. 81-90.

Smith, A.D.M., Sainsbury, K.J. & Stevens, R.A. 1999, 'Implementing effective fisheries-management systems ~ management strategy evaluation and the Australian partnership approach', *ICES Journal of Marine Science*, vol. 56, pp. 967-979.

Sorensen, D. & Gianola, D. 2002, *Likelihood, Bayesian, and MCMC Methods in Quantitative Genetics*, Springer-Verlag, New York.

Steinarsson, A. & Imsland, A.K. 2003, 'Size dependent variation in optimum growth temperature of red abalone (Haliotis rufescens)', *Aquaculture*, vol. 224, no. 1-4, pp. 353-362.

Stergiou, K.I., Moutopoulos, D.K. & Armenis, G. 2009, 'Perish legally and ecologically: the ineffectiveness of the minimum landing sizes in the Mediterranean Sea', *Fisheries Management and Ecology*, vol. 16, no. 5, pp. 368-375.

Stewart, J. 2008, 'A decision support system for setting legal minimum lengths of fish', *Fisheries Management and Ecology*, vol. 15, no. 4, pp. 291-301.

Stone, M. 1974, 'Cross-Validatory Choice and Assessment of Statistical Predictions', *Journal of the Royal Statistical Society. Series B (Methodological)*, vol. 36, pp. 111-147.

Su, X.Q., Antonas, K., Li, D. & Nichols, P. 2006, 'Seasonal variations of total lipid and fatty acid contents in the muscle of two Australian farmed abalone species', *Journal of Food Lipids*, vol. 13, no. 4, pp. 411-423.

Summerfelt, R.C. 1987, *Preface*, Age and growth in fishes. Papers presented at the International Symposium on Age and Growth of Fish. June 9-12, 1985, Iowa State University Press, Des Moines, Iowa.

Tarbath, D. & Gardner, C. 2009, *Tasmanian Abalone Fishery 2008*, Tasmanian Aquaculture and Fisheries Institute.

Tarbath, D., Mundy, C. & Haddon, M. 2008, *Tasmanian Abalone Fishery 2007*, Tasmanian Aquaculture and Fisheries Institute.

Tarbath, D.B. 2003, 'Population parameters of blacklip abalone (*Haliotis rubra* Leach) at the Acteons in south-east Tasmania', M.Sc. thesis, University of Tasmania.

Tarbath, D.B., Haddon, M. & Mundy, C. 2001, *East Coast Abalone Assessment: 2001*, Tasmanian Aquaculture and Fisheries Institute, Hobart.

Tarbath, D.B., Hodgson, K., Karlov, T. & Haddon, M. 2001, *Tasmanian abalone fishery 2000*, Tasmanian Aquaculture and Fisheries Institute, Hobart.

Tarr, R.J.Q. 1995, 'Growth and movement of the South African abalone *Haliotis midae*: A reassessment', *Marine and Freshwater Research*, vol. 46, no. 3, pp. 583-590.

Temby, N., Miller, K. & Mundy, C. 2007, 'Evidence of genetic subdivision among populations of blacklip abalone (*Haliotis rubra* Leach) in Tasmania.' *Marine and Freshwater Research*, vol. 58, pp. 733–742.

Travers, M.-A., Basuyaux, O., Le Goic, N., Huchette, S., Nicolas, J.-L., Koken, M. & Paillard, C. 2009, 'Influence of temperature and spawning effort on Haliotis tuberculata mortalities caused by Vibrio harveyi: an example of emerging vibriosis linked to global warming', *Global Change Biology*, vol. 15, pp. 1365–1376.

Troynikov, V.S., Day, R.W. & Leorke, A. 1998, 'Estimation of seasonal growth parameters using a stochastic Gompertz model for tagging data', *Journal of Shellfish Research*, vol. 17, no. 3, pp. 833-838.

Urban, H.J. 2002, 'Modeling growth of different developmental stages in bivalves', *Marine Ecology Progress Series*, vol. 238, pp. 109-114.

von Bertalanffy, L. 1938, 'A quantitative theory of organic growth (Inquiries on growth laws. II).' *Human Biology*, vol. 10, no. 2, pp. 181-213.

Walters, C. & Martell, S. 2004, *Fisheries Ecology and Management*, Princeton University press, Princeton and Oxford.

Wang, Y.-G., Thomas, M.R. & Somers, I.F. 1995, 'A maximum likelihood approach for estimating growth from tag-recapture data', *Canadian Journal of Fisheries and Aquatic Sciences*, vol. 52, pp. 252-259.

Wang, Y.G. 1998, 'Growth curves with explanatory variables and estimation of the effect of tagging', *Australian & New Zealand Journal of Statistics*, vol. 40, no. 3, pp. 299-304.

---- 1999, 'Estimating equations for parameters in stochastic growth models from tag-recapture data', *Biometrics*, vol. 55, no. 3, pp. 900-903.

Winsor, C.P. 1932, 'The Gompertz curve as a growth curve', *Proceedings of the National Academy of Sciences*, vol. 18, no. 1, pp. 1 - 8.

Worthington, D.G. & Andrew, N.L. 1997, 'Does covariation between growth and reproduction compromise the use of an alternative size limit for the blacklip abalone, *Haliotis rubra*, in NSW, Australia?' *Fisheries Research*, vol. 32, pp. 223-231.

---- 1998, 'Small-scale variation in demography and its implications for alternative size limits in the fishery for abalone in NSW, Australia', paper presented to North Pacific Symposium on Invertebrate Stock Assessment and Management.

Worthington, D.G., Andrew, N.L. & Bentley, N. 1998, 'Improved indices of a catch rate in the fishery for blacklip abalone, *Haliotis rubra*, in New South Wales, Australia', *Fisheries Research*, vol. 36, pp. 87-97.

Worthington, D.G., Andrew, N.L. & Hamer, G. 1995, 'Covariation between growth and morphology suggests alternative size limits for the abalone, *Haliotis rubra*, in NSW, Australia', *Fishery Bulletin U.S.*, vol. 93, pp. 551-561.

Yamaguchi, M. 1975, 'Estimating growth parameters from growth rate data', *Oecologia*, vol. 20, no. 4, pp. 321-332.

Zhou, S. 2007, 'Discriminating alternative stock-recruitment models and evaluating uncertainty in model structure', *Fisheries Research*, vol. 86, no. 2-3, pp. 268-279.

Dr Helidoniotis' thesis is titled: Growth of abalone (*Haliotis rubra*) with implications for its productivity.

Fay studied the growth rates among populations of abalone and the effect of temperature and fishing on stock biomass. This led to the development of a new theory in the link between temperature and growth rate, and has implications for adaptive fisheries management under predicted climate change.